Utrecht University
Institute for Theoretical Physics

Theoretical Physics Master Thesis

Soft Threshold Limit of Drell-Yan Angular Distributions

First examiner:
E.L.M.P. Laenen
Second examiner:
U. Gursoy
Daily supervisor:
J.K.L. Michel

Candidate:
Carlotta Casi

In cooperation with:
Nikhef

8 July, 2024

Abstract

The angular distribution of the final state leptons in the Drell-Yan process plays a key role in testing the QCD dynamics of Z/W bosons production and in measuring the values of masses and couplings of the EW sector of the SM. This angular distribution is in one-to-one correspondence to the set of production cross-sections for vector bosons of definite helicity (helicity cross sections) which feature sensitivity to soft and collinear QCD radiation. In this thesis, we calculate radiative corrections to the helicity cross sections up to next-to-next-to leading order (NNLO) in the strong coupling, focusing on the emission of a single and double gluon from the initial state quark-antiquark pair. We then study the behavior of these corrections in the soft threshold limit, where the dilepton pair invariant mass approaches the available center of mass energy. Finally, we use Soft-Collinear Effective Theory (SCET) to derive soft factorization theorems for Drell-Yan helicity cross sections ranging from the leading-power (LP) to the next-to-next-to-leading power (NNLP) in the soft expansion, perturbatively evaluate the relevant subleading soft functions, and perform a comparison to our expanded full-QCD results.

Contents

Chapter 1

Introduction

The main achievement of modern particle physics is the formulation of the Standard Model (SM) of fundamental interactions, which describes the electromagnetic, weak, and strong forces in a unique, renormalizable gauge theory with symmetry group $U(1) \times SU(2) \times SU(3)$. Despite its success, the SM is known to be incomplete, leaving several fundamental questions unanswered, and depends on several parameters that need to be extracted from experiments.

In this situation, it is therefore crucial to pursue the search for new physics beyond the Standard Model. High-energy particle physics experiments, such as those conducted at the Large Hadron Collider (LHC), aim to uncover phenomena that the SM cannot explain. A recent breakthrough in this direction has been the discovery of the Higgs boson [1, 2] and the determination of its properties [3], which appears to confirm the mechanism of electroweak symmetry breaking.

Whether the goal is to search for new physics or to test the SM as the fundamental theory of (almost all) fundamental interactions, if on one side we benefit from the great amount of data collected from particle colliders, on the other it is necessary to properly relate experimental verification with the theoretical predictions. In this sense, precision calculations for the strong (QCD) and electroweak (EW) sectors play a key role in determining the value of the SM couplings and masses, improve the understanding of parton distribution functions (PDFs), and enhance the overall precision of theoretical models. An important group of processes for the precision program are the ones involving the production and decay of intermediate Z/W bosons. Indeed, the production rates and properties of these bosons are sensitive to both QCD and EW corrections, making them ideal for testing the accuracy of higher-order calculations.

One of the main channels for Z/W bosons production is the Drell-Yan process [4], where the intermediate vector bosons are produced in an unpolarized proton-proton collision and decay into a lepton pair. We distinguish between neutral-current and charged-current Drell-Yan processes, respectively given by

$$pp \to Z/\gamma^* X \to \ell^+\ell^- \qquad pp \to W^+ X \to \ell^+\nu X \qquad pp \to W^- X \to \ell^-\nu X, \tag{1.1}$$

with X generic hadronic radiation in the final state. A key aspect in the study of

this process is the angular distribution of the leptons in the final states. This angular distribution is typically analyzed in the Collins-Soper frame [5], which is designed to minimize the influence of the initial state hadron motion and to facilitate the application of factorization techniques. At the Born level and at leading order in the electroweak interactions, this angular distribution can be written as

$$\frac{d\sigma}{d\cos\theta\, d\varphi} \propto (1+\cos^2\theta) + A\cos\theta, \tag{1.2}$$

with θ, φ polar and azimuthal angles, respectively, in the vector boson rest frame and A an angular coefficient. The inclusion of higher-orders QCD corrections results in a significant modification of this angular distribution, and additional terms must be included. It was shown in [6] that the general form of this distribution can be decomposed into a sum of nine real spherical harmonics, that is

$$\begin{aligned}\frac{d\sigma}{d\cos\theta\, d\varphi} \propto (1+\cos^2\theta) + \frac{A_0}{2}(1-3\cos^2\theta) + A_1\sin 2\theta\cos\varphi + \frac{A_2}{2}\sin 2\theta\cos 2\varphi + \\ A_3\sin\theta\cos\varphi + A_4\cos\theta + A_5\sin^2\theta\sin 2\varphi + A_6\sin 2\theta\sin\varphi + A_7\sin\theta\sin 2\varphi\end{aligned} \tag{1.3}$$

whose coefficients A_i depend on the lepton pair invariant mass, transverse momentum, and rapidity. In particular, because these coefficients encode all the sensitivity on the initial state QCD dynamics, their precise calculation and measurement provide critical tests of perturbative QCD and on the disentanglement of electroweak effects from QCD corrections.

This thesis is organized as follows. In chapter 2 we present the main results and techniques for treating scattering processes involving hadrons in the initial state. These include the discussion of the basic principle of Quantum Chromodynamics and of the Soft-Collinear-Effective-Theory. In chapter 3, we use the notation of [6] and [7] to relate the Drell-Yan angular coefficients to a set of production cross sections of definite helicity by decomposing the hadronic tensor into a set of Lorentz scalar structure functions. These cross-sections are then calculated at the Born level. In chapter 4 we then calculate these same cross sections in the presence of single and double real gluon emissions and study them in the soft threshold limit. In chapter 5 we rederive the LP factorization formula and derive the NNLP factorization formula. The prediction for the helicity cross sections computed in this formalism is then checked against the ones calculated in full QCD.

We conclude by discussing our results and future applications in chapter 6. Notation and conventions used in this thesis are then given in the two appendices A and B.

Chapter 2

Hadron Scattering

In this chapter, we present the principal results and mathematical formalism for treating scattering processes involving hadrons in the initial state. In section 2.1 we outline the main features of Quantum Chromodynamics (QCD), such as the QCD running coupling, the nature of infrared divergences, and factorization. In section 2.2 we instead review the Soft Collinear Effective Theory (SCET), the effective field theory describing soft and collinear degrees of freedom, and discuss its application to soft factorization theorems.

2.1 Quantum Chromodynamics

2.1.1 Degrees of freedom of QCD

Quantum Chromodynamics is the fundamental theory of strong interactions and is a gauge theory with symmetry group $SU(3)$. Its dynamical degrees of freedom are the quarks, that is the fermion fields representing the matter content of the theory, and the gluons, the massless spin 0 vector bosons mediating the interaction. Unlike electrically neutral photons, gluons carry the QCD conserved charge, the *color charge*, and can therefore couple with themselves. On the other hand, quarks, which come into three flavors organized in three generations of increasing masses, carry several quantum numbers, such as color charge, electric charge, and isospin. Because of these quantum numbers, quarks can interact through strong, electromagnetic, and weak force.

In the context of QCD, each quark flavor is represented by a three-component spinor field $q(x) = (q^1(x), q^2(x), q^3(x))^T$ -where each component is associated to one of the three colors "red", "blue", "green"- which transforms in the fundamental representation of the gauge group,

$$q^i(x) \longrightarrow \sum_{j=1}^{3} U_{ij}(x)\, q^j(x), \qquad U \in SU(N_c) \tag{2.1}$$

with $N_c = 3$ numbers of colors. Antiquarks are described by a three components row vector $\bar{q}^i(x)$ and trasform according to $\bar{q} \longrightarrow \bar{q}\, U^\dagger$, suppressing the color indices. Gauge fields instead, are Lie algebra valued 1-form, and as such can be written as $A_\mu = A^a_\mu(x)\, t_a$,

	Flavor	Q	T_3	*Mass [GeV]*
First Generation	*up (u)*	2/3	1/2	0.003
	down (d)	-1/3	-1/2	0.005
Second Generation	*charm (c)*	2/3	1/2	1.2
	strange (s)	-1/3	-1/2	0.1
Third Generation	*top (t)*	2/3	1/2	172
	bottom (b)	-1/3	-1/2	4.5

Table 2.1: Quarks quantum number, where Q denotes the charge and T_3 the isospin. Anti-quarks quantum numbers are not listed, as they have the same absolute value of the quantum numbers as their corresponding quark but with opposite signs.

where $A^a_\mu(x)$ are local differential forms, the gluon fields, transforming in the adjoint representation of $SU(N_c)$,

$$A^a_\mu(x) \longrightarrow U(x)A^a(x)U^\dagger(x) + \frac{i}{g}U(x)(\partial_\mu U^\dagger(x)), \tag{2.2}$$

where a is an internal index and runs from 1 to the dimension of the algebra (for $SU(N)$ this is N^2-1) and t_a are the generators of the color algebra in the fundamental representation. These generators are 3×3 hermitian traceless matrices defined as $t^a = \lambda_a/2$, with λ_a Gell-Mann matrices [8], and obey the following commutation relations,

$$[t_a, t_b] = if^{abc}t_c \tag{2.3}$$

with f^{abc} structure constants of the color algebra. These structure constants are real, totally anti-symmetric in all the indices, and determine the adjoint representation of the color algebra generators T^a, represented by $(N_c^2-1)\times(N_c^2-1)$ matrices defined by

$$(T^a)_{bc} = -if_{abc} \tag{2.4}$$

and which oìalso obey eq.(2.3). The normalization of these generators, in the fundamental and adjoint representation, is respectively defined by

$$\begin{aligned} \mathrm{Tr}[t_a t_b] &= T_F\,\delta_{ab} \qquad T_F = \frac{1}{2} \\ \mathrm{Tr}[T_a T_b] &= T_A\,\delta_{ab} \qquad T_A = N_c\,. \end{aligned} \tag{2.5}$$

In addition, given a representation R^a, we can define the quadratic Casimir operator $C(R) = R^a R^a$, which commutes with all the other generators in the same representation and, as such, is proportional to the identity via the Shur's lemma. For $R^a = t^a$ and $R^a = T^a$, the Casimir operator is equal to

$$\begin{aligned} t^a t^a &= C_F\, I \qquad C_F = \frac{N_c^2-1}{2N_c} \\ T^a T^a &= C_A\, I \qquad C_A = N_c\,. \end{aligned} \tag{2.6}$$

2.1.2 QCD lagrangian

We now start building the theoretical framework which describes the dynamics and the interactions of the quarks and gluon degrees of freedom. For this purpose, we need two more ingredients. The first is the covariant derivative

$$D_\mu = \partial_\mu - ig_s A^a_\mu t_a \,, \tag{2.7}$$

which is a gauge invariant operator, that is it is invariant under the transformations eq.(2.1),(2.2), that transforms covariantly under the action of an element of the color group, i.e. $Dq \to U(Dq)$. This derivative realized the matter fields-gauge fields coupling in a locally invariant manner via *minimal substitution*, and contains the term responsible for the quark-gluon vertex. The other ingredient is the field strength for the gluon fields. In geometric terms, the vector field A_μ in eq.(2.7) plays the role of a connection on the principal color bundle describing our $SU(N_c)$ gauge theory [9]. The curvature on this color bundle can thus be obtained canonically from the commutator between covariant derivatives acting on an arbitrary smooth function f, that is

$$[D_\mu, D_\nu] f(x) = -ig_s F_{\mu\nu} f(x) \,. \tag{2.8}$$

Being a Lie-algebra valued 2-form, the field strength can be expressed as $F_{\mu\nu} = F^a_{\mu\nu}(x) t_a$, where the coefficients are determined by the above commutator to be of the following form,

$$F^a_{\mu\nu} = \partial_\mu A^a_\nu - \partial_\nu A^a_\mu + ig_s f^{abc} A^b_\mu A^c_\nu \,. \tag{2.9}$$

Compared to the field strength of QED, these coefficients display a term proportional to the structure constants of the algebra. It is exactly this term that generates the vertices, i.e. the three- and four-gluons vertex, describing the self-coupling of the gauge bosons, which are indeed absent in abelian gauge theories.

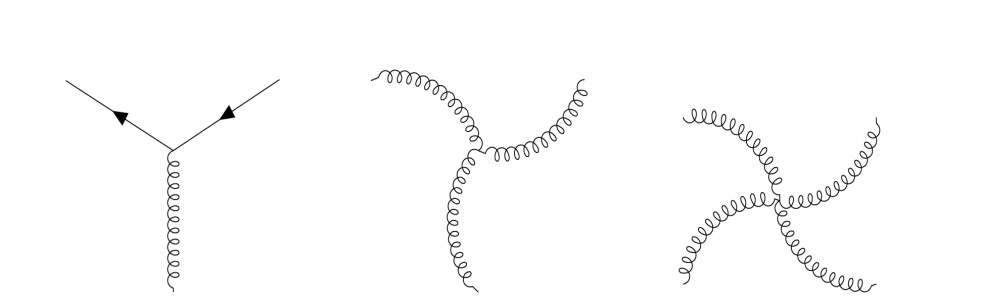

Figure 2.1: QCD vertices

The QCD Lagrangian can now be built according to a general prescription: to write down all the possible operators up to dimension four, constructed out of the degrees of

freedom of the theory and their four-derivatives, which are compatible with the given symmetries. For the strong force these symmetries are Poincarè invariance, local $SU(3)$ gauge symmetry and the discrete P and T symmetries[1]. This leaves us with with only one possible choice of operators which, including the canonical normalization for kinetic terms, leaves us with the Yang-Mills Lagrangian [10]

$$\mathcal{L}_{YM} = \sum_f \bar{q}^f(x)(i\not{D} - m_f)q^f(x) - \frac{1}{4}(F^a_{\mu\nu})^2, \tag{2.10}$$

with f labeling the flavor.

The Yang-Mills Lagrangian correctly describes the interactions of quarks and gluons in a purely classical formalism. In the quantized theory however, we must face two crucial issues due to the redundancy of degrees of freedom that local gauge symmetry brings with them. The first is how to deal with functional integrals over gauge field configurations that are not physically distinct. This overcounting of degrees of freedom does not affect calculations of gauge invariant quantities, as these are obtained through normalized partition functions, but it leads to ambiguities when computing gauge-dependent quantities obtained through generating functions, like the vector boson propagator. The second is that, unlike in QED, the amplitudes to produce timelike and longitudinally polarized gluons do not cancel out in intermediate matrix elements, thus implying that these unphysical states can be obtained with a non-zero probability. Both these problems can be simultaneously addressed through the *Faddeev-Popov method* [11]. This method consists of plugging in the path integral for the gluon propagator a delta function of the form $\delta(G(A))$, where $G(A)$ is the gauge condition, to restrict the integration domain to only physically distinct field configurations. The outcome is the appearance of an additional term in the action which, in the Feynman gauge, is of the form

$$\mathcal{L}_{g.f.} = -\frac{1}{2\xi}(\partial^\mu A^a_\mu) \tag{2.11}$$

and where ξ is a continuous parameter. In principle, there are many possible choices of gauges one can make, but from now on we will always work in the Feynman gauge as it has the advantage of preserving Lorentz symmetry. If we then include eq.(2.11) into the Lagrangian eq.(2.10), we get that the inverse gluon propagator is a non-singular matrix, which can therefore be inverted thus yielding to

$$a, \mu \xrightarrow{\quad k \quad} b, \nu \quad = \quad \frac{-i\delta^{ab}}{k^2 + i\varepsilon}\left(g_{\mu\nu} - (1-\xi)\frac{k_\mu k_\nu}{k^2}\right). \tag{2.12}$$

In practical calculations, the gauge parameter ξ is always set equal to a finite constant, which we choose to be $\xi = 1$ (the *Feynman-'t Hooft gauge*). If we were dealing with Abelian gauge theories, this would be the end of the story. In the nonabelian case

[1] QCD also displays an additional number of flavor symmetries with symmetry group $SU_L(N_f) \times SU_R(N_f) \times U_B(1) \times U_A(1)$, but since these are not relevant for studying the properties of quarks and gluons, they won't be taken into account.

however, the determinant of the Jacobian factor which accompanies the delta function of the Faddeev-Popov method depends on the gluon field, and therefore cannot be brought out of the path integral. A way out, is to express this determinant as a functional integral over anticommuting Grassmann fields, and this comes at the expense of supplementing the lagrangian with the term

$$\mathcal{L}_{gh} = -\bar{\eta}^a \left(\partial^2 \delta^{ac} + g \partial^\mu f^{abc} A^b_\mu \right) \eta^c \, . \tag{2.13}$$

Ghost η and anti-ghost $\bar{\eta}$ fields are fermionic fields in the adjoint representation of the gauge group. Hence, they cannot be associated with physical propagating particles, but they couple with the gauge fields. It can be shown that the contribution of diagrams containing ghost fields exactly compensates, to all orders in perturbation theory, with the one of diagrams involving unphysical polarized gluons, so that only transversely polarized gluons have to correctly be considered in computing S-matrix elements for scattering amplitudes.

The proof of this statement makes use of the Slavnov-Taylor [12, 13] identities, i.e. non-abelian generalization of the Ward-Takashi identities for QED, which in turn follow from a residual global symmetry displayed by the lagrangian

$$\mathcal{L}_{QCD} = \mathcal{L}_{YM} + \mathcal{L}_{gh} + \mathcal{L}_{g.f.}, \tag{2.14}$$

the BRST symmetry [14, 15]. This (super-)symmetry is furthermore crucial for establishing the renormalizability of non-abelian gauge theories, as it can be shown that the N-loops effective action has the same form as the tree-level action with renormalized parameters. Thus, in QCD, all the UV-divergences arising from loop diagrams can be absorbed in the bare parameters at the level of the lagrangian by a finite number of counterterms, while sub-divergences of many-loops graphs are canceled order by order in powers of the renormalized coupling.

The freedom we have in incorporating in the counterterms any finite part coming from divergent loop integrals is what determines the renormalization scheme. In this thesis, we adopt the *minimal subtraction* ($\overline{\text{MS}}$) scheme [16], in which the bare strong coupling is related to the renormalized coupling by

$$\frac{g_s^2(\varepsilon)}{4\pi} = \mu^{2\varepsilon} \alpha_s(\mu) Z_{\alpha_s}(\mu, \varepsilon) \, . \tag{2.15}$$

Here, the symbol μ denotes the renormalization scale and it is introduced by the regulator, which we take here as *dimensional regularization* [17] in $d = 4 - 2\varepsilon$ dimensions, to adjust the mass dimension of the action. The counterterm Z_{α_s} is instead defined as

$$Z_{\alpha_s}(\mu, \varepsilon) = \frac{e^{\varepsilon \gamma_E}}{(4\pi)^\varepsilon} \left[1 + \frac{\alpha_s(\mu)}{4\pi} \left(- \frac{\beta_0}{\varepsilon} \right) + \mathcal{O}(\alpha_s^2) \right]. \tag{2.16}$$

The coefficient involving the Eulero-Macheroni constant γ_E can be defined in several ways within the $\overline{\text{MS}}$ scheme, which are all equivalent in the limit $\varepsilon \to 0$; here we adopt the same

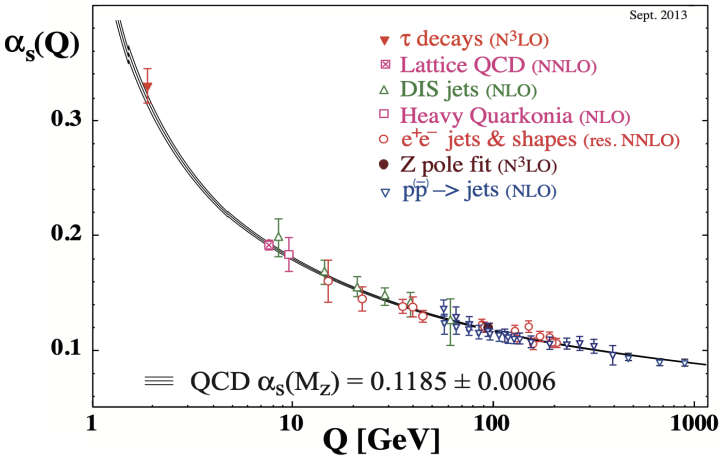

Figure 2.2: Dependence of the strong running coupling $\alpha_s(\mu)$ on the energy scale in GeV. Data from [19]

convention as in [18]. Unlike the renormalized coupling, which is a measurable parameter characterizing the strength of the interaction, the bare coupling is not a physical quantity and therefore it does not depend on the energy scale. Accordingly, the derivative of eq.(2.15) with respect to μ must vanish, thus determining

$$\begin{aligned}\beta(\mu,\varepsilon) = \mu\frac{d\alpha_s(\mu)}{d\mu} &= -2\varepsilon\alpha_s(\mu) - \mu\frac{d}{d\mu}\ln Z_{\alpha_s}(\mu,\varepsilon) \\ &= -2\varepsilon\alpha_s(\mu) - 2\alpha_s(\mu)\sum_{n=0}^{\infty}\beta_n\left(\frac{\alpha_s(\mu)}{4\pi}\right)^{n+1}\end{aligned} \tag{2.17}$$

This equation is the QCD beta function [20, 21] and its solution determines the explicit dependence of the running coupling α_s on the energy scale μ. If we set $\varepsilon = 0$, that is in four spacetime dimensions, the beta function corresponds to an expansion in powers of the coupling constant, whose coefficients β_n can be calculated from a set of elementary Green's functions, at present known up to five-loops [22, 23, 24]. Truncating the series at $n = 1$, we get the one-loop beta function

$$\beta^{1-\text{loop}}(\mu) = \mu\frac{d\alpha_s(\mu)}{d\mu} = -2\beta_0\frac{\alpha_s(\mu)^2}{4\pi}, \tag{2.18}$$

where the one-loop coefficient β_0 is given by

$$\beta_0 = \frac{11}{3}C_A - \frac{4}{3}T_F\, n_f, \tag{2.19}$$

and it is positive (for $n_f < 17$). Accordingly, the QCD beta function is negative, which means that the strength of the strong coupling α_s decreases as the energy scale μ increases.

This behavior, which persists also at higher orders, is characteristic of non-abelian gauge theories and is due to the fact that the contribution to the vacuum polarization from gauge boson self-interactions, which tends to make the coupling weaker at high energies, dominates over the contributions from fermions and scalars, which tend to screen the coupling. Indeed, the solution of eq.(2.18),

$$\alpha_s(\mu) = \frac{\alpha_s(\mu_0)}{1 + \alpha_s(\mu_0)\frac{\beta_0}{2\pi}\ln(\mu/\mu_0)} \tag{2.20}$$

displays a UV fixed point at zero coupling, where μ_0 is some initial reference energy scale, conventionally taken as the Z boson mass, at which $\alpha_s(M_Z) \simeq 0.1181$ [25]. Theories whose coupling becomes weaker at high energies are called *asymptotically free* [26, 27] and in the case of QCD this implies that, at sufficiently high energy scales, quarks and gluons behave as free, non interacting particles. On the other hand, as the energy scale decreases, the coupling constant becomes so large that it cannot be used as an expansion parameter anymore. The scale at which the coupling becomes strong is usually taken as the scale at which the coupling becomes infinite, that is

$$\Lambda_{\rm QCD}^{\rm 1-loop} = \mu_0 \exp\left[-\frac{2\pi}{\alpha_s(\mu_0)\beta_0} \right] \approx 200\,\text{MeV}\,. \tag{2.21}$$

Perturbation theory is thus valid only at physical scales $Q \sim \mu \lesssim 1$GeV, below which quarks and gluons are bounded together into color-singlet states, mesons (quark-antiquark pair) and baryons (three-quarks bound state), collectively referred to as hadrons. The fact that hadrons are color neutral is a phenomenon called *(color) confinement* [28] and indeed prevents colored particles, such colored hadrons, quarks and gluons, from being realized as physical observed states. Hence, in QCD, the asymptotic degrees of freedom are different from the degrees of freedom that initiate the scattering process. Because of this dichotomy, the description of the long-distance behavior of the theory requires particular care, as we will see in the next section.

2.1.3 Infrared Divergences

So far, we have only talked about UV divergences, which arise in loop diagrams and are induced by unconstrained momenta picking arbitrarily high values. QFTs of massless particles however also display another kind of divergences, namely the ones characterizing the long-distance behavior of the theory. These infrared divergences can appear both in loop diagrams and phase space integrals and are caused by external states being degenerate. As these degeneracies cannot be treated in perturbation theory, we cannot simply reabsorb these singularities at the level of the lagrangian, as previously done for their high-energy counterparts, but we have to come up with a different strategy. In general, the solution involves summing over a sufficiently large set of states, but how this sum is performed crucially depends on whether we are dealing with a process involving **initial state** or **final state radiation**. In this section we will focus on the first situation and see, applying it to the process $e^+e^- \to$ hadrons, how and to which extent it leads to

IR finite quantities. A discussion on the second case will instead be carried out in the next section.

The electron-positron annihilation and subsequent decay into a quark-antiquark pair can be mediated by any charge and color-neutral vector boson, i.e. either by a virtual photon γ^* or a Z boson. Assuming the center of mass energy of the process to be much lower than the production of the Z boson, we thus only consider

$$e^+e^- \longrightarrow \gamma^* \longrightarrow q\bar{q} \tag{2.22}$$

where, long after the collision, the $q\bar{q}$ pair then hadronize into singlet-coloured particles. At leading order in the electromagnetic coupling and in the center of mass frame of the virtual photon, the cross-section can be computed using

$$\sigma = \frac{1}{2E_{cm}^2} \int \sum_{c,s,p} |\mathcal{M}|^2 \, d\Phi \tag{2.23}$$

with E_{cm}^2 the center of mass energy, $d\Phi$ the final state phase space, and where the square matrix-element for the production and decay of the intermediate vector boson is averaged over spin, color, and polarization indices. Notice that the cross-section of eq.(2.23) is an example of **inclusive** observable, namely it is obtained by summing over every possible final state. At leading order in the strong coupling, and leaving the sum over quark species implicit for simplicity, the cross-section is equal to

$$\sigma_0 = \frac{N_c(e^2Q_q^2)}{4\pi E_{cm}^2} \left(\frac{4\pi\mu^2}{E_{cm}^2}\right)^{\varepsilon} \frac{(1-\varepsilon)^2}{(3-2\varepsilon)} \frac{\Gamma(1-\varepsilon)}{\Gamma(2-2\varepsilon)} \tag{2.24}$$

and is indeed finite in the limit $\varepsilon \to 0$. If we want to extract accurate predictions from the process eq.(2.22) however, we have to go beyond tree level and compute higher terms in the perturbative expansion. The NLO cross section receives contributions from all the **real emission** diagrams, which feature real on-shell radiation, and the diagrams including virtual corrections at first order in α_s. Both these contributions are displayed in Fig.2.3. Starting from the real emission case, if we insert the matrix element for the emission of a gluon from either quark and the anti-quark in eq.(2.23), we get the following cross-section

$$\sigma_R = \sigma_0 \, \frac{\alpha_s C_F}{2\pi} \left(\frac{4\pi\mu^2}{E_{cm}^2}\right)^{\varepsilon} \frac{\Gamma(1-\varepsilon)}{\Gamma(1-2\varepsilon)} \left[\frac{2}{\varepsilon^2} + \frac{3}{\varepsilon} + \frac{19}{2} - \frac{2\pi^2}{3} + \mathcal{O}(\varepsilon)\right]. \tag{2.25}$$

This expression is not finite in four spacetime dimensions as it contains divergences, which show up as single and double poles in ε. To see where these singularities come from, we notice that the amplitude for the one gluon bremsstrahlung contains the quark and the antiquark propagator, which are proportional to

$$\begin{aligned} (p_1 - k)^{-2} &= Q^2(1-x_1)^{-1} \\ (p_2 - k)^{-2} &= Q^2(1-x_2)^{-1} \, . \end{aligned} \tag{2.26}$$

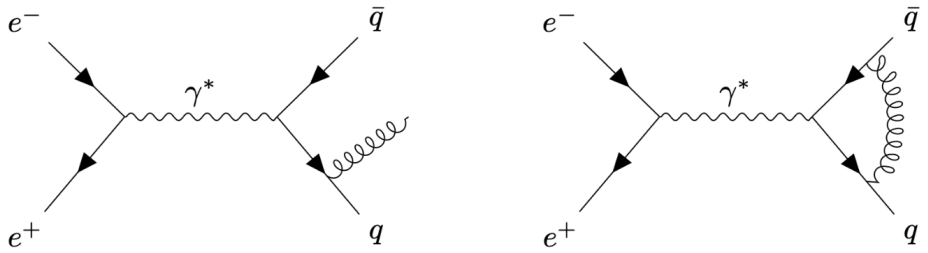

Figure 2.3: On the right, is the real emission diagram, where the gluon is emitted from the anti-quark. There is another real graph, where the gluon is emitted from the quark, which has not been reported. On the left, the virtual corrections feature the vertex correction.

In the *rhs* of this expression we have introduced the variables $x_i = 2p_i^0/Q$, with $i = 1, 2$, p_1, p_2 momenta of the quark and antiquark respectively, while we will label $x_3 = 2k^0/Q$, with k momentum of the emitted gluon. These variables represent the fraction of the total center of mass energy carried by the quarks and the gluon and satisfy $x_1 + x_2 + x_3 = 2$. The amplitude is singular in the limit $x_1 \to 1$ or $x_2 \to 1$, that is when all the energy available is retained either from the quark or from the antiquark. This is equivalent to stating that the propagators go on-shell, that is

$$(p_i - k)^{-2} \sim E_g(1 - \cos\theta_{k,p_i}) = 0, \qquad i = 1, 2 \tag{2.27}$$

with θ_k angle between the quark/antiquark and the emitted gluon. Eq.(2.27) is satisfied if $E_g \sim 0$, in which case we talk about **soft singularity** or if $\cos\theta_{k,p_1} = \cos\theta_{k,p_2} = 1$, which we call **collinear singularities**. The cross-section eq.(2.25) is therefore divergent because the final state is degenerate, indeed a configuration with a $q\bar{q}$ pair and a $q\bar{q}$ pair accompanied by (any amount of) soft and collinear gluons are indistinguishable from each other. A more thorough characterization of IR singularities involves Landau equations and pinch surfaces and can be found in [29, 30, 31].

However, we are not yet done, as we still have to calculate the contribution to the cross-section arising from the virtual diagram. A direct calculation shows that this is equal to

$$\sigma_V = \sigma_0 \frac{\alpha_s C_F}{2\pi} \left(\frac{4\pi\mu^2}{E_{cm}^2}\right)^{\varepsilon} \frac{\Gamma(1-\varepsilon)}{\Gamma(1-2\varepsilon)} \left[-\frac{2}{\varepsilon^2} - \frac{3}{\varepsilon} - 8 + \frac{2\pi^2}{3} + \mathcal{O}(\varepsilon) \right]. \tag{2.28}$$

Remarkably, even though the real and virtual cross-sections are individually singular, their divergent part cancels out when they are added together, thus making the NLO cross-section infrared finite.

For observables like the inclusive cross section, this cancellation between collinear and soft divergences can be proved to hold at all orders in perturbation theory. This property

is guaranteed by the Kinoshita-Lee-Nauenberg (KLN) theorem [32, 33], which states that any unitary theory is infrared finite if all the possible initial and finite states defined in a finite energy interval are summed over. Nonetheless, there are also some major observables for which this theorem does not apply. One of the most notable examples is the cross-section of a scattering process involving hadrons in the initial state. The reason why KLN theorem does not hold in this case is that, even though hadrons are the colliding particles, only their components, that is quarks and gluons, effectively participate in the interaction. At the same time, quarks and gluons do not exist as asymptotic states with definite energy and momentum, and the way they form into hadrons is non-perturbative. To compute such observables, we therefore rely on a property of the parton model known as factorization.

2.1.4 Factorization for hadron-hadron collision

Factorization refers to a universal procedure that consists of separating (more specifically, convoluting) long-distance non-perturbative effects from short-distance physics when calculating hadronic cross-sections. So far, factorization theorems have only been proven for a couple of inclusive processes, such as deep inelastic scattering, single particle inclusive annihilation, and Drell-Yan processes, provided all kinematics invariants are large and comparable with each other [34, 35].

We consider here a generic scattering process with two colliding hadrons A, B that produce a final state X with invariant mass

$$Q^2 = q^\mu q_\mu \,, \tag{2.29}$$

which sets the characteristic energy scale of the process, with q^μ the momentum of the intermediate vector boson. In the framework of the parton model [36], protons, like all the other hadrons, are described as bound states of constituents called *partons*. In fact, a parton can be either a quark or a gluon. In high energy scattering, where the momentum transfer is large, asymptotic freedom tells us that the protons' constituents behave as free particles and, since they do not exchange momenta, each of them can be thought as carrying a certain longitudinal[2] fraction x of the total hadron momentum, with $0 < x < 1$. If the density of the partons inside the proton is not too high, we can beside consider with a good approximation that only one parton from each proton participates in the interaction, with the other ones just passing through. We label the momentum fractions of the **interacting** partons a, b as

$$p_a^\mu = x_a P_a^\mu \qquad\qquad p_b^\mu = x_b P_b^\mu \,. \tag{2.30}$$

with P_a and P_b the hadrons A and B momenta respectively. On the other hand, in a suitable reference frame, such as the center of mass frame, the hadrons are moving at a relativistic speed, and therefore their length is contracted in the direction of the collision and their internal interactions are time-dilatated. In this frame, the characteristic time

[2]We assume that the hadrons carry zero or negligible transverse momentum before the collision.

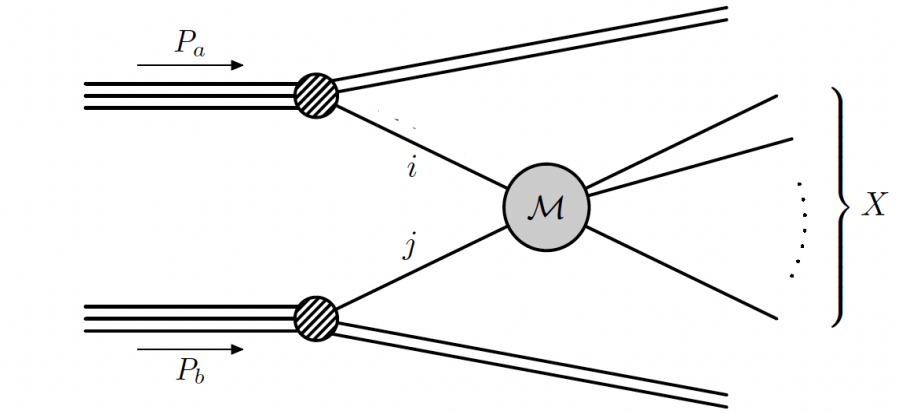

Figure 2.4: Diagram representing the collision $A(p_a) + B(P_b)$, where the extracted parton a, b interact to produce a final state X. Picture adapted from the reference [37].

scale of the annihilation process is much shorter than the time scale for the formation of any partonic intermediate state. Also, the interactions between the remaining partons occur too long after the annihilation to affect it. Because long-distance and short-distance physics do not influence each other, we can express the hadronic cross-section in terms of probabilities instead of amplitudes and write it as a series in powers of Λ_{QCD}/Q whose leading term is

$$d\sigma_{AB\to X} = \sum_{i,j} \int_{x_a}^{1} d\xi_a \int_{x_b}^{1} d\xi_b \, f_{i/A}(\xi_a) f_{j/B}(\xi_b) \, d\hat{\sigma}_{ij\to X}\left(\frac{x_a}{\xi_a}, \frac{x_b}{\xi_b}\right). \tag{2.31}$$

This expression is known as the *factorization formula* and is valid in the approximation that the hard scattering scale Q is much greater than the non-perturbative scale Λ_{QCD}. Here, the non-perturbative physics is encoded in the parton distribution functions (PDFs) $f_{i/H}(\xi)$, corresponding to the probability density to find a parton i inside the hadron H carrying a fraction between ξ and $\xi + d\xi$ of the total hadron momentum. Since these distributions describe the internal structure of the hadron, they are universal, in the sense that they only depend on the type of parton inside the hadron but not on the specific scattering process and, being non-perturbative objects, they have to be determined from experiments [38, 39] or from lattice QCD calculations [40]. The term $d\hat{\sigma}_{ab\to X}$ represents instead the partonic cross section for the process $(i + j \to X)$, that is

$$d\hat{\sigma}_{ij\to X} = \frac{1}{2s} \langle |\mathcal{M}_{i+j\to X}|^2 \rangle d\Phi \tag{2.32}$$

with $d\Phi$ Lorentz invariant phase space and $\langle |\mathcal{M}_{i+j\to X}|^2 \rangle$ matrix element averaged over all relevant internal and external indices, including spin and color. In particular, $d\hat{\sigma}_{ij\to X}$ is calculable in perturbation theory and UV finite because divergences from loop diagrams can be removed through the renormalization procedure. However, this is not true for

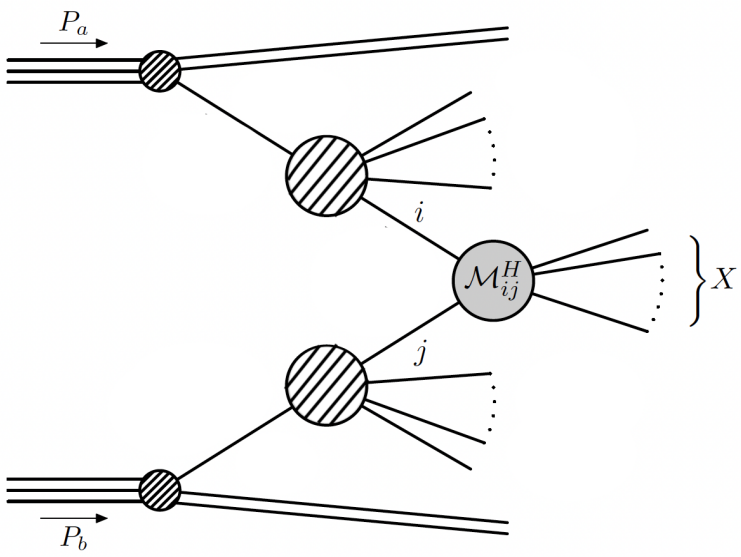

Figure 2.5: Factorization in presence of radiative emissions. Picture adapted from the one of reference [37].

IR divergences, and this cross section will indeed generally display uncancelled collinear divergences.

To describe where these IR divergences originate from, we refer to Fig.2.5. There, the two **extracted** parton a, b with momenta

$$p_a^\mu = \xi_a P_a^\mu \qquad p_b^\mu = \xi_b P_b^\mu \tag{2.33}$$

undergo a collinear splitting splitting, that is they emit a daughter partons i, j which then interact and produce the final state X. Being $\xi_{a,b}$ the total momentum fractions of the partons within the hadron and $x_{a,b}$ the momentum fractions of the interacting partons, we can define the variables

$$z_a = \frac{q_a}{p_a} = \frac{x_a}{\xi_a} \qquad z_b = \frac{q_b}{p_b} = \frac{x_b}{\xi_b}, \tag{2.34}$$

with z_a, $z_b \in [0,1]$ representing the total fraction of the parton momenta p_a and p_b that participate in the interaction after the collinear emission. Because the splitting happens at longer time scales than the hard scattering collision, we can write the partonic cross section as a convolution in turn, i.e.

$$d\hat{\sigma}_{ij\to X} = \sum_{i,j} \int dz_a \int dz_b \, \Gamma_{ik}(z_a) \, d\hat{\sigma}^H_{kl\to X}(z_a, z_b) \, \Gamma_{lj}(z_b) \, . \tag{2.35}$$

In this formula, $d\hat{\sigma}^H_{ij\to X}$ denotes the cross-section relative to the hard scattering process, while $\Gamma_{ij}(z)$ are called transition functions, and describe the probability that the parent

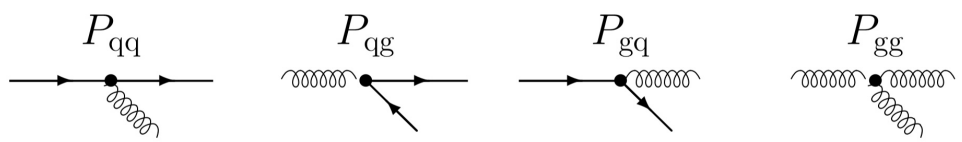

Figure 2.6: Leading order Altarelli-Parisi splitting functions. Picture taken from [41]

parton j emits the daughter parton i with a fraction z of its momentum. While the hard scattering cross section is ultraviolet dominated (and therefore admits an expansion in powers of α_s) and infrared free, the transition functions are the objects containing the IR divergences. Indeed, expanding these functions in powers of α_s, one has that

$$\Gamma_{ij}(z) = \Gamma_{ij}^{(0)}(z) + \left(\frac{\alpha_s}{4\pi}\right)\Gamma_{ij}^{(1)}(z) + \mathcal{O}(\alpha_s^2)\,, \tag{2.36}$$

where n indicates the number of collinear splittings and whose coefficient, up to NLO in the $\overline{\mathrm{MS}}$ scheme, contains collinear divergences which manifest themselves as $1/\varepsilon$ poles,

$$\begin{aligned}\Gamma_{ij}^{(0)}(z) &= \delta_{ij}\,\delta(1-z)\\ \Gamma_{ij}^{(1)}(z) &= \left[-\frac{1}{\varepsilon} - \ln\left(\frac{\mu^2}{Q^2}\right)\right] P_{ij}^{(0)}(z)\,.\end{aligned} \tag{2.37}$$

The functions $P_{ij}(z)$ in the NLO coefficient are the Altarelli-Parisi splitting functions (or DGLAP kernels) and are computable in perturbation theory, with $P_{ij}^{(0)}(z)$ indicating the leading term in their power expansion. Since $i, j = q, g$, there are in total four possible splitting functions, which are displayed in Fig. 2.6 and whose explicit expression depends on the specific parent and daughter parton i, j. If we now expand $d\hat{\sigma}$ and $d\hat{\sigma}^H$ up to first order in α_s and use eq.(2.36), (2.37), the partonic cross section eq.(2.35) reads

$$\begin{aligned}d\hat{\sigma}_{ij\to X}^{(0)} + \left(\frac{\alpha_s}{4\pi}\right) d\hat{\sigma}_{ij\to X}^{(1)} = d\hat{\sigma}_{ij\to X}^{H,(0)} + \left(\frac{\alpha_s}{4\pi}\right)\Bigg\{ d\hat{\sigma}_{ij\to X}^{H,(1)} + \left[-\frac{1}{\varepsilon} - \ln\left(\frac{\mu^2}{Q^2}\right)\right]\\ \times\Bigg[\sum_k \int dz_a\, P_{ik}^{(0)}(z_a)\, d\hat{\sigma}_{kj\to X}^{H,(0)}(z_a, z_b)\\ + \sum_l \int dz_b\, d\hat{\sigma}_{il\to X}^{H,(0)}(z_a, z_b)\, P_{lj}^{(0)}(z_a)\Bigg]\Bigg\}\end{aligned} \tag{2.38}$$

up to corrections $\mathcal{O}(\alpha_s^2)$. Even though the partonic cross section is not finite, by convoluting it with the parton distribution functions one can eventually obtain a finite hadronic cross section by reabsorbing the $1/\varepsilon$ pole into the PDFs. These functions can indeed be defined by hadron matrix elements of operators acting on hadronic states and counting the number of partons carrying a fraction ξ of the hadron's momentum [42].

When treated in dimensional regularization, they exhibit both UV and IR divergences, which cancel in dimensional regularization. The UV divergences can be absorbed into the definition of the PDF, and therefore have to be treated via renormalization and acquire a dependence on the unit mass μ_R. The dependence of the PDFs on the energy scale μ_R is given by the famous DGLAP (Dokshitzer-Gribov-Lipatov-Altarelli-Parisi) equations [43, 44, 45], describing how the PDF evolve with changes in the energy scale accounting for the emission and absorption of partons. The IR divergence instead, which is not removed by renormalization, can be incorporated into the PDF by defining the *renormalized* PDF,

$$f_i^{\text{ren}}(\xi,\mu) = f_i(\xi) - \frac{1}{\varepsilon}\left(\frac{\alpha_s}{4\pi}\right)\sum_h \int_0^1 \frac{dz}{z}\, f_i\left(\frac{x}{z}\right) P_{ih}^{(0)}(z)\,. \tag{2.39}$$

In this way, and after the renormalization procedure, we obtain that the hadronic cross section is indeed finite. Especially, since the PDFs depend on the specific parton but not on the hadron, one can consider the hadronic cross section eq.(2.31) and write it for colliding partons instead of for colliding hadrons. Expanding the hadronic cross section in powers of α_s, and matching all the terms of its expansion with their respective convolution of renormalized PDFs and partonic cross section, the hadronic cross section is found to be equal to

$$d\sigma_{AB\to X} = \sum_{i,j}\int_{x_a}^1 d\xi_a \int_{x_b}^1 d\xi_b\, f_{i/A}^{\text{ren}}(\xi_a,\mu) f_{j/B}^{\text{ren}}(\xi_b,\mu)\, d\hat{\sigma}_{ij\to X}\left(\frac{x_a}{\xi_a},\frac{x_b}{\xi_b},Q^2,\mu\right), \tag{2.40}$$

with the partonic cross section given by

$$\begin{aligned} d\hat{\sigma}_{ij\to X}(z_a,z_b,Q^2,\mu) = {} & d\hat{\sigma}_{ij\to X}^{H,(0)}(z_a,z_b,Q^2) + \left(\frac{\alpha_s}{4\pi}\right) d\hat{\sigma}_{ij\to X}^{H,(1)}(z_a,z_b,Q^2) \\ & + \left(\frac{\alpha_s}{4\pi}\right)\ln\left(\frac{\mu^2}{Q^2}\right)\sum_k \int dz_a\, P_{ik}^{(0)}(z_a)\, d\hat{\sigma}_{kj\to X}^{H,(0)}(z_a,z_b) \\ & + \left(\frac{\alpha_s}{4\pi}\right)\ln\left(\frac{\mu^2}{Q^2}\right)\sum_l \int dz_b\, d\hat{\sigma}_{il\to X}^{H,(0)}(z_a,z_b)\, P_{lj}^{(0)}(z_a)\Bigg]. \end{aligned} \tag{2.41}$$

Hence, factorization exploits the separation of scales, the non-perturbative one encoded in the parton distribution functions, and the hard scale encoded in the partonic cross-section, to find a finite expression for the hadronic cross-section. Nonetheless, as clear from the cross-section of eq.(2.41), the presence of radiative emissions implies the existence of multiple energy scales. Indeed, only the hard scattering cross section $\hat{\sigma}_{ij}^H \sim Q^2$, while collinear and soft modes have an infrared origin, and therefore happen at scales $<< Q^2$. The natural implementation of the description of physical processes involving multiple energy scales is given by effective field theories, which are discussed in the next section.

2.2 Factorization in the Soft Collinear Effective Theory

2.2.1 What is an EFT?

An effective field theory (EFT) is a quantum field theory that describes physics at some energy scale Λ_l while systematically incorporating the effects of higher energy scales $\sim \Lambda_h$. This separation of scales is achieved by an expansion in powers of Λ_l/Λ_h, which is ensured to be small provided the low energy Λ_l and the high energy scale Λ_h satisfy $\Lambda_l << \Lambda_h$. In this way, physical quantities can be calculated up to a finite order in the power expansion, which can be chosen to be as small as desired, thus enabling one to adjust the accuracy of the theoretical prediction. Generally, the low energy scale is taken to be the one of a typical momentum scale p, while the hard scale corresponds to the hard scattering scale Q.

Being a QFT in all regards, an EFT admits its lagrangian, as well as renormalization and regularization schemes [46]. However, unlike normal QFTs, the effective lagrangian can include operators of dimension greater than d, which are however suppressed by powers of the high energy scale Q, that is

$$\mathcal{L}_{\text{EFT}} = \mathcal{L}_{\mathcal{D}\leq d} + \frac{\mathcal{L}_{d+1}}{Q} + \frac{\mathcal{L}_{d+2}}{Q^2} + \dots . \tag{2.42}$$

where every term of this sum can be written as

$$\mathcal{L}_{\mathcal{D}} = \sum_i c_i \mathcal{O}^i_{\mathcal{D}} \, . \tag{2.43}$$

The dimension $\mathcal{D}$ of the operators $\mathcal{O}_i$ depends on the power counting parameter of the EFT, while c_i are the coefficients of the effective lagrangian, which are determined by the underlying high energy theory and incapsulate the effects of high-energy degrees of freedom. According to the method used in the construction of the EFT, these coefficients can be either determined experimentally or derived analytically. In particular, we distinguish between:

- **top-down EFT:** A top-down EFT is the low energy limit of a known high-energy theory. Notable examples are the Fermi Theory of Weak Interactions [47], which is a low energy theory of the SM, where the masses of the W, Z boson have been integrated out, and the HQET (Heavy Quark Effective Theory) [48, 49, 50], derived from QCD. Because the full theory is known, the coefficients c_i are determined by comparing a set of Green functions in the EFT and the full theory, known as the matching procedure.

- **bottom-up EFT:** In the bottom-up approach, the high energy theory is not known. Therefore, an effective lagrangian is constructed by including higher-dimensional operators consistent with the symmetries of the theory and the coefficients c_i are treated as free parameters that are constrained by experimental data. Examples of this approach are the chiral perturbation theory (χPT) [51, 52] used to describe low-energy QCD interactions among pions, and the Standard Model Effective Field Theory (SMEFT) [53].

In this section, we review SCET [54, 55, 56, 57, 58, 59], which is a top-down effective theory describing QCD in the infrared. Unlike in the HQEF, where high momentum modes of heavy quarks are integrated out, in SCET we do not integrate out entire degrees of freedom, but only off-shell modes. In this way, this effective theory can describe multiple momentum regions, such as soft, ultrasoft, and various collinear modes. For this reason, it can be used to describe a wide range of physical processes, such as hard scattering inclusive processes, jet production, and beta decays, and has multiple applications, such as the resummation of Sudakov logarithms and factorization theorems. In this thesis, SCET will be used to formulate soft factorization theorems for pp collisions. Our discussion follows mainly reference [60] with some integrations from references [61] and [18]. The power expansion will be performed in position space, as done in ref.[60], unlike in the more usual label momentum formalism.

2.2.2 SCET degrees of freedom

SCET describes the dynamics and interactions of soft and collinear degrees of freedom in the presence of a hard interaction. Particles involved in these kinds of processes carry energies much larger than their masses and therefore are better described in terms of lightcone coordinates. A basis for these coordinates is constructed by picking a lightlike vector $n^\mu = (1, \vec{n})$ which describes the direction of motion of one of the colliding particles, and another auxiliary vector $\bar{n} = (1, -\vec{n})$, satisfying $n^2 = \bar{n}^2 = 0$, $n \cdot \bar{n} = 2$. A common choice for this basis is

$$n^\mu = (1, 0, 0, 1) \qquad \bar{n}^\mu = (1, 0, 0, -1)\,. \tag{2.44}$$

In this way, every four vector p can be decomposed into a collinear component, proportional to n^μ, an anti-collinear one, proportional to $\bar{n}^\mu$ and a transverse component orthogonal to both as

$$p^\mu = (\bar{n} \cdot p)\frac{n^\mu}{2} + (n \cdot p)\frac{\bar{n}^\mu}{2} + p_\perp^\mu\,. \tag{2.45}$$

with $\vec{p}_\perp = (0, p^1, p^2, 0)$. In general, we will represent four momenta in terms of their components by writing $p^\mu = (p^+, p^-, \vec{p}_\perp)$, where $p^+ = (\bar{n} \cdot p)$ and $p^- = (n \cdot p)$. In this notation, and using the properties of the vectors eq.(2.44), we can easily derive the following product rules

$$p \cdot q = \frac{1}{2}(p_- q_+ + p_+ q_-) - \vec{p}_\perp \cdot \vec{q}_\perp \qquad p^2 = p^+ p^- - \vec{p}_\perp^{\,2} \tag{2.46}$$

using the standard euclidean metric, while in Minkowski metric $p_\perp^2 = -\vec{p}_\perp^{\,2}$. In addition, we can also decompose the metric and the gamma matrices in lightcone coordinates, which are equal to

$$g^{\mu\nu} = \frac{n^\mu \bar{n}^\nu}{2} + \frac{\bar{n}^\mu n^\nu}{2} + g_\perp^{\mu\nu} \qquad \gamma^\mu = \not{n}\frac{n^\mu}{2} + \not{\bar{n}}\frac{\bar{n}^\mu}{2} + \gamma_\perp^\mu\,. \tag{2.47}$$

Lightcone coordinates can now be used for describing the infrared degrees of freedom of SCET, which include collinear and soft particles. For example, considering the collision between two protons of momenta P_a and P_b in the center of mass frame, these can be parametrized as $P_a^\mu = (0, P_a^-, 0, 0)$ and $P_b^\mu = (P_b^+, 0, 0, 0)$, assuming the proton of momentum P_a moves in the direction n^μ and the proton of momenta P_b in direction $\bar{n}^\mu$. Hence, since for n-collinear particles the dominant component is the minus component, we have that $p^- \gg |\vec{p}_\perp| \gg p^+$ satisfying $p^+ p^- \sim p_\perp^2$, so that n-collinear modes have scaling

$$p_n \sim (\lambda^2, 1, \lambda)\, Q \tag{2.48}$$

in terms of the power counting parameter $\lambda \ll 1$. The same argument holds the other way around for anti-collinear modes, which satisfy $p^+ \gg |\vec{p}_\perp| \gg p^-$ and therefore

$$p_{\bar{n}} \sim (1, \lambda^2, \lambda)\, Q\,. \tag{2.49}$$

The precise definition of the power counting parameter λ is not unique and depends on the process under consideration. For examples, assuming p_n and $p_{\bar{n}}$ are the modes inside the colliding protons, we have $\lambda = \Lambda_{\rm QCD}/Q$. On the other hand, unlike collinear modes, soft modes have no preferential direction and therefore scale homogeneously in λ. We call *soft modes* the ones with scaling

$$p_s \sim (\lambda, \lambda, \lambda)\, Q\,. \tag{2.50}$$

Note that soft modes have the same virtuality as collinear modes, that is $p_s^2 \sim p_n^2 \sim \lambda^2 Q^2$ and are both consistent with the fact that SCET degrees of freedom describe off-shell fluctuations with $p^2 \ll Q^2$. However, since the plus and minus components of soft momenta are larger than the corresponding n and $\bar{n}$ collinear ones, interactions between soft and collinear modes must be integrated out and incorporated into the matching coefficient. In addition, the condition that SCET modes satisfy $p^2 \lesssim Q^2$ allows the presence of *ultrasoft modes*

$$p_{us} \sim (\lambda^2, \lambda^2, \lambda^2)\, Q \tag{2.51}$$

and, unlike soft modes, their interactions with collinear modes are indeed included in the effective lagrangian.

According to the specific process and observables under consideration, the relevant modes of the effective theory can be either the collinear and ultrasoft ones or the collinear and soft ones. These effective theories are known respectively as SCET_I and SCET_II, whose relevant modes are displayed in Fig. 2.7. In particular, because the perpendicular component of soft and collinear modes has the same virtuality (while for ultrasoft modes this component is always power suppressed) SCET_II is used for studying processes involving transverse momentum dependent observables.

2.2.3 SCET Lagrangian

Because in SCET the hard interaction is disentangled from the infrared dynamics, the general form of the SCET lagrangian is given by

$$\mathcal{L}_{\rm SCET} = \mathcal{L}_{\rm hard} + \mathcal{L}_{\rm dyn}\,. \tag{2.52}$$

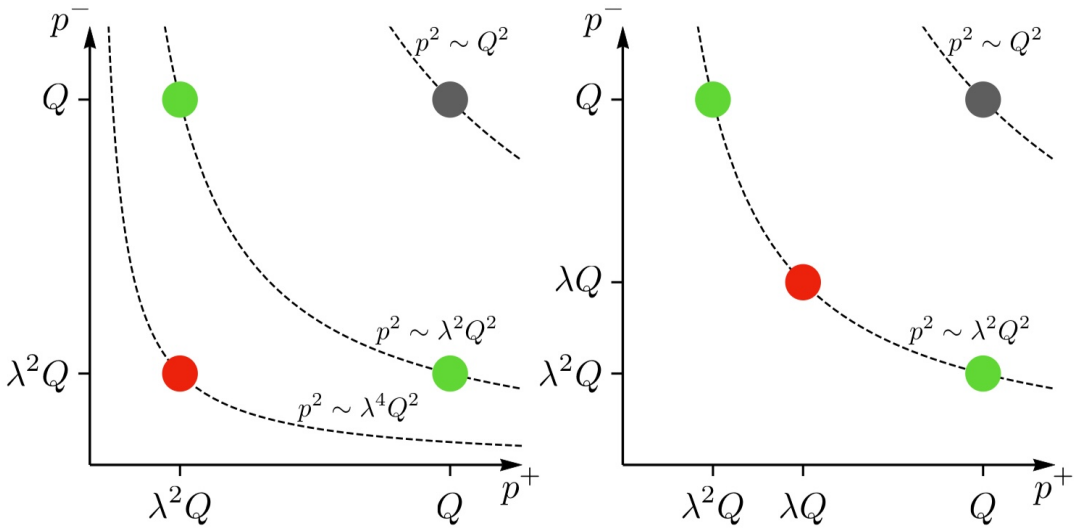

Figure 2.7: Modes of SCET_I (right) and SCET_II (left) in the (p^+, p^-) plane, with $p^2 \sim p_\perp^2 \sim p^+ p^-$ indicating their virtuality. Note that in SCET_II all the modes lie in the same hyperbola. Red, green, and grey dots correspond to (ultra)soft, collinear, and hard modes respectively. Image taken from ref. [37].

Here, $\mathcal{L}_\text{hard}$ is composed of hard scattering operators encoding short-distance physics that arise from matching QCD onto SCET, while $\mathcal{L}_\text{dyn}$ described the dynamics of soft and collinear degrees of freedom. According to the discussion carried out in the next section, the dynamical Lagrangian describes the interaction of soft and ultrasoft modes among themselves and of collinear and ultrasoft modes. At leading order in the power counting parameter λ, we then have that

$$\mathcal{L}^{(0)}_\text{dyn} = \sum_{j=c,\bar{c}} \mathcal{L}^{(0)}_j + \mathcal{L}^{(0)}_{us} + \mathcal{L}^{(0)}_s, \tag{2.53}$$

where c, $\bar{c}$ label the individual collinear sectors.

The degrees of freedom that enter the Lagrangian, are the quarks and gluon fields. However, unlike in QCD, in SCET quarks and gluons are represented by multiple fields, whose power counting can be determined from the ones of the relevant SCET modes. In particular, following the notation of [60], we have

$$\begin{aligned}
&\text{collinear quark} : \xi_n \sim \lambda \\
&\text{ultrasoft quark} : \psi_s \sim \lambda^3 \\
&\text{collinear gluon} : A_c = (n \cdot A_c, \bar{n} \cdot A_c, A_{c,\perp}) \sim (\lambda^2, 1, \lambda) \\
&\text{ultrasoft gluon} : A_s = (n \cdot A_s, \bar{n} \cdot A_s, A_{s,\perp}) \sim (\lambda^2, \lambda^2, \lambda^2)\,.
\end{aligned} \tag{2.54}$$

Note that the collinear and ultrasoft gluon fields have the same scaling as the collinear and soft modes of eq.(2.48), (2.51), which is necessary for constructing the covariant

derivative. In particular, since the theory comprises both collinear and soft fields, we introduce the following covariant derivatives

$$iD_\mu^s = i\partial_\mu + gA_\mu^s \qquad iD_\mu^c = i\partial_\mu + gA_\mu^c \tag{2.55}$$

where four derivative ∂_μ and the gluon fields have the same scaling. In turn, these covariant derivatives can be used for constructing the field strengths

$$F_{\mu\nu}^s = ig[iD_\mu^s, iD_\nu^s] \qquad F_{\mu\nu}^c = ig[iD_\mu^c, iD_\nu^c]\,. \tag{2.56}$$

For our purposes, it is sufficient to look at the collinear part $\mathcal{L}_{n_i}^{(0)}$ only, where for simplicity, we restrict our discussion to a single collinear sector $n_i = n$. This Lagrangian is then given by

$$\mathcal{L}_c = \mathcal{L}_{c\xi} + \mathcal{L}_{cg} \tag{2.57}$$

where the first denotes the dynamics and interactions of collinear quarks and the second the ones for collinear gluons. For the derivation of factorization theorems in chapter 5, $\mathcal{L}_{n\xi}$ suffices. In order to determine the form of this lagrangian, we have to write down all the possible LP operators consistent with the symmetry of the theory. For SCET, these are $SU(N_c)$ gauge invariance and reparametrization invariance, where this last is related to the fact that the choice of the directions n and $\bar{n}$ explicitly breaks Lorentz invariance. These symmetries are treated in e.g. chapter 4.4 of reference [60], and we won't discuss them further here. Instead, we will report the form of the leading power lagrangian for collinear ξ fields, that is

$$\mathcal{L}_{c\xi}^{(0)} = \bar{\xi}\frac{\bar{n}\!\!\!/}{2}\left[in\cdot D + i\not{D}_{c,\perp}\frac{1}{i\bar{n}\cdot D_c}\,i\not{D}_{c,\perp}\right]\xi\,. \tag{2.58}$$

Here, the first term denotes the interaction between collinear and soft particles and the second of collinear particles with other collinear particles. The covariant derivative appearing in this expression is given by

$$in\cdot D = in\cdot\partial + gn\cdot A_c(x) + gn\cdot A_s(x_-), \tag{2.59}$$

where $A_s(x_-)$ is the leading power term in the power expansion of the ultrasoft gluon field around the point $x_-^\mu = (x\cdot\bar{n})n^\mu/2$.

One of the main characteristics of SCET is the presence of Wilson lines. Wilson lines are path-ordered exponential of gauge fields over a continuous path that transform as

$$W(x,y) \longrightarrow U(x)W(x,y)U^\dagger(y) \tag{2.60}$$

with $U \in SU(N)$ and x, y point in the path. In SCET, we generally deal with Wilson lines extending to infinity, that is $x = -\infty$ or $y = +\infty$. In particular, one has

$$\begin{aligned} W_c(x) &= \mathcal{P}\left[ig\int_{-\infty}^0 ds\,\bar{n}\cdot A_c(x+s\bar{n})\right] \\ S_c(x) &= \mathcal{P}\left[ig\int_{-\infty}^0 ds\,\bar{n}\cdot A_s(x+s\bar{n})\right] \end{aligned} \tag{2.61}$$

which denote respectively the collinear and soft Wilson lines, with $\mathcal{P}$ path-ordering symbol. In the effective theory, these exponentials of gauge fields serve a double purpose. First, they can be used for constructing non-local gauge invariant building blocks, which can then be employed for building a gauge invariant lagrangian. For example, one can define the following gauge invariant combination involving collinear and anti-collinear fields,

$$\chi_c(x) \equiv W_c^\dagger(x)\xi_c(x) \qquad\qquad \chi_{\bar{c}}(x) \equiv W_{\bar{c}}^\dagger(x)\xi_{\bar{c}}(x)\,. \tag{2.62}$$

In addition, Wilson lines can be used to factorize the contribution of ultrasoft gluons from the leading power collinear lagrangian, which is known as *decoupling transformation*. To show how these transformations work, consider the Lagrangian

$$\mathcal{L}_{c+s} = \bar{\xi}\frac{\bar{n}\!\!\!/}{2} in\cdot D\xi = \bar{\xi}\frac{\bar{n}\!\!\!/}{2}\big(in\cdot\partial + gn\cdot A_c(x) + gn\cdot A_s(x_-)\big)\xi \tag{2.63}$$

describing the interaction between collinear quarks and ultrasoft gluons, and apply the following field redefinitions

$$\begin{aligned}\xi(x) &\to S_n(x_-)\xi^{(0)}(x)\\ A_c^\mu(x) &\to S_n(x_-)A_c^{(0),\mu}(x)S_n^\dagger(x_-)\,.\end{aligned} \tag{2.64}$$

By using that the covariant derivative along a Wilson line vanishes, one can prove that this substitution has the effect of decoupling the ultrasoft gluons from the leading power lagrangian, as

$$\mathcal{L}_{c+s} \to \bar{\xi}^{(0)}\frac{\bar{n}\!\!\!/}{2} n\cdot D_c^{(0)}\xi^{(0)}(x) = \bar{\xi}^{(0)}\frac{\bar{n}\!\!\!/}{2}\big(in\cdot\partial + gn\cdot A_c^{(0)}(x)\big)\xi^{(0)}(x), \tag{2.65}$$

where indeed the ultrasoft gluon field $A_s(x_-)$ no longer appear. However, it is important to remark that this only holds at leading power, and the subleading power terms of the collinear Lagrangian still feature interactions between collinear quarks and ultrasoft gluons. Eventually, one can generalize the form of the decoupling transformations eq.(2.64) to the gauge-invariant collinear fields of eq.(2.62), case in which they have the following form

$$\chi_c(x) \to S_n(x_-)\chi_c^{(0)}(x) \qquad\qquad \chi_{\bar{c}}(x) \to S_{\bar{n}}(x_+)\chi_{\bar{c}}^{(0)}(x)\,. \tag{2.66}$$

Chapter 3

Drell-Yan angular distributions

In this chapter, we introduce the neutral current Drell-Yan process and derive the helicity decomposition of the amplitude that leads us to the definition of helicity cross-section and Drell-Yan angular coefficients. This decomposition at the amplitude level enables us to map the dileptons' angular coefficients into the fully differential cross section in terms of the Collins Soper (CS) frame angles. For this reason, it represents the main and most crucial ingredient in the derivation of our results in the full QCD framework.

3.1 Overwiew

The Drell-Yan (DY) process was introduced in the early '70s by S. Drell and T.M.Yan [4] and refers to the massive dilepton production from unpolarized proton-proton (pp) scattering, which produce an intermediate vector boson via $q\bar{q}$ annihilation. In this thesis, we are interested in the kinematic region where the intermediate vector boson that carries the interaction is produced at small or moderate transverse momentum $q_T << Q$, with Q hard scale. This choice is motivated by two main reasons. The first is that the majority of the events contributing to the total cross section occur when the vector boson is produced at small q_T. The second is that, assuming the colliding protons carry negligible transverse momentum, the vector boson acquires a small transverse component after additional particles, such as soft gluons, are radiated from the initial state partons. Therefore, the study of low-q_T vector boson production is particularly relevant for understanding the dynamics of single and multiparticle soft radiation from the colling quark-antiquark pair. At the same time, the angular distribution of the final state lepton is highly sensitive to initial state radiation. Indeed, at the Born level, this distribution is symmetric with respect to the polar angle ϑ of the vector boson rest frame, and the differential cross section is proportional to $d\sigma/d\Omega \propto 1 + \cos^2\vartheta$, with Ω solid angle. We explicitly derive this distribution in section 3.3.3, when treating the Drell-Yan process at the tree level. On the other hand, if $q_T \neq 0$, the lab frame no longer corresponds to the frame where the vector boson is at rest, which leads us to introduce the Collins-Soper (CS) frame in section 3.2.1. In this frame, the dilepton angular distribution also acquires a dependence on the azimuthal angle φ, and the differential cross section can be written as a linear

combination of spherical harmonics in the CS angles ϑ, φ, whose coefficients A_i (angular coefficients) encodes all the dependence of the cross-section on the initial state QCD dynamics, as shown in section 3.2.3. The connection between angular coefficients and soft radiation is made explicit by showing that these angular coefficients are in one-to-one correspondence to the set of production cross-sections for vector bosons of definite helicity. These helicity cross sections can be derived by carrying out a full decomposition of the leptonic and hadron tensors into structure functions of definite helicity, as we show in section 3.2.2. The decomposition into Lorentz-scalar structure functions already appears in the literature for the study of the angular dependence of dilepton production [6, 62, 63]. Here, we closely follow the discussion of ref.[18] and ref.[64], of which the material of section 3.2 is a short review.

3.2 Factorization and CS decomposition

We now consider the production of the intermediate vector boson from the unpolarized pp scattering and its subsequent decay into a lepton pair. Since the decomposition we are going to derive holds as well for the more general case of a set of colorless particles, we will refer to the final state simply as L. The intermediate vector boson V created in the collision is created by the annihilation of a quark and antiquark pair extracted from the colliding protons and can be either an (off-shell) virtual photon γ^* or an electroweak boson Z, $W^\pm$. In this thesis, we only consider the neutral current Drell-Yan process

$$qq \longrightarrow \gamma^*/ZX \longrightarrow LX \tag{3.1}$$

where $V = \gamma^*/Z$ and with X denoting a generic undetected final state radiation. At leading order in the EW interaction, the matrix element factorizes into

$$\mathcal{M}(pp \to \gamma^*/ZX \to LX) = \mathcal{M}^{\mu}_{V\to L}\,\langle X|J_{V,\mu}|pp\rangle, \tag{3.2}$$

where $\mathcal{M}^{\mu}_{V\to L}$ is the amplitude for the propagation and decay of the vector boson V, while J^{μ}_{V} denotes the electroweak current that couples with the $q\bar{q}$ pair. Including the charges and electroweak couplings, the current for $V = \gamma/Z$ has the following expression

$$J^{\mu}_{\gamma} = |e| \sum_f Q_f\, \bar{q}_f\, \gamma^\mu\, q_f \qquad\qquad J^{\mu}_{Z} = -|e| \sum_f \bar{q}_f\, \gamma^\mu (v_f - a_f\gamma^5) q_f \tag{3.3}$$

with the sum over f extending to all the quarks flavor and where v_f and a_f denote the vector and axial coupling. Integrating the amplitude over phase and working at fixed values of the vector boson momentum, the hadronic cross section in the lab frame, which we take here as the center of mass frame, can be written as

$$\frac{d\sigma}{d^4q} = \frac{1}{2E^2_{cm}} \sum_{VV'} L_{\mu\nu,VV'}(q)\, W^{\mu\nu}_{VV'}(q, p_a, p_b) \tag{3.4}$$

with $E^2_{cm} = (P_a + P_b)^2$. To obtain testable theoretical prediction, we will frequently parametrize the cross-section in terms of the lab frame quantities, such as the invariant

mass of the dilepton final state $Q^2 = q^2 > 0$, the rapidity Y and the vector boson transverse momentum $\vec{q}_T$, which are in one-to-one correspondence with the Lorentz invariants constructed out of the momenta q, P_a and P_b.

Looking back at eq.(3.4), the tensor $W^{\mu\nu}_{VV'}$ is the hadronic tensor, which encodes the initial state QCD dynamics of the $q\bar{q}$ annihilation and is given by

$$W^{\mu\nu}_{VV'}(q, P_a, P_b) = \sum\!\!\!\!\!\!\int_X \langle pp|J^{\mu\,\dagger}_V|X\rangle \langle X|J^{\nu}_{V'}|pp\rangle \, \delta^4(P_a + P_b - q - p_X) \,, \tag{3.5}$$

considering the averaged over spins implicit. Here, the integral sum runs over all possible hadronic final states X of total four-momentum p_X integrated over their respective phase space. After this integration, the hadronic tensor indeed depends only on the vector boson four-momentum q and the protons momenta P_a and P_b parametrized by

$$P^{\mu}_a = \frac{E_{cm}}{2}(1,0,0,1) \qquad\qquad P^{\mu}_b \qquad P^{\mu}_b = \frac{E_{cm}}{2}(1,0,0,-1), \tag{3.6}$$

where the momentum fractions ξ_a and ξ_b have been introduced in section 2.1.4.

In the fully differential cross-section, the hadronic tensor appears together with the leptonic tensor $L^{\mu\nu}_{VV'}(q)$, which describes the propagation of the vector boson and its decay into the final state L. This tensor is given by

$$\begin{aligned} L_{VV'}(q) &= \int d\Phi_L(q)\, L^{\mu\nu}_{VV'}(\Phi_L) \\ L^{\mu\nu}_{VV'}(\Phi_L) &= \mathcal{M}^{\mu\,*}_{V\to L}\, \mathcal{M}^{\nu}_{V\to L} \end{aligned} \tag{3.7}$$

and is obtained from the full leptonic tensor $L^{\mu\nu}_{VV'}(\Phi_L)$ after integration over the dilepton phase space. Since the final state consists of two particles, we can parametrize this phase space as

$$d\Phi_L(q) = \left[\prod_{i=1,2} \frac{d^4 p_i}{(2\pi)^3}\, \theta(p_i^0)\, \delta(p_i^2)\right] (2\pi)^4\, \delta^4(q - \sum_{i=1,2} p_i) \tag{3.8}$$

which depends on the four momentum of the vector boson q so that, after the integration, $L_{\mu\nu}$ indeed depends on q. Note in particular that we consider the leptons to be massless, a convention that we will adopt throughout the rest of the thesis.

A clear separation of the hadronic and leptonic contributions to the cross-section can be obtained by carrying out a decomposition of these tensors into structure functions. In particular, as we will see in section 3.2.3, the contribution of the leptonic tensor to the helicity differential cross sections merely corresponds to a constant prefactor, and therefore this decomposition will be carried out for the hadronic tensor only. Moreover, this choice makes the application of factorization theorems more effective, as done in chapter 5. Therefore, our goal now is to decompose $W^{\mu\nu}_{VV}(q, P_a, P_b)$ into a set of Lorentz scalar structure functions by projecting it into a frame constructed out of the momenta q, P_a, P_b and their invariants. It directly follows that, since the hadronic tensor also depends on this set of momenta, any Lorentz scalar structure function constructed in

this way must depend on the Lorentz invariants formed out of q, P_a, P_b. Out of these six invariants, three of them contain non-trivial kinematical information, that is

$$\begin{aligned} q^2 &= Q^2 \\ s_{aq} &= 2q \cdot p_a = E_{cm} m_T \, e^{-Y} \\ s_{bq} &= 2q \cdot p_b = E_{cm} m_T \, e^{Y} \end{aligned} \tag{3.9}$$

which are in one-to-one correspondence with the lab-frame kinematic variables Q^2, Y, q_T^2. The other three instead encode the beam parameters

$$P_a^2 = P_b^2 = 0 \qquad s_{ab} = 2p_a \cdot p_b, \tag{3.10}$$

where we consider the protons (and consequently also the quark and antiquark) to be massless.

In addition, since the current J_γ^μ is conserved in QCD, that is $\partial_\mu J_\gamma^\mu = 0$, gauge invariance implies that

$$q_\mu W_{\gamma\gamma}^{\mu\nu} = q_\nu W_{\gamma\gamma}^{\mu\nu} = 0 \, . \tag{3.11}$$

The same however does not straightforwardly hold for J_Z^μ as the axial-vector current is not conserved in QCD. Consequently, the hadronic tensor can be generally written as a sum of a conserved part, satisfying eq.(3.11), and a non-conserved part. proportional to q^μ or q^ν, that is

$$\begin{aligned} W^{\mu\nu} &= W_{\text{cons.}}^{\mu\nu} + (\text{terms} \propto q^\mu \ \text{ or } \ q^\nu) \\ q_\mu W_{\text{cons.}}^{\mu\nu} &= q_\mu W_{\text{cons.}}^{\mu\nu} = 0, \end{aligned} \tag{3.12}$$

where $W_{\text{cons.}}$ is obtained from squaring the conserved part of the current J_Z^μ. The same can be likewise adapted to the leptonic tensor, which can be decomposed into a conserved part satisfying $q_\mu L_{\text{cons.}}^{\mu\nu} = q_\mu L_{\text{cons.}}^{\mu\nu} = 0$ and a non-conserved part, which only survives when is contracted with the non-conserved part of the hadronic tensor. However, as a result of considering leptons masses to vanish $m_\ell = 0$, the leptonic current is always conserved, so that the non-conserved part of the hadronic tensor can be consistently ignored as it does not contribute to physical observables. This fact has the important consequence that we only need to introduce three (instead of four) polarization vectors to describe the vector boson polarization state.

3.2.1 Collins-Soper frame

In this section, we construct the reference frame onto which project the hadronic tensor. We start by picking one time-like vector and three-spacelike vectors, which we label t^μ and x^μ, y^μ, z^μ respectively. We then align the timelike vector with the direction of the vector boson propagation by setting it equal to

$$t^\mu = \frac{q^\mu}{\sqrt{q^2}} \, . \tag{3.13}$$

This choice ensures that the timelike vector is properly normalized and provides a natural covariant basis for analyzing the vector boson decay products. The remaining vectors are instead chosen to be linear combinations of the momenta P_a, P_b, and q. Starting from the z axis, this is chosen to lie in the direction of the colliding proton, that is we write it as a linear combination

$$z^\mu = \lambda_a P_a + \lambda_b P_b, \tag{3.14}$$

with λ_a and λ_b functions of the kinematic invariants. Requiring the vector to be spacelike $z^2 = -1$ and orthogonal to the timelike vector $z \cdot t = 0$, we obtain that

$$z^\mu = \frac{s_{bq}\, P_a^\mu - s_{aq}\, P_b^\mu}{\sqrt{s_{ab} s_{aq} s_{bq}}} \tag{3.15}$$

up to an overall conventional minus sign. Indeed, z^μ is not symmetric under $P_a \leftrightarrow P_b$, and it changes sign when the quarks momenta are exchanged. To complete the orthonormal basis, we only need to determine x^μ and y^μ. We choose x^μ to be invariant under the exchange $P_a \leftrightarrow P_b$, ensuring that it remains aligned with a specific direction in the transverse plane that does not distinguish between the two protons. Thus, we can write it as a linear combination,

$$x^\mu = \frac{c_x}{\sqrt{q^2}}\left(q^\mu - \kappa_a\, P_a^\mu - \kappa_b\, P_b^\mu\right) \tag{3.16}$$

whose coefficients c_x, κ_a and κ_b can be fixed by imposing the constraints $x^2 = -1$ and $t \cdot x = z \cdot x = 0$, which leaves us with

$$x^\mu = \frac{s_{aq} s_{bq} q^\mu - s_{bq} q^2 P_a^\mu - s_{bq} q^2 P_b^\mu}{\left[s_{aq} s_{bq} q^2 (s_{aq} s_{bq} - s_{ab} q^2)\right]^{1/2}}\,. \tag{3.17}$$

At this point, the remaining spacelike vector y^μ can be simply picked to form a right-handed coordinate system with t^μ, x^μ and z^μ, that is we set it equal to

$$y^\mu = \varepsilon^{\mu\nu\rho\sigma} t_\nu x_\rho z_\sigma\,. \tag{3.18}$$

Here, ε refers to the totally antisymmetric Levi-Civita symbol (for which we adopt the convention $\epsilon^{0123} = +1$), so that it straightforwardly holds that y^μ satisfy $t \cdot y = x \cdot y = z \cdot y$ and that $y^2 = -1$. Thus, we have just constructed a reference frame of normalized and mutually orthogonal unit vectors, which define a frame where they have components $t^\mu = (1,0,0,0)$, $x^\mu = (0,1,0,0)$, $y^\mu = (0,0,1,0)$ and $z^\mu = (0,0,0,1)$. In particular, since t^μ is given by eq.(3.13), this frame corresponds to the reference frame where the vector boson is at rest, that is $q^\mu = (\sqrt{q^2},0,0,0)$. The proof that $\{t^\mu, x^\mu, y^\mu, z^\mu\}$ actually corresponds to the Collins Soper (CS) frame [5] can be found in [7], where the derivation of the CS frame has been carried out for the general case of colliding hadrons $h(P_a)$, $h(P_b)$ with potentially distinct masses.

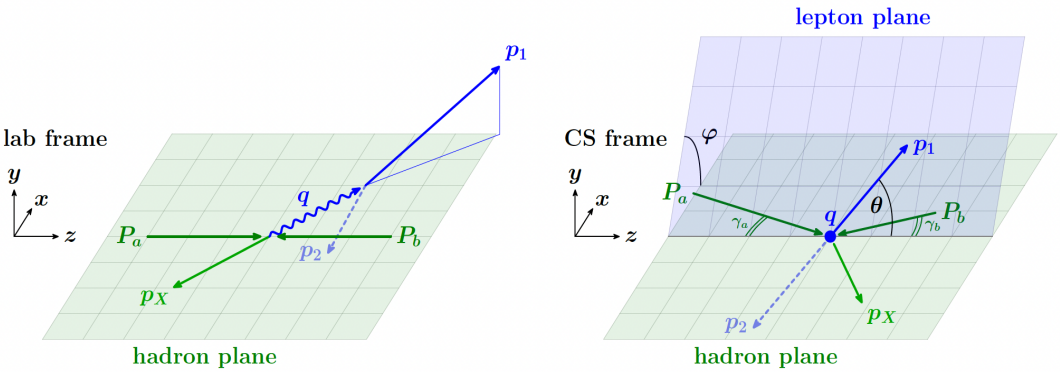

Figure 3.1: In the lab frame (right) the hadron plane is defined by the (x, z) plane where the scattering $p(P_a)p(P_b) \to V(q)X(p_X)$ takes place. The z axis corresponds to the direction of the protons collision and V has non-vanishing three momentum $\vec{q}$. In the CS frame (left) instead, the vector boson is at rest, and the protons' directions form angles γ_a, γ_b with respect to the z^μ axis and equal in the massless limit $m_p = 0$. The lepton plane is the plane where spanned by the momenta of the leptons p_1 and p_2, which are emitted back to back. The angles ϑ and φ correspond to the CS angles. Picture taken from ref.[7].

3.2.2 Hadronic tensor decomposition

We now construct polarization vectors from the orthonormal basis of the Collins-Soper frame, which ensures that they are covariant. We define these polarization vectors as

$$\varepsilon_\pm^\mu = \frac{1}{\sqrt{2}}(x^\mu \mp iy^\mu), \qquad \varepsilon_0^\mu = z^\mu, \tag{3.19}$$

which corresponds to positive/negative helicity and longitudinal polarization with respect to the z^μ axis. Using these vectors, we decompose the hadronic tensor into its components corresponding to different helicity states,

$$W_{\lambda\lambda'}(q, s_{ab}, s_{bq}) \equiv \varepsilon_\lambda^\mu \varepsilon_{\lambda'}^{*\,\nu} W^{\mu\nu}(q, P_a, P_b), \qquad \lambda = \{+, -, 0\}\,. \tag{3.20}$$

Because $W^{\mu\nu}$ is hermitian, that is $W^{\mu\nu *} = W^{\nu\mu}$ as it follows from its definition eq.(3.5), its symmetric components are purely real and its antisymmetric purely imaginary, so that $W_{\lambda\lambda'}(q, s_{ab}, s_{bq})$ corresponds to nine real-valued Lorentz scalar structure functions.

Here, following ref. [7], we use the following combinations:

$$\begin{aligned}
W_{-1} &= W_{++} + W_{--} && = (x_\mu x_\nu + y_\mu y_\nu) W^{\mu\nu} \\
W_0 &= 2W_{00} && = 2 z^\mu z^\nu W^{\mu\nu} \\
W_1 &= -\frac{1}{\sqrt{2}}(W_{+0} + W_{0+} + W_{-0} + W_{0-}) && = -(x_\mu z_\nu + x_\nu z_\nu) W^{\mu\nu} \\
W_2 &= -2(W_{+-} + W_{-+}) && = 2(y_\mu y_\nu - x_\mu x_\nu) W^{\mu\nu} \\
W_3 &= -\sqrt{2}(W_{+0} + W_{0+} - W_{-0} - W_{0-}) && = 2i(y_\mu z_\nu - y_\nu z_\mu) W^{\mu\nu} \\
W_4 &= 2(W_{++} - W_{--}) && = 2i(x_\mu y_\nu - x_\nu y_\mu) W^{\mu\nu} \\
W_5 &= -i(W_{+-} - W_{-+}) && = -(x_\mu y_\nu + x_\nu y_\mu) W^{\mu\nu} \\
W_6 &= -\frac{i}{\sqrt{2}}(W_{+0} - W_{0+} - W_{-0} + W_{0-}) && = -(y_\mu z_\nu + y_\nu z_\mu) W^{\mu\nu} \\
W_7 &= -i\sqrt{2}(W_{+0} - W_{0+} + W_{-0} - W_{0-}) && - 2i(x_\mu z_\nu - x_\nu z_\mu) W^{\mu\nu} \,.
\end{aligned} \tag{3.21}$$

which correspond to the tensor components of the hadronic tensor evaluated in the CS frame. For this reason, we refer to this expression as *CS decomposition*. In addition, we define the inclusive hadronic structure function, which describes an unpolarized or longitudinally polarized vector boson, and is therefore proportional to the total inclusive scattering probability irrespective of the helicity states of the initial and final-state particles,

$$W_{\text{incl}} = W_{++} + W_{--} + W_{00} = W_{-1} + \frac{1}{2} W_0 \,. \tag{3.22}$$

The second equality of eq.(3.21) is what defines the projectors $P_i^{\mu\nu}$, $i = -1, ..7$. These projectors are orthogonal operators satisfying $P_{\mu\nu_i} P^{\mu\nu\,-1} = \mathbb{I}$, where the inverse $P_i^{\mu\nu\,-1} \equiv P_i^{\mu\nu}$ differ from its corresponding $P^{\mu\nu}{}_i$ by a mere costant factor. Using this identity, we find that

$$L_{\mu\nu} W^{\mu\nu} = \sum_{i=-1}^{7} P_i^{\mu\nu} L_{\mu\nu}\, P_{\mu\nu_i} W^{\mu\nu} = \sum_{i=-1} L_i W^i \,, \tag{3.23}$$

where we have defined the leptonic structure functions as

$$L_i(q) = \int d\Phi_L(q)\, P_i^{\mu\nu}\, L_{\mu\nu}(\Phi_L) \,. \tag{3.24}$$

Inserting now eq.(3.23) into eq.(3.4), the differential cross section can be written in terms of the following sum

$$\frac{d\sigma}{d^4 q} = \frac{1}{2E_{cm}^2} \sum_{i=-1}^{7} L_i(q^2) W_i(q^2, s_{aq}, s_{bq}) \,. \tag{3.25}$$

This formula is totally general and it is valid for every value of the transverse momentum q_T and for any number of radiative emissions from the colliding quark in the initial state.

These radiative emissions, which will be studied in chapter 4, lead to a modification of the hadronic tensor and hence to the hadronic structure functions $W_i(q^2, s_{aq}, s_{bq})$. However, since the leptonic sector is not modified, they leave the leptonic functions $L_i(q)$ unchanged. For this reason, we analyze the leptonic tensor in the next section of this chapter, where the results we derive are valid for all the processes considered in the rest of this thesis.

3.2.3 Leptonic tensor and angular distribution

The full differential leptonic tensor $L_{VV'}(\Phi_L)$ for the decay $Z/\gamma^* \to \ell^+\ell^-$ given in eq.(3.7), parametrized in terms of the leptons momenta p_1 and p_2, is equal to

$$L^{\mu\nu}(p_1, p_2) = \frac{24\pi}{q^2}\Big[L_+(q^2)(p_1^\mu p_2^\nu + p_1^\nu p_2^\mu - g^{\mu\nu}(p_1 \cdot p_2)) + iL_-(q^2)\,\varepsilon^{\mu\nu\rho\sigma}(p_1)_\rho(p_2)_\sigma\Big] \quad (3.26)$$

. In this expression, $L_+(q^2)$ and $L_-(q^2)$ are scalar coefficients for the parity-conserving and parity-violating part of the leptonic tensor and they are respectively given by the contraction of the leptonic tensor with the symmetric (antisymmetric) projectors $P_i^{\mu\nu}$. Consequently, $L_+(q^2)$ can only appear in combination with the parity even hadronic structure function $W_{-1,0,1,2,5,6}$ and $L_-(q^2)$ with the parity odd $W_{3,4,7}$. The normalization is instead chosen in accordance with ref.[7], where these scalar coefficients have been explicitly calculated for $V = \gamma^*, Z$ and are reported below,

$$\begin{aligned}
\text{parity even}: \quad & L_{+\gamma\gamma}(q^2) = \frac{2}{3}\frac{\alpha_{em}}{q^2}, && L_{+ZZ}(q^2) = \frac{2}{3}\frac{\alpha_{em}}{q^2}\,(v_l^2 + a_l^2)|P_Z(q^2)|^2 \\
& L_{+\gamma Z}(q^2) = \frac{2}{3}\frac{\alpha_{em}}{q^2}(-v_l)\,P_Z(q^2), && L_{+Z\gamma}(q^2) = L^*_{+\gamma Z}(q^2) \\
\text{parity odd}: \quad & L_{-\gamma\gamma}(q^2) = 0, && L_{-ZZ}(q^2) = \frac{2}{3}\frac{\alpha_{em}}{q^2}\,(-2v_l a_l)|P_Z(q^2)|^2 \\
& L_{-\gamma Z}(q^2) = \frac{2}{3}\frac{\alpha_{em}}{q^2}(a_l)\,P_Z(q^2), && L_{-Z\gamma}(q^2) = L^*_{+\gamma Z}(q^2)\,,
\end{aligned} \quad (3.27)$$

where we have introduced the shorthand notation $P_V(q^2)$ for the reduced propagator

$$P_V(q^2) = \frac{q^2}{q^2 - m_V^2 + i\Gamma_V m_V}\,. \quad (3.28)$$

The angular dependence of the leptonic tensor can be now pointed out by parametrizing the leptons momenta and the leptonic phase space in terms of the CS angles ϑ and φ, in terms of which they are respectively given by

$$d\Phi_L(q) = \frac{d\cos\vartheta\, d\varphi}{32\pi^2}, \qquad p_{1,2} = \frac{Q}{2}(t^\mu \pm x^\mu \sin\vartheta\cos\varphi \pm y^\mu \sin\vartheta\sin\varphi \pm z^\mu\cos\vartheta) \quad (3.29)$$

where the negatively charged lepton of momentum p_1 has been chosen to move in the hemisphere where $\cos\vartheta > 0$. In virtue of the orthonormality of the CS frame basis vectors,

the contraction of the projectors $P_i^{\mu\nu}$ with the leptonic tensor eq.(3.26) integrated over the phase space allows one to write the leptonic structure functions of eq.(3.24) as

$$L_i(q^2) = \int_{-1}^{1} d\cos\vartheta \int_0^{2\pi} d\varphi \, L_i(q^2, \vartheta, \varphi) \tag{3.30}$$

where the functions $L_i(q^2, \vartheta, \varphi)$ are equal to

$$L_i(q^2, \vartheta, \varphi) = \frac{3}{16\pi} L_{\pm(i)}(q^2)\, g_i(\theta, \varphi) = \frac{3}{16\pi} \begin{cases} L_+(q^2)\, g_i(\theta, \varphi) & i = -1, 0, 1, 2, 5, 6 \\ L_-(q^2)\, g_i(\theta, \varphi) & i = 3, 4, 7 \end{cases} \tag{3.31}$$

with $g_i(\theta, \varphi)$ denoting spherical harmonics in terms of the CS angles, which are listed in app.B.1 and $L_{\pm,VV'}$ given by eq.(3.27).

We can now investigate the dependence of the cross-section on the CS angles by plugging eq.(3.30) and eq.(3.31) into eq.(3.25), which let us obtain a fully differential cross-section, namely a cross-section differential in the vector boson four-momentum and solid angle, as

$$\begin{aligned} \frac{d\sigma}{d^4q} &= \int_{-1}^{1} d\cos\vartheta \int_0^{2\pi} d\varphi \, \frac{d\sigma}{d^4q \, d\cos \, d\varphi} \\ \frac{d\sigma}{d^4q \, d\cos \, d\varphi} &= \frac{1}{2s} \sum_{i=-1}^{7} L_i(q^2) W^i(q^2) = \frac{3}{16\pi} \sum_{i=-1}^{7} \frac{d\sigma^{(i)}}{d^4q} \, g_i(\vartheta, \varphi) \end{aligned} \tag{3.32}$$

where in the last step we have defined the *helicity cross sections*

$$\frac{d\sigma^{(i)}}{d^4q} = \frac{1}{2s} L_{\pm(i)}(q^2) W^i(q^2) \, . \tag{3.33}$$

Accordingly, we will call

$$\langle |\mathcal{M}|^2 \rangle_i = L_{\pm(i)}(q^2) W^i(q^2) \tag{3.34}$$

helicity matrix elements, which are the objects we are going to calculate and check in the soft threshold limit. As anticipated in 3.1, the helicity cross sections will be the main subject of our further investigation, being in bijection with the angular distributions of the final state dilepton. To prove this correspondence, we expand the fully differential cross section eq.(3.32) and write it as a linear combination of the spherical harmonics $g_i(\theta, \varphi)$. This yields to

$$\frac{d\sigma}{d^4q \, d\cos \, d\varphi} = \frac{3}{16\pi} \frac{d\sigma^{\text{incl}}}{d^4q} \left[(1 + \cos^2\vartheta) + \frac{A_0}{2}(1 - 3\cos^2\vartheta) + \sum_{i=1}^{7} A_i \, g_i(\vartheta, \varphi) \right], \tag{3.35}$$

where the inclusive cross section (that is, the cross-section obtained from W_{incl} of eq.(3.22) has been factored out. Here, the symbols A_i denote precisely the *angular coefficients*,

defined as the ratio of the helicity cross sections (3.33) and the inclusive helicity cross-section $d\hat{\sigma}_{\text{incl}}$,

$$A_i = \frac{d\sigma^{(i)}}{d\sigma_{\text{incl}}} \equiv \frac{d\sigma^{(i)}}{d\sigma^{-1} + \frac{1}{2}d\sigma^0} \,. \tag{3.36}$$

These angular coefficients have already been calculated up to $\mathcal{O}(\alpha_s^2)$ for both the neutral and charged Drell-Yan process [6, 65] and experimentally determined by the ATLAS collaboration [66]. The study of these angular coefficients in soft threshold limit will be carried out in the next chapter. Instead, we dedicate the end of the present one to the application of the setup carried out in this section to the Drell-Yan scattering at tree level.

3.3 Tree-level Drell-Yan process

3.3.1 Tree level amplitude

As discussed in section 2.1.3, only interactions between quarks and gluons are computable in perturbative QCD, but not between hadrons. Therefore, we now focus on the partonic process

$$q(p_a)\bar{q}(p_b) \to V(q)X(p_X) \,. \tag{3.37}$$

The relevant quantities, such as hadronic tensor and differential cross sections, which depend on the initial QCD dynamics can be calculated by using the same expression derived before provided we replace all the hadronic variables with partonic variables (e.g. protons momenta with partons momenta $P_a \to p_a$, $P_b \to p_b$, $E_{cm}^2 \to s$,...). The connection between the quantities we derive here and the ones presented in the previous section is then obtained by convoluting the first with the parton distribution functions, as shown in section 2.1.4.

The total amplitude for the neutral Drell-Yan process is given by the sum of the amplitude for the production and decay of an off-shell photon and the one for the production and decay of a Z boson. Starting from the case in which the intermediate vector boson is a virtual photon, we obtain that the amplitude for this process reads

$$i\mathcal{M}_\gamma = \delta_{ij} Q_f e^2 [\bar{v}(p_b)\gamma^\mu u(p_a)] \frac{i}{q^2 - i0} [\bar{u}(p_1)\gamma_\mu v(p_2)] \tag{3.38}$$

where the sum over flavors and color indices is left implicit. The relation $\gamma^0(\gamma^\mu)^\dagger\gamma^0 = \gamma^\mu$ and that γ^0 is self-adjoint $\gamma^0 = (\gamma^0)^\dagger$, allows us to compute the conjugate of the bispinor product appearing in the expression above. Averaging over color indices and using the completeness relations for spinors app.A.2.2 for the average over spin indices, we then obtain that the matrix element squared for $VV' = \gamma\gamma$ is given by the product of aleptonic

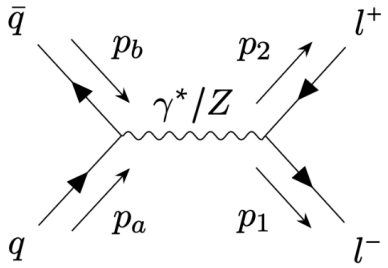

Figure 3.2: Drell Yan process at tree level.

tensor and hadronic tensor, respectively given by

$$L_{\mu\nu} = \frac{e^2}{q^4}\,\mathrm{Tr}[\gamma^\mu \not{p}_1 \gamma^\nu \not{p}_2] \tag{3.39}$$

$$W^{\mu\nu}_{\gamma\gamma\,\mathrm{LO}} = \frac{Q_f^2 e^2}{4N_c^2}\mathrm{Tr}[\gamma^\mu \not{p}_b \gamma^\nu \not{p}_a]\,. \tag{3.40}$$

where we have chosen the normalization of these tensors to include all the numerical factors and couplings in their definition. Moreover, we only reserve the label referring to the order of the perturbative expansion in α_s to the hadronic tensor as, as stated in section 3.2.2, the leptonic tensors we derive in this section are the same we obtain for single/multiple gluon emissions.
If the vector boson is instead a Z boson, the amplitude at tree level is equal to

$$i\mathcal{M}_Z = e^2\delta_{ij}[\bar{v}(p_b)\gamma^\mu(v_f - a_f\gamma^5)u(p_a)]\, i\frac{P_Z(q^2)}{q^2}[\bar{u}(p_1)\gamma_\mu(v_l - a_l\gamma^5)v(p_2)], \tag{3.41}$$

where the Dirac matrix γ^5 is hermitian and anticommute with all the other Dirac matrices, $\{\gamma^5, \gamma^\mu\} = 0$, for $\mu = 0, 1, 2, 3$. Using this property, we can easily compute the conjugate matrix, so as to obtain

$$L^{\mu\nu}_{ZZ} = \frac{e^2}{q^4}|P_Z(q^2)|^2\,\mathrm{Tr}[\not{p}_1\gamma^\mu(v_l - a_l\gamma^5)\not{p}_2\gamma^\nu(v_l - a_l\gamma^5)] \tag{3.42}$$

$$W^{\mu\nu}_{ZZ\,\mathrm{LO}} = \frac{e^2}{4N_c}\mathrm{Tr}[\not{p}_b\gamma^\mu(v_f - a_f\gamma^5)\not{p}_a\gamma^\nu(v_f - a_f\gamma^5)]\,. \tag{3.43}$$

To compute the full square matrix element for the tree-level DY process we now only miss the contribution of the interference matrix elements. This contribution is equal to

$$\mathcal{M}_\gamma\mathcal{M}_Z^* + \mathcal{M}_Z\mathcal{M}_\gamma^* = \mathcal{M}_\gamma\mathcal{M}_Z^* + (\mathcal{M}_\gamma\mathcal{M}_Z^*)^* = 2\,\mathrm{Re}(\mathcal{M}_\gamma\mathcal{M}_Z^*), \tag{3.44}$$

whose expression can be computed explicit from the amplitudes eq.(3.38) and eq.(3.41),

and is equal to the product of the following tensors,

$$L^{\mu\nu}_{\gamma/Z} = \frac{e^2}{q^4} P_Z(q^2)\mathrm{Tr}[\not{p}_1\gamma^\mu\not{p}_2\gamma^\nu(v_l - a_l\gamma^5)] \qquad L^{\mu\nu}_{Z\gamma} = (L^{\mu\nu}_{\gamma/Z})^* \tag{3.45}$$

$$W^{\mu\nu}_{\gamma/Z_{\mathrm{LO}}} = \frac{Q_f e^2}{4N_c}\mathrm{Tr}[\not{p}_b\gamma^\mu\not{p}_a\gamma^\nu(v_f - a_f\gamma^5)] \qquad W^{\mu\nu}_{Z\gamma_{\mathrm{LO}}} = (W^{\mu\nu}_{\gamma/Z_{\mathrm{LO}}})^* \,. \tag{3.46}$$

Now that we have the full amplitude for the process, we can project the hadronic tensor into hadronic structure functions.

3.3.2 Hadronic tensor decomposition at tree level

For the decomposition into structure functions, we proceed as in the previous section, namely working the single cases $V, V' = \gamma^*/Z$ separately. Starting from $VV' = \gamma\gamma$, we we can express the trace of eq.(3.40) as

$$\mathrm{Tr}[\gamma^\mu\not{p}_b\gamma^\nu\not{p}_a] = 4\big(p_a^\mu p_b^\nu + p_a^\nu p_b^\mu - g^{\mu\nu}(p_a\cdot p_b)\big)\,. \tag{3.47}$$

This shows that the hadronic tensor $W^{\mu\nu}_{\gamma\gamma\,\mathrm{LO}}$ is symmetric, consistently with the requirement that electromagnetic interactions are parity conserving. At its turn, this implies immediately that the contraction with the antisymmetric projectors must vanish, that is we can immediately set $W_{3,4,7} = 0$. Moreover, being the photon a massless particle, it can only carry transverse polarization, so that $z_\mu W^{\mu\nu}_{\gamma\gamma\,\mathrm{LO}} = z_\nu W^{\mu\nu}_{\gamma\gamma\,\mathrm{LO}} = 0$, namely the helicity projection of the hadron tensor along the beam axis vanish, and therefore also $W_{0,1,6} = 0$. Likewise, also the quark and antiquark (since we work in the massless case) can only be polarized either in the x or the y direction, which results in four possible initial states $|++\rangle$, $|--\rangle$, $|+-\rangle$, $|-+\rangle$. The corresponding projections of the hadronic tensor onto these helicity states are accordingly W_{++}, W_{--}, W_{+-}, W_{-+}. The photon however is a boson of spin 1, so the only way two massless spinors can annihilate into such a particle is if they carry the same polarization. As a result $W_{+-} = W_{-+} = 0$, so the only non-vanishing structure function turns out to be

$$W^{-1}_{\gamma\gamma\,\mathrm{LO}} = \frac{4\pi\alpha_{em}Q_f^2}{N_c}\,q^2 \tag{3.48}$$

where we have used that $\alpha_{em} = e^2/4\pi$.

Considering now the hadronic tensor $W^{\mu\nu}_{ZZ_{\mathrm{LO}}}$ given by eq.(3.43), this can be written as a sum of a symmetric part and an antisymmetric part as follows

$$W^{\mu\nu}_{ZZ} = \frac{e^2}{4N_c}\Big[(v_f^2 + a_f^2)\mathrm{Tr}[\not{p}_b\gamma^\mu\not{p}_a\gamma^\nu] - 2v_f a_f\mathrm{Tr}[\not{p}_b\gamma^\mu\not{p}_a\gamma^\nu\gamma^5]\Big] \tag{3.49}$$

by exploiting the linearity of the trace. In particular, the symmetric part is equal to the electromagnetic hadronic tensor apart from a factor $1/Q_f^2$, while the antisymmetric one is proportional to the Levi-Civita tensor $\epsilon^{\mu\nu\rho\sigma}$ in virtue of the identities eq.(A.6). Because the Levi-Civita symbol is antisymmetric in all the indices, this second term survives

only when contracted with $P^{\mu\nu}_{3,4,7}$ and vanishes otherwise. Among these projectors, the one including z^μ, that is $P^{\mu\nu}_{3,7}$ yields zero, again because quarks only carry transverse polarization so that the vector boson cannot be produced longitudinal. This leaves us with only two non-vanishing structure functions,

$$\begin{aligned} W^{-1}_{\gamma\gamma\,\mathrm{LO}} &= \frac{4\pi\alpha_{em}}{N_c}\, q^2\,(v_f^2 + a_f^2) \\ W^{4}_{\gamma\gamma\,\mathrm{LO}} &= \frac{4\pi\alpha_{em}}{N_c}\, q^2\,(-4 v_f a_f)\,. \end{aligned} \tag{3.50}$$

As last, we consider the tensor for the case $VV' = \gamma/Z$ (the other one follows trivially)

$$W^{\mu\nu}_{\gamma/Z\,\mathrm{LO}} = \frac{Q_f e^2}{4N_c}\Big[v_f \mathrm{Tr}[\not{p}_b \gamma^\mu \not{p}_a \gamma^\nu] - a_f \mathrm{Tr}[\not{p}_b \gamma^\mu \not{p}_a \gamma^\nu \gamma^5]\Big], \tag{3.51}$$

which is equal to the tensor of eq.(3.49) apart from a different normalization involving EW couplings. According to the results previously obtained for the hadronic structure functions, is now easy to derive that

$$\begin{aligned} W^{-1}_{\gamma/Z\,\mathrm{LO}} &= v_f W^{-1}_{\gamma\gamma\,\mathrm{LO}} = \frac{4\pi\alpha_{em} Q_f}{N_c}\, q^2\, v_f \\ W^{4}_{\gamma/Z\,\mathrm{LO}} &= \frac{Q_f^2}{2v_f} W^{4}_{ZZ\,\mathrm{LO}} = \frac{4\pi\alpha_{em} Q_f}{N_c}\, q^2\,(-2a_f)\,. \end{aligned} \tag{3.52}$$

3.3.3 LO hadronic cross section

The main purpose of this section is to highlight the general steps that lead to the calculation of the hadronic cross section based on the formalism developed in section 3.2. The relevant formulas, concepts, and normalization choices presented here directly generalize for higher orders in α_s. Firstly, we work out the phase space. At tree-level, the total phase space is simply given by the dileptons phase space, in which we insert the identity

$$1 = \int d^4q\, \delta^4(q - (p_1 + p_2))\,. \tag{3.53}$$

where we have used that $p_a + p_b = p_1 + p_2$. As a result, the total phase space factorizes into the phase space for the decaying leptons and the phase space of the intermediate vector boson, that is $d\Phi = d\Phi_L \times d^4$, plus a delta function involving momentum conservation. If we remain differential with respect to the vector boson momentum and integrate the matrix element square over the leptonic phase space, we obtain that the total hadronic cross section can be written as

$$\frac{d\sigma^{\mathrm{LO}}}{d^4q} = \sum_{ij} \int_0^1 d\xi_a \int_0^1 d\xi_b\, f_i(\xi_a) f_j(\xi_b)\, \frac{d\hat{\sigma}^{\mathrm{LO}}}{d^4q}\, \delta^4(q - (p_a + p_b))\,. \tag{3.54}$$

Focusing now on the total partonic cross-section, this is given in eq.(2.32) by summing over all possible combinations of intermediated vector bosons $V, V' = \gamma/Z$. Also, we have seen in eq.(3.35) that this cross-section can be factorized into an angular-dependent part and a part depending on the hard dynamics of the process. Putting everything together, this implies that we can write

$$\frac{d\hat{\sigma}^{\mathrm{LO}}}{d^4q} = \sum_{VV'} \frac{d\hat{\sigma}^{\mathrm{LO}}_{VV'}}{d^4q} = \frac{3}{16\pi} \sum_{VV'} \int_1^1 \cos\theta \int d\phi \, \frac{d\hat{\sigma}^{(i)}_{VV'}}{d^4q} \, g_i(\theta,\phi) \, . \tag{3.55}$$

Plugging now this equation into eq.(3.54) and expressing the helicity cross sections in terms of the helicity matrix elements eq.(3.34), we hence obtain that the total hadronic cross section can be expressed as the following sum

$$\frac{d\sigma^{\mathrm{LO}}}{d^4q} = \frac{3}{16\pi} \sum_{VV'} \int_1^1 \cos\theta \int d\phi \, \frac{d\sigma^{\mathrm{LO}}_{VV',i}}{d^4q} \, g_i(\theta,\phi) \tag{3.56}$$

where we have defined the *hadronic helicity cross sections* as

$$\frac{d\sigma^{\mathrm{LO}}_{VV',i}}{d^4q} = \frac{1}{2E_{cm}^2} \sum_{ij} \int \frac{d\xi_a}{\xi_a} \int \frac{d\xi_b}{\xi_b} \, f_i(\xi_a) f_j(\xi_b) \langle |\mathcal{M}|^2_{VV'} \rangle_i \, \delta^4(q - (p_a + p_b)) \tag{3.57}$$

In the last step, we have used that the flux factor is related to the hadronic center of mass energy by $s = \xi_a \xi_b E_{cm}^2$. As stated in section 3.2, we want to express this cross-section in terms of the invariant mass Q^2 and the transverse momentum $\vec{q}_T$ of the vector boson and of the rapidity Y. To do so, it is useful to work in lightcone coordinates, defined in section 2.2.2. From the definition eq.(3.6), we notice that the protons momenta P_a and P_b only admit minus and plus components respectively, so that the vector boson momentum can be written as

$$q^\mu = (q^-, \vec{q}_T, q^+) = (x_a P_a^-, \vec{q}_T, x_b P_b^+) \, , \tag{3.58}$$

where the energy fractions x_a and x_b have been defined in eq.(2.30) and we recall correspond to the momentum fractions of the partons that participate in the annihilation. Using this parametrization, we can easily derive the following identity

$$d^4q = \frac{1}{2} \, dq^- dq^+ d^2\vec{q}_T = \left(\frac{P_a^+ P_b^-}{2} \right) dx_a \, dx_b \, d^2\vec{q}_T \, . \tag{3.59}$$

In addition to the volume element, we also have to express the delta function in lightcone coordinates. This can be done by noticing that the normalization condition imposes that

$$1 = \int d^4q \, \delta(q) = \int \frac{1}{2} dq^- dq^+ d^2q_T \, \left[2 \, \delta^-(q^-) \delta^+(q^+) \delta^2(\vec{q}_T) \right] \tag{3.60}$$

and therefore in four dimensions, the delta function in lighcone coordinates is always accompanied by a factor 2. Moreover, using the scaling properties of the delta function,

we obtain

$$\begin{aligned}\delta^4(q-(p_a+p_b)) &= 2\delta^-(q^- - \xi_a P_a^-)\,\delta^+(q^+ - \xi_b P_b^+)\,\delta^2(\vec{q}_T) \\ &= \frac{2}{P_a^- P_b^+}\delta^-\left(\frac{q^-}{P_a^-} - \xi_a\right)\delta^+\left(\frac{q^+}{P_b^+} - \xi_b\right)\delta^2(\vec{q}_T)\,. \end{aligned} \tag{3.61}$$

In this expression, not only does the numerical factor in front of the delta functions exactly cancel the Jacobian factor of the change of coordinates (which is crucial to restoring the correct mass dimension of the cross-section), but also the plus and minus delta function set

$$\xi_a = x_a = \frac{q^-}{P_a^-} \qquad \xi_b = x_b = \frac{q^+}{P_a^+}\,. \tag{3.62}$$

This is indeed what we expect from a tree-level process where, without any parton splitting, the momentum fraction of the parton extracted from the proton is the same one that carries the parton participating in the interaction. Integrating now the δ^- and δ^+ distributions against the momentum fractions ξ_a and ξ_b, the cross sections eq.(3.57) can be written as

$$\frac{d\sigma^{\mathrm{LO}}_{VV',i}}{dx_a\,dx_b\,d\vec{q}_T} = \frac{1}{2E_{cm}^2}\sum_{ij}\frac{f_i(x_a)}{x_a}\,\frac{f_j(x_b)}{x_b}\,\langle|\mathcal{M}|^2_{VV'}\rangle_i\,\delta^2(\vec{q}_T)\,. \tag{3.63}$$

where the delta function $\delta(\vec{q}_T)$ enforces that the vector boson is produced at zero transverse momentum. We will see that this is no more true at higher orders. Recalling now that in section 3.3.2, we have found that the hadronic structure functions are only non-vanishing for $i=-1$ ($VV'=\gamma\gamma$) and for $i=-1,4$ ($VV'=ZZ$ and $VV'=\gamma/Z, Z/\gamma$), it follows that these are also the only indices for which the hadronic helicity cross-section do not vanish. According to eq.(3.56), these helicity cross-section are related to the total hadronic cross section by integration over the solid angles. For $g_1(\theta,\varphi)=1+\cos\theta^2$ and $g_4(\theta,\varphi)=\cos\theta$ this integration yields respectively

$$\int_{-1}^{1} d\cos\vartheta\int_0^{2\pi} d\varphi\; g_i(\vartheta,\varphi) = \begin{cases}\dfrac{16\pi}{3} & i-1\\ 0 & i=4\end{cases} \tag{3.64}$$

implying that the projection of the hadronic tensor with $i=-1$ solely contributes to the whole final hadronic cross-section. Hence, using this fact and inserting now eq.(3.63) into eq.(3.56), we obtain

$$\frac{d\sigma^{\mathrm{LO}}}{dx_a dx_b\,d\vec{q}_T} = \frac{1}{2E_{cm}^2}\sum_{VV'}\sum_{ij}\frac{f_i(x_a)}{x_a}\,\frac{f_j(x_b)}{x_b}\,\langle|\mathcal{M}|^2_{VV'}\rangle_{-1}\;\delta^2(\vec{q}_T)\,. \tag{3.65}$$

From now on we will generally consider cross-sections inclusive in the momentum $\vec{q}_T$, which we therefore integrate over. In this way, the cross-section is only differential in the parameters x_a and x_b that, since the protons momenta P_a and P_b are fixed,

can be determined experimentally if the four-momentum of the vector boson is known. Nonetheless, due to the difficulties of determining q in collider experiments, it is more useful to express this cross-section in terms of the invariant mass Q^2 and the rapidity of the lepton pair Y. The relevance change of coordinates in this case is

$$Q^2 = q^2 = x_a x_b\, S \qquad Y = \ln\sqrt{\frac{x_a}{x_b}} \tag{3.66}$$

with $S = E_{cm}^2 = (P_a + P_b)^2$ center of mass energy, which features the following Jacobian factor

$$dQ^2 dY = \frac{Q^2}{x_a x_b}\, dx_a dx_b\,. \tag{3.67}$$

Hence, eventually using that $i, j = q, \bar{q}$ we can finally write the cross section as

$$\frac{d\sigma^{\mathrm{LO}}}{dQ^2\, dY} = \frac{1}{E_{cm}^2} \sum_q \hat{\sigma}_B \left[f_q(x_a) f_{\bar{q}}(x_b) + f_{\bar{q}}(x_a) f_q(x_b) \right]. \tag{3.68}$$

where we have defined the total Born cross section $\hat{\sigma}_B$ as the sum over all the intermediate vector bosons VV' of the cross sections $\hat{\sigma}_B^{VV'}$. These cross-section can be finally evaluated using eq.(3.33), (3.27) and the results of the previous section, and are equal to

$$\hat{\sigma}_B^{VV'} = \frac{1}{2Q^2} \langle |\mathcal{M}|^2_{VV'} \rangle_{-1} = \begin{cases} \dfrac{4\pi\alpha_{em}^2 Q_f^2}{3\, N_c\, Q^2} & VV' = \gamma\gamma \\ \dfrac{4\pi\alpha_{em}^2}{3\, N_c\, Q^2} \left| P_Z(q^2) \right|^2 \cdot (v_f^2 + a_f^2)(v_l^2 + a_l^2) & VV' = ZZ \\ \dfrac{4\pi\alpha_{em}^2 Q_f}{3\, N_c Q^2} \, \mathrm{Re}\{P_Z(q^2)\}\, (-v_l v_f) & VV' = \gamma/Z,\ Z/\gamma \end{cases} . \tag{3.69}$$

The tree-level calculation constitutes the only case of this thesis where we explicitly compute the total hadronic cross-section. Indeed, as we have seen, the integration over the CS angles generally involves a loss of information on the angular distribution of the dilepton pair due to the vanishing of some of the spherical harmonics $g_i(\theta, \varphi)$. For this reason, for the single and double gluon emission, we will only focus on the helicity hadronic cross sections.

Chapter 4

Radiative corrections to the Drell-Yan process

In this chapter, radiative corrections to the Drell-Yan cross section are calculated at NLO in section 4.1, and NNLO in section 4.2 of its perturbative expansion. In both cases, we first compute the relevant cut diagrams contributing to the square matrix element and determine the hadronic tensor, which we project into structure functions. Using the scaling properties of soft and collinear fields derived in SCET, the behavior of these structure functions is then studied in the limit of soft threshold. The soft expanded helicity cross sections $\hat{\sigma}_i(z_a, z_b)$ are finally computed explicitly, providing the full-theory calculation that we will test in the next section by means of soft factorization theorems.

4.1 One-gluon emission

4.1.1 Amplitude at $\mathcal{O}(\alpha_s)$

The first order real correction to the DY process is similar to the one already seen in section 2.1.3 for the case of the $q\bar{q}$ annihilation into hadrons, but with the gluon being emitted from the initial state quark/antiquark. This is the only contribution we have to account for, as other types of processes[1] are forbidden by γ, Z being neutral. Therefore, we now focus on the subprocess

$$q(p_a) + \bar{q}(p_b) \longrightarrow V(q) + g(k), \tag{4.1}$$

with g emitted gluon of momentum k. The amplitude for this partonic subprocess is constructed by summing the amplitudes relative to the two processes displayed in Fig. 4.1, namely one where the gluon is emitted by the quark and one where is emitted by the antiquark. In the case the vector boson is a virtual photon, the amplitude reads

$$i\mathcal{M}_{R,\gamma} = g_s e^2 Q_f [\bar{v}(p_b) S_\gamma^{\mu\alpha} u(p_a)] \varepsilon_\alpha^*(k) \frac{i}{q^2} [\bar{u}(p_1)\gamma_\mu v(p_2)] \tag{4.2}$$

[1] If the vector boson is a charged W boson, one should also consider the subprocess $q + g \longrightarrow W + q$

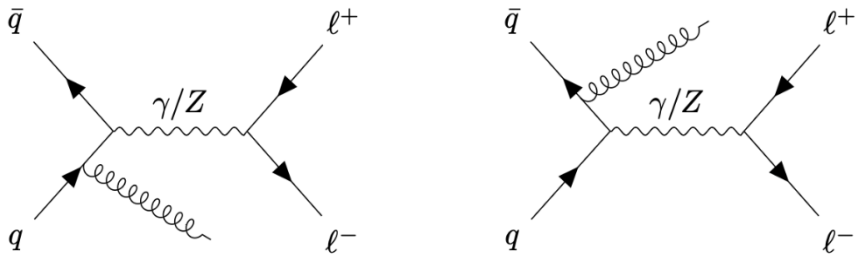

Figure 4.1: Diagrams contributing to the amplitude for the first order radiative correction to the DY process.

where the tensor $S^{\mu\alpha}$ describes the spin states of the emitting particle and the emitted gluon and is given by

$$S_\gamma^{\mu\alpha} = \left[\gamma^\mu \frac{\not{p}_a - \not{k}}{(p_a-k)^2}\gamma^\alpha - \gamma^\alpha \frac{\not{p}_b - \not{k}}{(p_b-k)^2}\gamma^\mu\right](t^a)_i^j \tag{4.3}$$

including the color generators. Taking the complex conjugate or the matrix element eq.(4.52), the spinor product $[\bar{v}S^{\mu\alpha}u]$ transforms as $[\bar{u}S^{\alpha\mu}v]$, while the complex conjugate of color generators is equal to their transpose $t^a_{ij} = t^{a\,\dagger}_{ij} = t^{a\,*}_{ji}$, being these matrices hermitian. The multiplication of $\mathcal{M}_{R,i}$ with $\mathcal{M}^*_{R,i}$, averaged over spin, color, and polarization indices, leaves us with the matrix element squared, which factorizes into a leptonic tensor of the same form as the tree level one, given by eq. (3.39), and a hadronic tensor of the form

$$W^{\mu\nu}_{R,\gamma\gamma} = -g_s^2 \frac{Q_f^2 e^2}{4N_c} C_F \mathrm{Tr}[\not{p}_b S_\gamma^{\mu\alpha} \not{p}_a S_{\gamma,\alpha}{}^\nu]\,. \tag{4.4}$$

The minus sign comes from the sum over polarizations, where every cut gives a factor $(-g_{\alpha\beta})$, with α, β polarization indices, while the factor C_F comes from the color structure $(t^a t^a)^j_j$ of the cut diagrams, that after color average indeed gives

$$\frac{1}{N_c}\sum_{a=1}^{N_c^2-1}\mathrm{Tr}[t_a t_a] = \sum_{a=1}^{N_c-1}\frac{\delta_{aa}}{N_c^2}T_F = \frac{N_c^2-1}{N_c}T_F = C_F,$$

where eq.(2.5), (2.6) have been used.

If $VV' = ZZ$, we replace the QED current J^μ_γ with the EW current J^μ_Z of eq.3.3, which leaves us with an amplitude of the same form as the one of eq.(4.2) but with the tensor of eq.(4.3) replaced by

$$S_Z^{\mu\alpha} = v_f S_\gamma^{\mu\nu} - a_f S_5^{\mu\alpha}\,. \tag{4.5}$$

and with the vector boson propagator replaced by the reduced propagator for Z boson production. This tensor is now given by the combination of a parity-conserving part,

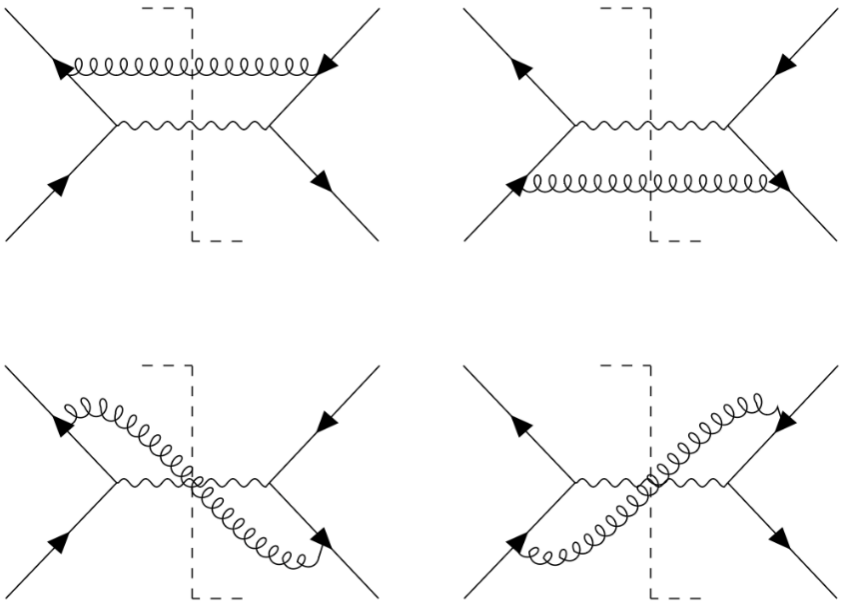

Figure 4.2: Set of cut diagrams arising from the Drell-Yan process matrix element at $\mathcal{O}(\alpha_s)$.

proportional to the vector coupling and given by the $S_\gamma^{\mu\nu}$ tensor for the electromagnetic interaction, and a parity-odd part proportional to the axial coupling, where

$$S_5^{\mu\alpha} = \left[\gamma^\mu\gamma^5 \frac{\not{p}_a - \not{k}}{(p_a-k)^2}\gamma^\alpha - \gamma^\alpha \frac{\not{p}_b - \not{k}}{(p_b-k)^2}\gamma^\mu\gamma^5\right]. \tag{4.6}$$

Squaring amplitude and averaging over all the indices, the leptonic sector does not modify, so that the leptonic tensor is again equal to the tree level one of eq.(3.42), while the hadronic tensor is given by

$$W_{R,ZZ}^{\mu\nu} = -g_s^2 \frac{e^2}{4N_c} C_F \,\mathrm{Tr}[\not{p}_b S_Z^{\mu\alpha} \not{p}_a S_\alpha{}_Z^{\nu}]\,. \tag{4.7}$$

Our main purpose is now to study the power expansion in soft gluon momentum of the structure functions in which the hadronic tensors eq.(4.4) and eq.(4.7) factorizes onto. Moreover, the cross sections we are going to derive restrict to the cases $VV' = \gamma\gamma$ and $VV' = ZZ$, which we want to compare to analyze how the angular distribution of the lepton gets modified when introducing a parity-violating interaction, such as the EW one, compared to the parity conserving QED interaction. For this reason, the computation of the interference term contributing to the total α_s square amplitude is not carried out here but can be found instead in app.B.2.

4.1.2 Hadronic tensor decomposition at $\mathcal{O}(\alpha_s)$

For one gluon emission, momentum conservation reads $q = p_a + p_b - k$, where q, p_a, and p_b are the variables we have chosen the hadronic tensor to depend on. However, because the fourth kinematic variable, namely the gluon momentum, is automatically constraint by the other ones, we can exploit this freedom to decide on which set of three momenta we want to specify the kinematic dependence of the hadronic tensors $W^{\mu\nu}_{R,\gamma\gamma}$ and $W^{\mu\nu}_{R,ZZ}$. For taking the soft limit, the most obvious choice is to pick p_a, p_b, and k. In this section however, we first derive structure functions in terms of q, p_a, and p_b and then use momentum conservation to restore the gluon momentum k when considering the limit of small gluon momentum in section 4.1.3. The reason for this choice will become clear soon. For the moment, we as usual start by treating the photon case and rewrite the Dirac structure of eq.(4.3) as

$$S^{\mu\alpha} = \gamma^\mu \frac{\not{q} - \not{p}_b}{(p_b - q)^2}\gamma^\alpha - \gamma^\alpha \frac{\not{q} - \not{p}_a}{(p_a - q)^2}\gamma^\mu \,. \tag{4.8}$$

In addition, because the projectors $P_i^{\mu\nu}$ depends on the Lorenz invariants q^2, s_{aq} and s_{bq}, we define partonic-like Mandelstam variables s, t, u related to these invariants by

$$s = (p_a + p_b)^2 = s_{ab} \qquad t = (p_b - q)^2 = -s_{bq} + q^2 \qquad u = (p_a - q)^2 = -s_{aq} + q^2 \tag{4.9}$$

and satisfying $s + t + u = q^2$. Using these identities, we can express both the hadronic tensor of eq.(4.4) and the projectors in terms of s, t, and u. Thus, performing their contraction and isolating the function of the kinematic variables from constant factors and couplings, we obtain that the structure functions can be written as

$$W^i_{R,\gamma\gamma} = g_s^2\, C_F \left(\frac{8\pi\alpha_{em}Q_f^2}{N_c}\right) T^i_R \qquad i = \text{incl}, \ldots 7 \tag{4.10}$$

where the functions T^i are equal to

$$\begin{aligned}
T^{\text{incl}}_R &= \left(\frac{(q^2+u)^2 + (q^2+t)^2}{ut}\right) \\
T^0_R &= \left(\frac{q^2-u}{q^2-t} + \frac{q^2-t}{q^2-u}\right) \\
T^1_R &= \sqrt{\frac{q^2 s}{tu}}\left(\frac{q^2-u}{q^2-t} - \frac{q^2-t}{q^2-u}\right) \\
T^2_R &= \left(\frac{q^2-u}{q^2-t} + \frac{q^2-t}{q^2-u}\right)
\end{aligned} \tag{4.11}$$

and the ones with $i = 3, 4, 5, 6, 7$ vanish identically. As a result of the transverse momentum contribution introduced by the emitted gluon, some structure functions, which were equal to zero in the tree-level calculation, have now switched on. These correspond

to the projection of the hadron tensor onto longitudinal ($i = 0$) and transverse ($i = 2$) polarization states and a combination of both ($i = 1$). In particular, we notice that the transverse and longitudinal projections are the same at this order, thus implying, according to our discussion of section 3.2.3, that also $A_0 = A_2$. This equality is known as Lam-Tung relation [67] and has been proven to hold only up to NLO [68].

Focusing now on the Z boson production case, we can write the tensor eq.(4.7) interms of the dirac structure $S_\gamma^{\mu\nu}$ and $S_5^{\mu\nu}$. This operation allows us to once again decompose the hadronic tensor into a symmetric and an antisymmetric part,

$$W^{\mu\nu}_{R,ZZ} = -g_s^2 \frac{e^2}{4N_c} C_F \Big[(v_f^2 + a_f^2)\mathrm{Tr}[\not{p}_b S_\gamma^{\mu\alpha} \not{p}_a S_{\alpha\gamma}{}^{\nu}] - 2v_f a_f \mathrm{Tr}[\not{p}_b S_\gamma^{\mu\alpha} \not{p}_a S_{\alpha 5}{}^{\nu}] \Big]. \tag{4.12}$$

where the symmetric part is proportional to the tensor $W^{\mu\nu}_{R,\gamma\gamma}$. Accordingly, the structure functions with $i = \{incl, 1, 0, 1, 2\}$ will have the same form as the ones of eq.(4.11) apart from a multiplying factor involving coupling terms, that is

$$W^i_{R,ZZ} = g_s^2 C_F \left(\frac{8\pi\alpha_{em}}{N_c} (v_f^2 + a_f^2) \right) T^i_R, \qquad i = \mathrm{incl}, 0, 1, 2\,. \tag{4.13}$$

The antisymmetric part instead, is responsible for the function with $i = 4$, also present at tree level and quantifying the difference between left-handed and right-handed helicity states, and turns on the one with $i = 3$ as well, and which corresponds again to a combination of transverse and longitudinal helicity states. For these two indices, we thus have that

$$W^i_{R,ZZ} = g_s^2 C_F \left(\frac{8\pi\alpha_{em}}{N_c} (-4v_f a_f) \right) T^i_R, \qquad i = 3, 4 \tag{4.14}$$

with

$$\begin{aligned} T_R^3 &= \sqrt{\frac{(q^2-u)(q^2-t)}{ut}} \left(\frac{q^2-u}{q^2-t} - \frac{q^2-t}{q^2-u} \right) \\ T_R^4 &= \sqrt{\frac{q^2 s}{(q^2-t)(q^2-u)}} \left(\frac{(q^2-u)^2 + (q^2-t)^2}{ut} \right). \end{aligned} \tag{4.15}$$

The other structure functions, with indices $i = 5, 6, 7$ instead vanish. Hence, the projections of the hadronic tensor for both photon and Z boson production can be written in terms of the same functions of the kinematic variables, which divide into parity-even and parity-odd ones, respectively given by eq.(4.11) and (4.15). Moreover, the reason we have decided to write these functions in terms of the Mandelstam variables eq.(4.9) and the invariant mass q^2 is to directly compare them with the ones calculated in [6], with which they agree apart from constant factors involving powers of 2.

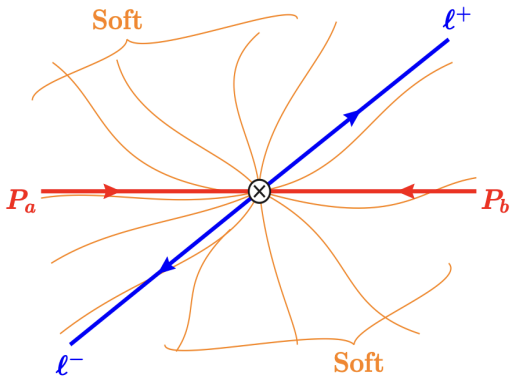

Figure 4.3: Drell-Yan process at soft threshold. Image taken from reference [69].

4.1.3 Soft limit

In section 2.2.2, we have seen that the hierarchy of the momentum components of collinear, anticollinear, and soft fields is encoded in the powers of the small parameter λ that defines their scalings. In the case of the Drell-Yan process at soft threshold, the modes p_n and $p_{\bar{n}}$ correspond to the collinear and anticollinear modes inside the colliding protons, and therefore $\lambda = \Lambda_{\text{QCD}}/Q$. On the other hand, protons do not contain soft degrees of freedom, and therefore the scaling of the soft modes p_s cannot be expressed in terms of the same small power counting parameter. Instead, we notice that, using conservation of momentum $p_a + p_b - p_X = q$, the plus and minus component of the hadronic radiation p_X can be written as

$$p_X^- = (1 - z_a)\, Q \qquad p_X^+ = (1 - z_b)\, Q\,. \tag{4.16}$$

Using that the radiation is on shell $p_X^- p_X^+ \sim p_\perp^2$ and that in SCET_{II} soft radiation scale homogeneously in λ, the scaling of soft and collinear modes is given by

$$p_c^\mu \sim \left(\frac{\Lambda_{\text{QCD}}^2}{Q}, Q, \Lambda_{\text{QCD}}\right) \qquad p_{\bar{c}}^\mu \sim \left(Q, \frac{\Lambda_{\text{QCD}}^2}{Q}, \Lambda_{\text{QCD}}\right) \qquad p_X^\mu \sim (\lambda, \lambda, \lambda)\, Q \tag{4.17}$$

with $\lambda = \sqrt{(1 - z_a)(1 - z_b)}$. These modes are depicted in fig. (4.3). Because at NLO the hadronic radiation p_X^μ is equal to the emitted gluon momentum k^μ, we can use the scaling just derived to identify distinct regions of momentum space where different types of particles dominate, and eventually to isolate the gluon's contribution to the structure functions T^i in the regime where it is emitted at soft threshold. To see this, let us first pick T^{incl} and use the identity $q^2 = t + u + s$ and the definition of these Mandelstam variables in eq.(4.9) to express this structure function in terms of k, p_a, and p_b. The result is

$$T_R^{\text{incl}} = \frac{[(p_a \cdot p_b) - (p_a \cdot k)]^2 + [(p_a \cdot p_b) - (p_b \cdot k)]^2}{(p_a \cdot k)(p_b \cdot k)}\,. \tag{4.18}$$

This expression features three distinct products of the collinear and soft momentum, which can be worked out using the scalings eq.(4.17) which, in lightcone coordinates give

$$(p_a \cdot k) = p_a^- k^+ \sim \lambda Q^2 \qquad (p_b \cdot k) = p_b^+ k^- \sim \lambda Q^2 \qquad (p_a \cdot p_b) = p_a^- p_b^+ \sim Q^2 \,. \tag{4.19}$$

Therefore, in the numerator of T_R^{incl}, the products $(p_a \cdot k)$ and $(p_b \cdot k)$ are power suppressed with respect to $(p_a \cdot p_b)$ and only amount to small corrections and can thus be discarded. Hence, in the limit of soft gluon momentum, the inclusive hadronic structure function can be written as

$$T_R^{\text{incl}} = 2\,\frac{(p_a \cdot p_b)^2}{(p_a \cdot k)(p_b \cdot k)}[1 + \mathcal{O}(\lambda)] \tag{4.20}$$

where the result has been expressed in lightcone coordinates and only the LP term has been written explicitly. We can now repeat the same steps for the other structure functions. In particular, since the variables s, t and u are in bijection with the scalar products $(p_a \cdot p_b)$, $(p_a \cdot k)$ and $(p_b \cdot k)$ respectively, the scalings of eq.(4.19) are sufficient for treating the T^is for all the indices i. For example, considering $i = 0, 2$, we have that

$$T_R^0 = T_R^2 = \frac{[(p_a \cdot p_b) - (p_a \cdot k)]^2 + [(p_a \cdot p_b) - (p_b \cdot k)]^2}{[(p_a \cdot p_b) - (p_a \cdot k)] \cdot [(p_a \cdot p_b) - (p_b \cdot k)]} = 2[1 + \mathcal{O}(\lambda^2)], \tag{4.21}$$

where the correction of order λ is absent in this case. The last function, among the parity even ones, which we still have to determine the scale of, is T_R^1. From its explicit expression in eq.(4.11), we notice that this is similar to T_R^0, but unlikely to this last it features a difference of ratios $(q^2 - u)/(q^2 - t)$ and $(q^2 - t)/(q^2 - u)$, which makes it vanishing at leading power. Hence, in this case, instead of directly useing the scaling of eq.(4.19), we expand in powers of the dimensioneless ratios $(p_a \cdot k)/(p_a \cdot p_b) \sim \lambda$ and $(p_b \cdot k)/(p_a \cdot p_b) \sim \lambda$. This results in

$$\begin{aligned} T_R^1 &= \sqrt{\frac{q^2(p_a \cdot p_b)}{(p_a \cdot k)(p_b \cdot k)}}\left(\frac{[(p_a \cdot p_b) - (p_b \cdot k)]^2 - [(p_a \cdot p_b) - (p_b \cdot k)]^2}{[(p_a \cdot p_b) - (p_a \cdot k)][(p_a \cdot p_b) - (p_b \cdot k)]}\right) \\ &= \sqrt{\frac{q^2(p_a \cdot p_b)}{(p_a \cdot k)(p_b \cdot k)}}\left[-2\left(\frac{(p_a \cdot k)}{(p_a \cdot p_b)} - \frac{(p_b \cdot k)}{(p_a \cdot p_b)}\right) + \mathcal{O}(\lambda^2)\right] \\ &= 2\left[\sqrt{\frac{p_b \cdot k}{p_a \cdot k}} - \sqrt{\frac{p_a \cdot k}{p_b \cdot k}}\right] + \mathcal{O}(\lambda) \end{aligned} \tag{4.22}$$

where in the last step we have used that at soft threshold $q^2 = (p_a \cdot p_b) + \mathcal{O}(\lambda)$. The scaling of the remaining antisymmetric structure functions is now easy to determine by noticing that their explicit form can lead back to one of the symmetric ones we have just examined. In particular, we find that in the soft limit, the functions T^4 and T^{incl}, and T_R^3 and T_R^1 have the same LP term. This can shown by noticing that

$$T_R^4 = \mathcal{C}\, T^{incl} \qquad\qquad \frac{T_R^3}{T_R^1} = \mathcal{C} \tag{4.23}$$

where $\mathcal{C}$ depends on the kinematic invariants and has scaling

$$\mathcal{C} = \sqrt{\frac{q^2(p_a \cdot p_b)}{[(p_a \cdot p_b) - (p_a \cdot k)][(p_a \cdot p_b) - (p_b \cdot k)]}} = 1 + \mathcal{O}(\lambda), \tag{4.24}$$

which proves our statement. Eventually, we thus have determined the expression and the relative scaling of the LP power term of the expansion in soft gluon momentum of all the structure functions T^i. In particular, we have found that

$$T_R^{incl} \sim T_R^4 \sim \lambda^{-2} \qquad T_R^0 \sim T_R^2 \sim T_R^1 \sim T_R^3 \sim \lambda^0, \tag{4.25}$$

where T_R^{incl} and T_R^4 are the most singular hadronic function in the limit $\lambda \to 0$ and therefore are the most sensitive to soft emissions. This fact should be of no surprise since these functions are also the only ones that do not vanish at LO, and that therefore provide the most dominant contribution to the cross-section and leptons angular distribution. Instead, according to the EFT prediction, every contraction of the hadronic tensor with z^μ produces a structure function whose scaling is suppressed by a power of λ with respect to the inclusive structure functions. However, the more general relation holds $W^{1,3} \leq \lambda^n W^{\text{incl}}$ with $n \in \mathbb{N}$(for every number of emissions). Therefore, even though we would expect $W^{1,3} \sim \lambda W^{\text{incl}}$ if the inequality would be saturated, we have a suppression of two powers of λ with respect to the inclusive structure function.

These soft expanded hadronic functions can be now used to construct soft helicity matrix elements which we will use for calculating the helicity cross-section at soft threshold. We first notice that the expansion of the T^is always gives a factor of 2 which we can incorporate in the overall normalization of the matrix elements. Instead, we include the Casimir invariant C_F into the definition of soft hadronic structure function and define

$$T_R^i \equiv \frac{2}{C_F}\, T_{R,\text{soft}}^i [1 + \mathcal{O}(\lambda)]\,. \tag{4.26}$$

If we now insert this relation into eq. (4.10) for the hadronic structure functions $W_{R,\gamma\gamma}^i$, and then use these to construct helicity matrix elements according to eq.(3.34), for $VV' = \gamma\gamma$ we can parametrize soft helicity matrix elements as follows

$$\langle |\mathcal{M}_{\gamma\gamma}|_R^2 \rangle_i = g_s^2\, 8\, \hat{\sigma}_B^{\gamma\gamma}\, T_{R,\text{soft}}^i, \tag{4.27}$$

where $i \in \{incl, 0, 1, 2\}$ and where the explicit expression for the Born level cross section is given in eq.(3.69). The same can be done for the hadronic structure functions $W_{R,ZZ}^i$ of eq.(4.14) and eq.(4.14). In this case however, the functions with $i \in \{incl, 0, 1, 2\}$ feature a different functions of the coupling $v_{l,f}$ and $a_{l,f}$ with respect to the ones with $i \in \{3, 4\}$. To introduce the same notation for both sets of indices, we define

$$\hat{\sigma}_{B,\pm}^{ZZ} \equiv \begin{cases} \hat{\sigma}_{B,+}^{ZZ} = \hat{\sigma}_B^{ZZ} & i = incl, 0, 1, 2 \\ \hat{\sigma}_{B,-}^{ZZ} = \hat{\sigma}_B^{ZZ} \cdot \dfrac{8 v_f v_l a_f a_l}{(v_f^2 + a_f^2)(v_l^2 + a_l^2)} & i = 3, 4 \end{cases} \tag{4.28}$$

where the explicit expression of the Born cross section $\hat{\sigma}_B^{ZZ}$ is also given in eq.(3.69). With this definition, we can eventually write the soft helicity matrix elements for $VV' = ZZ$ as

$$\langle|\mathcal{M}_{ZZ}|^2_R\rangle_i = g_s^2\, 8\, \hat{\sigma}_B^{ZZ,\pm}\, T^i_{R,\text{soft}}\,, \tag{4.29}$$

with $i \in \{incl, 0, 1, 2, 3, 4\}$. Notice that these matrix elements have the same normalization for the cases $VV' = \gamma\gamma$ and $VV' = ZZ$ as they should be, and the only difference in their expression is given by the value of the Born cross section. Specifically, since the soft structure functions T^i_{soft} are the same in both cases, we can simply write

$$\langle|\mathcal{M}|^2_R\rangle_i = g_s^2\, 8\, \hat{\sigma}\, T^i_{R,\text{soft}}, \tag{4.30}$$

where it is clear that, if we consider the vector boson is a photon, we have $\widetilde{\sigma}_B = \hat{\sigma}_B^{\gamma\gamma}$ and $i \in \{incl, 0, 1, 2\}$ and if the vector boson is a Z boson $\widetilde{\sigma}_B = \hat{\sigma}_{B,\pm}^{ZZ}$ and and $i \in \{incl, 0, 1, 2, 3, 4\}$. In virtue of this simplified notation we have introduced, we will also drop the label VV' in the calculation of the cross-section we will carry out in the next section since this is specified from the specific choice we make for $\widetilde{\sigma}_B$.

4.1.4 Hadronic Cross Section for single real emission

As anticipated at the end of section 3.3.3, we now only focus on the partonic helicity cross sections. We choose to express these cross sections as differential with respect to the parameters x_a and x_b and to integrate over the transverse momentum of the intermediate vector boson. We start by considering the total phase space $d\Phi_{2\to3}$, which we split into a phase space for the decaying leptons, a phase space for the emitted gluon, and phase space for the intermediate vector boson by inserting the delta function eq.(3.53). As a result, we get that

$$d\Phi_{2\to3} = d\Phi_L \times \left[\frac{d^4q}{(2\pi)^4}\frac{d^4k}{(2\pi)^3}\theta(k^0)\delta(k^2)\right](2\pi)^4\delta(q + k - p_a - p_b)\,. \tag{4.31}$$

Keeping q fixed, we can apply the change of coordinates of eq.(3.59) and integrate immediately over $\vec{q}_T$. Both the integration over the gluon momentum and over the transverse momentum are going to be performed in dimensional regularization as the cross section will display infrared divergences. This follows from the discussion of section 2.1.3, where we have seen that the NLO cross section is finite only if real *and virtual* contributions are added together. Consequently, we here generalize the definition given in eq.(3.57) for the helicity hadronic cross section at tree level to

$$\frac{d\sigma^i_R}{dx_a\, dx_b} = \sum_{ij}\int\frac{d\xi_a}{\xi_a}\int\frac{d\xi_b}{\xi_b}\, f_i(\xi_a)\, f_j(\xi_b)\, \hat{\sigma}^i_R\left(\frac{x_a}{\xi_a}, \frac{x_b}{\xi_b}, Q^2, \varepsilon\right) \tag{4.32}$$

where

$$\hat{\sigma}^i_R\left(\frac{x_a}{\xi_a}, \frac{x_b}{\xi_b}, Q^2, \varepsilon\right) = \frac{\mu^{2\varepsilon}}{4(2\pi)^2}\int\frac{d^{(d-2)}q_T}{(2\pi)^{d-2}}\int d\Phi_g\, \langle|\mathcal{M}|^2_R\rangle_i\,. \tag{4.33}$$

With this choice of normalization, the jacobian factor coming from the change of coordinates cancels against the flux factor E_{cm}^2 in front of the hadronic helicity cross-section. At the same time, all the ε dependence is absorbed into the regularized partonic cross section, which after the integration over $\vec{q}_T$ only depends on the ratios x_a/ξ_a and x_b/ξ_b and Q^2. In addition, we add a $\mu^{(d-4)}$ for every power of the coupling constant g_s^2 when working in dimensional regularization. Focusing on eq.(4.33), we first write the gluon phase space d dimensions, which based on eq.(4.31) reads

$$\int d\Phi_g^d = \int \frac{d^d k}{(2\pi)^{d-1}} \delta(k^2)\, \theta(k^0) (2\pi)^d \delta^d(q + k - p_a - p_b)\,. \tag{4.34}$$

Expressing it in lightcone coordinates, both the volume element $d^d k$ and the d-dimensional delta function δ^d factorize into a plus and minus and a transverse component in $(d-2)$ dimensions. Therefore, integrating out $d^{d-2}(\vec{q}_T - \vec{k}_T)$ against $d^{d-2}k_T$ and leaving out for the moment the theta function $\theta(k^0)$, we obtain

$$\int d\Phi_g = (2\pi) \int dk^+ dk^- \delta(k^+ k^- - q_T^2)\, \delta^-(q^- + k^- - p_a^-)\, \delta^+(q^+ + k^+ - p_b^+)\,. \tag{4.35}$$

Hence, inserting this identity into eq.(4.33) and integrating over the plus and minus components of the gluon momenta, we obtain that

$$\hat{\sigma}_R^i = \frac{g_s^2}{(4\pi)} \mu^{2\varepsilon}\, 4\, \widetilde{\sigma}_B^{\mathrm{DY}} \int \frac{d^{d-2} q_T}{(2\pi)^{d-2}}\, T^i_{R,\,\mathrm{soft}}(k^+, k^-)\, \delta(k^+ k^- - q_T^2), \tag{4.36}$$

where we have used eq.(4.30) for expressing the soft matrix element in terms of the soft hadronic functions $T^i_{R,\,\mathrm{soft}}$. Also, as seen in the previous section, these function only depends on the scalar products $(p_a \cdot k)$ and $(p_b \cdot k)$ and thus only on the components k^+, k^- of the gluon momenta. After the integration over the gluon phase space, the value of these components is fixed by the δ^+ and δ^- distribution to be equal to

$$\begin{aligned} k^- &= p_a^- - q^- = (\xi_a - x_a) P_a^- = (\xi_a - x_a) \frac{p_a^-}{\xi_a} = (1 - z_a) p_a^- = \bar{z}_a\, p_a^- \\ k^+ &= p_b^+ - q^+ = (\xi_b - x_b) P_b^+ = (\xi_b - x_b) \frac{p_b^+}{\xi_b} = (1 - z_b) p_b^+ = \bar{z}_b\, p_b^+ \end{aligned} \tag{4.37}$$

where the variables $z_i = x_i/\xi_i$ have been defined in section 2.1.4 and $\bar{z}_{ab}$ are short-hand notations for $(1 - z_{ab})$. As last, we perform the integration over the transverse momentum in eq.(4.36). We notice that $d^{d-2}q_T$ denotes the integral over the $(d-2)$ components of the vector $\vec{q}_T$ while in the argument of the delta function, we have its modulus $q_T^2 = \vec{q}_T \cdot \vec{q}_T = \sum_i^{d-2} (q_T)^i$. Hence, it is now useful to express the volume element $d^{d-2}q_T$ in lightcone coordinates, that is

$$d^{(d-2)}\vec{q}_T = dq_T\, q_T^{(d-2)-1}\, d\Omega_{(d-2)} = \frac{1}{2} dq_T^2\, (q_T^2)^{(d-4)/2} d\Omega_{(d-2)} \tag{4.38}$$

where $d\Omega_{(d-2)}$ denotes the angle subtended by a $(d-1)$ dimensional unit sphere in a $d-$ dimensional Euclidean space. Using the general formula

$$\int_{\Omega_n} d\Omega_n = \frac{2\pi^{n/2}}{\Gamma(n/2)}\,, \tag{4.39}$$

and the identity eq.(4.38), the normalized volume element over q_T can be written as

$$\int \frac{d^{d-2}q_T}{(2\pi)^{d-2}} = \frac{(4\pi)^{\varepsilon-1}}{\Gamma(1-\varepsilon)} \int dq_T^2\, (q_T^2)^{-\varepsilon}\,. \tag{4.40}$$

Thanks to this relation,we can now easily integrate out the delta function of eq.(4.64), which fixes the value of the transverse momentum to $q_T^2 = k^+k^-$ and gives back a theta function $\theta(k^+k^-)$, which ensures that $q_T^2 > 0$. In the $\overline{\text{MS}}$ eq.(4.36) therefore becomes

$$\hat{\sigma}_R^i = \left(\frac{\alpha_s}{4\pi}\right)\frac{e^{\varepsilon\gamma_E}\mu^{2\varepsilon}}{\Gamma(1-\varepsilon)}\; 4\,\widetilde{\sigma}_B\, T^i_{R,\text{soft}}(k^+,k^-)(k^+k^-)^{-\varepsilon}\,\theta(k^0)\theta(k^+k^-), \tag{4.41}$$

after reinstating the Heaviside theta functions. At this point, consistently with eq.(4.37), which defines a bijection between the gluon momenta $k^\pm$ and the parameters z_a and z_b, we can rewrite the whole cross-section in terms of these dimensionless ratios. Using the definition of the variable $z_{a,b} = x_{a,b}/\xi_{a,b}$, the real hadronic cross sections of eq.(4.32) becomes

$$\frac{d\sigma_R^i}{dx_a\,dx_b} = \sum_{ij}\int\frac{dz_a}{z_a}\int\frac{dz_b}{z_b}\, f_i\!\left(\frac{x_a}{z_a}\right) f_j\!\left(\frac{z_b}{x_b}\right)\hat{\sigma}_R^i(z_a,z_b,Q^2,\varepsilon) \tag{4.42}$$

and where the cross sections $\hat{\sigma}_R^i(z_a,z_b,Q^2,\varepsilon)$ are given by using eq.(4.37) into eq.(4.41). In addition, we can absorbed the factor $(Q^2\bar{z}_a\bar{z}_b)^{-\varepsilon}$ coming from dimensional regularization into the soft hadronic functions $T^i_{R,\text{soft}}$, which at their turn gain an ε dependence,

$$T^i_{R,\text{soft}}(z_a,z_b,Q^2,\varepsilon) = Q^{-2\varepsilon}(1-z_a)^{-\varepsilon}(1-z_b)^{-\varepsilon}\, T^i_{R,\text{soft}}(z_a,z_b)\,. \tag{4.43}$$

The cross-section $\sigma_R(z_a,z_b,Q^2,\varepsilon)$ can be then calculated by expanding these regularized soft structure functions around $\varepsilon = 0$. As we have seen in the previous section, $T^i_{R,}$ with $i = 0,1,2,3$ scale as λ^0, and therefore their cross-section is finite in this limit. Expressing these functions, i.e. eq.(4.21) and (4.22) in terms of the variables $\bar{z}_a$ and $\bar{z}_b$ according to the normalization prescription defined in eq.(4.26), we thus have that

$$\begin{aligned} T^0_{R,\text{soft}} &= T^2_{R,\text{soft}} = C_F\,(Q^2\bar{z}_a\bar{z}_b)^{-\varepsilon} + \mathcal{O}(\lambda) \\ T^1_{R,\text{soft}} &\sim T^3_{R,\text{soft}} = C_F\,(Q^2\bar{z}_a\bar{z}_b)^{-\varepsilon}\left(\sqrt{\frac{\bar{z}_a}{\bar{z}_b}} - \sqrt{\frac{\bar{z}_b}{\bar{z}_a}}\right) + \mathcal{O}(\lambda) \end{aligned} \tag{4.44}$$

Hence, expanding around four spacetime dimensions, we obtain the following partonic cross-sections

$$\begin{aligned} \hat{\sigma}^0_R(z_a,z_b,Q^2) &= \left(\frac{\alpha_s}{4\pi}\right) 4\,C_F\,\widetilde{\sigma}_B\;\theta(\bar{z}_a)\theta(\bar{z}_b) \\ \hat{\sigma}^1_R(z_a,z_b,Q^2) &= \left(\frac{\alpha_s}{4\pi}\right) 4\,C_F\,\widetilde{\sigma}_B\left(\sqrt{\frac{\bar{z}_a}{\bar{z}_b}} - \sqrt{\frac{\bar{z}_b}{\bar{z}_a}}\right)\theta(\bar{z}_a)\theta(\bar{z}_b) \end{aligned} \tag{4.45}$$

where $\hat{\sigma}^0_R(z_a, z_b, Q^2) = \hat{\sigma}^2_R(z_a, z_b, Q^2)$ and $\sigma^1_R(z_a, z_b, Q^2) \sim \sigma^3_R(z_a, z_b, Q^2)$ is understood. Focusing now on $T^{\text{incl}}_{R,\text{soft}} \sim T^4_{R,\text{soft}}$, they have scaling λ^{-2}. Clearly, in the limit of vanishing gluon momentum $\lambda \to 0$, these functions are singular. The finite part of the cross sections σ^{soft}_R and σ^{soft}_R can thus be obtained by the λ^0 term of their power expansion. Hence, expanding eq.(4.18) up to zeroth order in λ and changing variable to $\bar{z}_a$, $\bar{z}_b$, the inclusive soft hadronic function reads

$$T^{\text{incl}}_{R,\text{soft}} = C_F\,(Q^2 \bar{z}_a \bar{z}_b)^{-\varepsilon}\left[\frac{1}{\bar{z}_a\,\bar{z}_b} - \frac{1}{\bar{z}_a} - \frac{1}{\bar{z}_b} + \frac{1}{2}\left(\frac{\bar{z}_a}{\bar{z}_b} + \frac{\bar{z}_b}{\bar{z}_a}\right)\right] + \mathcal{O}(\lambda)\,. \tag{4.46}$$

From the discussion carried out in section 2.1.4, we know that the inclusive cross section displays a UV pole, which cancels out against the UV pole of the virtual contribution, and a double IR pole, which gets canceled by the one of the lowest order Altarelli-Parisi kernel. To make this double pole manifest, we use the identity

$$\frac{1}{z^{1+\varepsilon}} = -\frac{\delta(z)}{\varepsilon} + \mathcal{L}_0(z) - \varepsilon\mathcal{L}_1(z) + \mathcal{O}(\varepsilon^2) \tag{4.47}$$

where the distributions $\mathcal{L}_0$ and $\mathcal{L}_1$ are defined in terms of the *plus distribution* (see app.A.1) and are given by

$$\mathcal{L}_0(z) = \left[\frac{1}{z}\right]_+ \qquad\qquad \mathcal{L}_1(z) = \left[\frac{\ln(z)}{z}\right]_+ . \tag{4.48}$$

We now plug the identity eq.(4.47) into the soft inclusive hadronic function eq.(4.46) and expand around $\varepsilon = 0$ up to the first order. The expression we obtain in this way can in turn be inserted into eq.(4.41) and, minimally subtracting the singular part,

$$\begin{aligned}[\hat{\sigma}^{\text{incl}}_R]_{\text{sing}}(z_a, z_b) = \left(\frac{\alpha_s}{4\pi}\right) 4\widetilde{\sigma}_B\, C_F \times \\ \left[\frac{1}{\varepsilon^2}\,\delta(\bar{z}_a)\delta(\bar{z}_b) + \frac{1}{\varepsilon}\Big[\delta(\bar{z}_a)\big(1 - \bar{z}_b/2 - \mathcal{L}_0(\bar{z}_b)\big) + (\bar{z}_a \leftrightarrow \bar{z}_b)\Big]\right]\end{aligned} \tag{4.49}$$

we obtain that the finite inclusive hadronic cross section is equal to

$$\begin{aligned}\hat{\sigma}^{\text{incl}}_R(z_a, z_b) = \left(\frac{\alpha_s}{4\pi}\right) 4\widetilde{\sigma}_B\, C_F \Bigg\{ &-\frac{1}{12}\delta(\bar{z}_a)\delta(\bar{z}_b)(\pi^2 - 6\ln^2 M^2) + \delta(\bar{z}_a)\mathcal{L}_1(\bar{z}_b) + \delta(\bar{z}_b)\mathcal{L}_1(\bar{z}_a) \\ &\mathcal{L}_0(\bar{z}_a)\mathcal{L}_0(\bar{z}_b) + \Bigg[-\delta(\bar{z}_a)\Big[(\ln M^2 + \log(\bar{z}_b))\Big(1 - \frac{\bar{z}_b}{2}\Big) \\ &+ \mathcal{L}_0(\bar{z}_b)\ln M^2 + \mathcal{L}_0(\bar{z}_a)\Big(1 - \frac{\bar{z}_b}{2}\Big) + (\bar{z}_a \longleftrightarrow \bar{z}_b)\Bigg]\Bigg\}\end{aligned} \tag{4.50}$$

where M^2 is a shorthand notation for $M^2 = \mu^2/Q^2$. Clearly, the leadinf power cross section $\hat{\sigma}^4_R(z_a, z_b)$ has the same form.

4.2 Two-gluons emission

4.2.1 Amplitude at $\mathcal{O}(\alpha_s^2)$

We now consider the order α_s^2 radiative correction to the DY process in the case the vector boson is a virtual photon. This choice is supported by the fact that, as we have seen in section 4.1.3, the LP contribution of the (only non-vanishing) parity-odd structure functions T_R^3 and T_R^4 is, except from terms of order λ, the same as the parity-even structure functions T_R^1 and T_R^{incl}. Therefore, we can simply focus on the QED process knowing that, apart from a normalization factor involving the vector and axial couplings, the results we derive also hold if the intermediate vector boson is a Z-boson. The second order real correction to the unpolarized proton-proton scattering is given by the 2 gluons emission process

$$q(p_a) + \bar{q}(p_b) \longrightarrow \gamma(q) + g(k_1) + g(k_2), \tag{4.51}$$

where the two gluons can be radiated either from the quark/antiquark or by an additional gluon emitted from the quark/antiquark line. The relevant vertices are dispalyed in fig.4.4. The amplitude can be now written as

$$i\mathcal{M}_{RR} = g_s^2 Q_f e^2\, \bar{v}(p_b)\Bigg[\sum_{perm}\sum_{\bullet} S_{\bullet}^{\mu\alpha_1\alpha_2}\, \epsilon^*_{\alpha_1}(k_1)\epsilon^*_{\alpha_2}(k_2)\Bigg]u(p_a)\frac{i}{q^2}[\bar{u}(p_1)\gamma_\mu v(p_2)] \tag{4.52}$$

where the first sum accounts for the permutation of the external gluon lines ($\alpha_1 \longleftrightarrow \alpha_2$) and the second for the topologically independent types of vertices, i.e. $\bullet = \{gg\gamma\}$, $\{\gamma gg\}$, $\{g\gamma g\}$, $\{2g\gamma\}$, $\{\gamma 2g\}$. Again, we label $S_{\bullet}^{\mu\alpha_1\alpha_2}$ the tensors constructed out of momentum vectors and Dirac matrices which describe the spin structure of the vertices. Including their color structure, these tensors are given by

$$\begin{aligned}
S_{gg\gamma}^{\mu\alpha_1\alpha_2} &= \left[\gamma^\mu \frac{\not{p}_a - \not{k}_1 - \not{k}_2}{(p_a-k_1-k_2)^2}\gamma^{\alpha_1}\frac{\not{p}_a - \not{k}_2}{(p_a-k_2)^2}\gamma^{\alpha_2}\right](t^a t^b)^l_m \\
S_{\gamma gg}^{\mu\alpha_1\alpha_2} &= \left[\gamma^{\alpha_1} \frac{\not{p}_b - \not{k}_1}{(p_b-k_1)^2}\gamma^{\alpha_2}\frac{\not{p}_b - \not{k}_1 - \not{k}_2}{(p_b-k_1-k_2)^2}\gamma^{\mu}\right](t^a t^b)^l_m \\
S_{g\gamma g}^{\mu\alpha_1\alpha_2} &= \left[-\gamma^{\alpha_1} \frac{\not{p}_b - \not{k}_1}{(p_b-k_1)^2}\gamma^{\mu}\frac{\not{p}_a - \not{k}_2}{(p_a-k_2)^2}\gamma^{\alpha_2}\right](t^a t^b)^l_m \\
S_{2g\gamma}^{\mu\alpha_1\alpha_2} &= \left[\gamma^{mu} \frac{\not{p}_a - \not{k}_1 - \not{k}_2}{(p_a-k_1-k_2)^2}\frac{V^{\alpha_1\alpha_2}}{(k_1+k_2)^2}\right]([t^a,t^b])^l_m \\
S_{2g\gamma}^{\mu\alpha_1\alpha_2} &= \left[\frac{-V^{\alpha_1\alpha_2}}{(k_1+k_2)^2}\frac{\not{p}_b - \not{k}_1}{(p_b-k_1)^2}\gamma^{\mu}\right]([t^a,t^b])^l_m
\end{aligned}$$

$$V^{\alpha_1\alpha_2} = g^{\alpha_1\alpha_2}(\not{k}_2 - \not{k}_1) + \gamma^{\alpha_1}(2k_1+k_2)^{\alpha_2} - \gamma^{\alpha_2}(2k_2+k_1)^{\alpha_1} \tag{4.53}$$

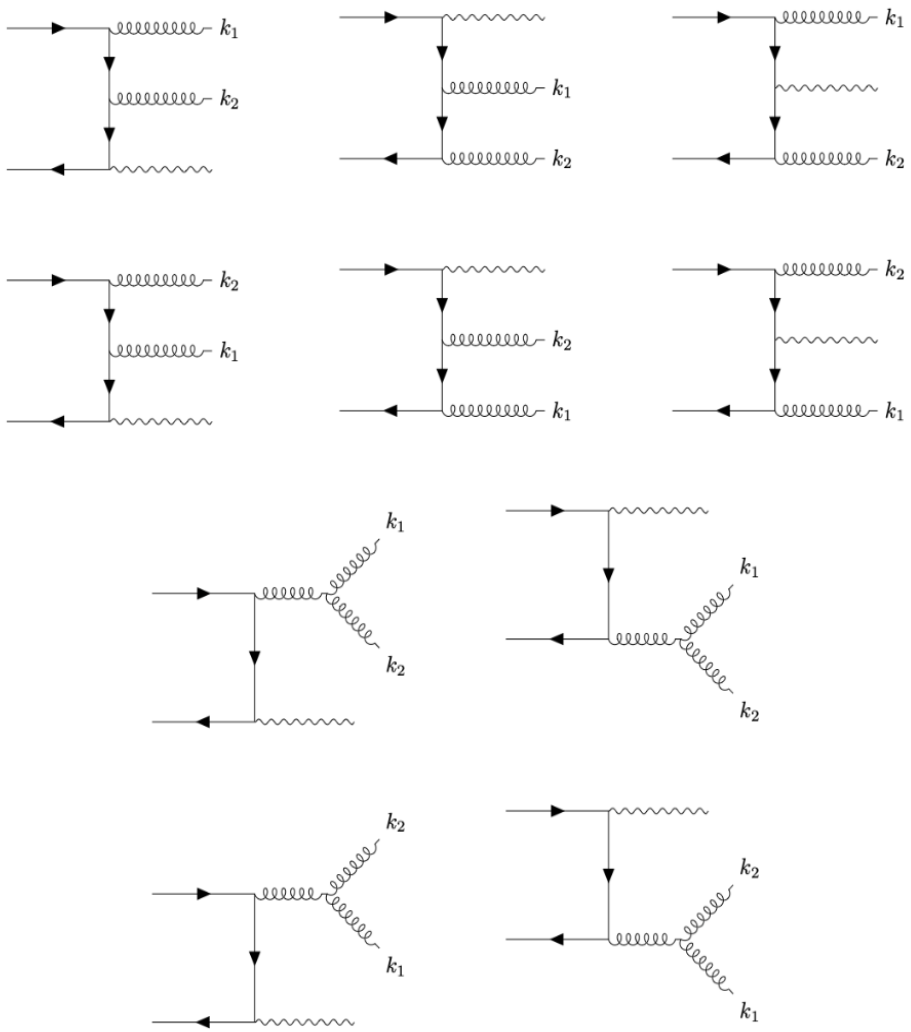

Figure 4.4: 2-gluons emission vertices. The diagrams constructed out of the vertices in the first two lines include both C_F^2 and $C_F C_A$ color structure. Diagrams constructed out of the vertices of the third and fourth lines only include $C_F C_A$ color structure. In particular, the abelian contribution of the total 2-gluon emission amplitude does not include the vertices of the last two lines.

where, for the vertex involving the three-gluon coupling, eq.(2.3) have been used. Squaring the matrix element (4.52) and averaging over spin, color and polarization leaves us with the following hadronic tensor

$$W_{RR} = \frac{g_s^4 e^2 Q_f^2}{4N_c^2} \sum_{perm} \sum_{\bullet,\,\star} \mathrm{Tr}[\not{p}_b S_\bullet^{\mu\alpha_1\alpha_2} \not{p}_a \tilde{S^\nu}_{\alpha_1\alpha_2,\star}] \tag{4.54}$$

where $\tilde{S^\nu}_{\alpha_1\alpha_2,\bullet} = \gamma^0 (S_\bullet^{\nu\beta_1\beta_2})^* \gamma^0 g_{\alpha_1\beta_1} g_{\alpha_2\beta_2}$. Having two possible permutations and five independent vertices, this tensor is given by the sum of $(2\times 5)^2 = 100$ traces. Also, the permutation of the external gluon lines implies the permutation of the vertices, so that $t^a t^b \to t^b t^a$, while the complex conjugate of the color generators is equal to their transpose (as these are self-adjoin matrices) as we have already seen for the one-gluon emission case. Accordingly, each of the traces making up the hadronic tensor eq.(4.54) carry one of the following two color structures,

$$(t^a t^b)^l_m (t^b t^a)^m_l \qquad\qquad (t^a t^b)^l_m (t^a t^b)^m_l \tag{4.55}$$

In the first case, the first (second) emitted gluon is color-connected to itself, while cut diagrams involving the second have crossing gluon lines. When summing over the color indices, these two structure can be explicitly evaluated using eq.(2.5) and eq.(2.6) and correspond to

$$\begin{aligned} &\frac{1}{N_c}\mathrm{Tr}[t^a t^a t^b t^b] = \frac{C_F^2}{N_c}\mathrm{Tr}[\mathbb{I}] = C_F^2 \\ &\frac{1}{N_c}\mathrm{Tr}[t^a t^b t^a t^b] = -\frac{1}{4N_c^2}\sum_{a=1}^{N_c^2-1}\delta_{aa} = C_F(C_F - C_A/2)\,. \end{aligned} \tag{4.56}$$

In particular, since $C(F) \sim N_c$ and $\big(C(F) - C(A)/2\big) \sim N_c^{-1}$, cut diagrams with crossing gluon lines are suppressed by a factor $1/N_c^2$ relative to the diagrams with non-crossing lines. On the other hand, $S_\bullet^{\mu\alpha_1\alpha_2}$ tensors with $\bullet = \{2g\gamma\}, \{\gamma 2g\}$ are proportional to the commutator of color generators, so that in reality we have an additional color structure besides the ones of eq.(4.55), that is $([t^a, t^b])^l_m ([t^b, t^a])^k_m$. Since this structure though is not independent from the other two, as

$$\frac{1}{N_c}([t^a, t^b])^l_k ([t^b, t^a])^k_l = \frac{2}{N_c}\big(\mathrm{Tr}[t^a t^a t^b t^b] - \mathrm{Tr}[t^a t^b t^a t^b]\big) = C_F C_A \tag{4.57}$$

we can pick any two out of these three functions of the Casimir operators as color basis. For practical convenience, we choose this basis to be formed out of C_F^2 and $C_F C_A$, and therefore any observable depending on the initial state dynamics can be written as a linear combination of these two terms.

4.2.2 Hadronic tensor decomposition at order $\mathcal{O}(\alpha_s^2)$ and scaling

The information we now want to extract from the square matrix element of the second order radiative correction is the form and the scaling of the LP term of its helicity

components in the soft limit. However, considering the higher complexity of $W^{\mu\nu}_{RR}$ compared to $W^{\mu\nu}_{R}$, is not practical to first project the hadronic tensor into structure functions and then take its soft limit as done for the one gluon case. Indeed, this would only bring to a full power expansion in soft momentum, of which we would then discard subleading power terms. What we can do instead, is to exploit the fact that the contraction with the projectors $P^i_{\mu\nu}$ and the expansion in powers of the small parameter λ are commuting operations. Hence, we can first take the soft limit at the amplitude level by using that $k_1^\mu \sim k_2^\mu \sim (\lambda,\lambda,\lambda)Q$ in the $S^{\mu\alpha_1\alpha_2}_{\bullet}$ tensors of eq.(4.53). A unique parameter λ is sufficient as the two gluons are identical. These tensors, and therefore the amplitude, scale all homogeneously as λ^{-2}, as we expect in the case of two soft singularities, while the hadronic tensor -which is constructed out of two of these dirac structures- therefore scales as λ^{-4}. Then, we can expand the projectors $P^i_{\mu\nu}$ in the same way, whose leading power term is proportional to λ^0 as they are non-singular. Contracting the soft-expanded projectors with the soft-expanded hadronic tensor allows us to directly construct the soft helicity matrix elements as given by eq.(3.34), which can be written as

$$\langle|\mathcal{M}|^2_{RR}\rangle_i = g_s^4\, 8\, \hat{\sigma}_B^{\gamma\gamma}\, T^i_{RR,\text{soft}}, \tag{4.58}$$

where we have multiplied by 1/2 because the two gluons are identical. Here, we only give the explicit expression for the abelian term of $T^{incl}_{RR,\text{soft}}$ and of $T^0_{RR,\text{soft}}$, that is

$$\begin{aligned} T^{\text{incl}}_{RR,\text{soft}} &= C_F^2\, \frac{p_a^- p_b^+}{k_1^+ k_1^- k_2^+ k_2^-} + \mathcal{O}(C_F C_A) \\ T^0_{RR,\text{soft}} &= C_F^2 \left(\frac{1}{k_1^- k_1^+} + \frac{1}{k_2^- k_2^+}\right) + \mathcal{O}(C_F C_A)\,. \end{aligned} \tag{4.59}$$

Evidently, with the term abelian we refer to diagrams with color structure C_F^2, where the name derives from the fact that the vertices involved in these diagrams also appear in commutative gauge theories such as QED. All the other functions $T^i_{RR,\text{soft}}$ depend instead on the scalar product between the gluons transverse momenta $(\vec{k}_{1,T}\cdot\vec{k}_{2,T})$, which makes them azimuthally asymmetric. In this case, the derivation of the helicity cross sections involves integration over the angle spanned by the transverse momenta $\vec{k}_{T,1}$ and $\vec{k}_{T,2}$ in dimensional regularization (which should hide additional collinear singularities). For simplicity, we therefore focus on the C_F^2 term of $T^i_{RR,\text{soft}}$ for $i \in \{incl, 0\}$ only. Note that, as given from eq.(4.59), $T^{incl}_{RR,\text{soft}}$ has the same form of $T^{incl}_{R,\text{soft}}$ (see eq.(4.18)) but with k^+k^- replaced by $k_1^+k_1^-k_2^+k_2^-$. The same cannot be stated for $T^0_{RR,\text{soft}}$, since the leading power term of $T^0_{R,\text{soft}}$ was simply the identity. The exponentiation properties of the amplitude are hard to check in QCD but easy to compute using soft factorization theorems, as these constitute all order ansatz. We will explicitly apply these theorems to the calculation of the single real and double real emission at LP and NNLP in the next chapter.

4.2.3 Hadronic cross section for double real emission

The discussion presented in this section will closely follow the one carried out in section 4.1.4 and, as in that case, we first start by splitting the phase space $d\Phi_{2\to4}$ by using the identity eq.(3.53). As a result, we obtain

$$d\Phi_{2\to4} = d\Phi_L \times \left[\frac{d^4q}{(2\pi)^4}\prod_{i=1}^{2}\frac{d^4k_i}{(2\pi)^3}\theta(k_i^0)\delta(k_i^2)\right](2\pi)^4\delta^4(q+k_1+k_2-p_a-p_b)\,. \tag{4.60}$$

Remaining differential with respect to q, expressing the volume element d^4q as $dx_a\,dx_b\,d^2q_T$ using eq.(3.59) and integrating over transverse momentum, the hadronic helicity cross sections for the double real emission reads

$$\frac{d\sigma^i_{RR}}{dx_a dx_b} = \sum_{ij}\int\frac{d\xi_a}{\xi_a}\int\frac{d\xi_b}{\xi_b}\,f_i(\xi_a)\,f_j(\xi_b)\,\hat{\sigma}^i_{RR}\left(\frac{xi_a}{\xi_a},\frac{x_b}{\xi_b},Q^2,\varepsilon\right). \tag{4.61}$$

In total analogy to the single gluon emission, the partonic cross section in this expression is defined as

$$\hat{\sigma}^i_{RR}\left(\frac{\xi_a}{\xi_a},\frac{x_b}{\xi_b},Q^2,\varepsilon\right) = \frac{\mu^{4\varepsilon}}{4(2\pi)^2}\int\frac{d^{d-2}q_T}{(2\pi)^{d-2}}\int d^d\Phi_{2g}\,\langle|\mathcal{M}|^2_{RR}\rangle_i \tag{4.62}$$

using the same normalizaiton as before and where $d\Phi_{2g}$ denotes the two-gluons phase space. Moreover, we have introduced a factor $\mu^{4\varepsilon}$ to compensate for the power g_s^4 of the strong coupling in the double real helicity matrix element. Focusing on the phase space first, expressing it in lightcone coordinates gives

$$\begin{aligned}\int\frac{d^{d-2}q_T}{(2\pi)^{d-2}}\int d^d\Phi_{2g} = \frac{1}{2}\int\frac{d^{d-2}k_{T,1}}{(2\pi)^{d-2}}\int\frac{d^{d-2}k_{T,2}}{(2\pi)^{d-2}}\int dk_1^+\,dk_1^-\,dk_2^+\,dk_2^-\,\delta(k_1^+k_1^- - k_{T,1}^2)\\ \times\,\delta(k_2^+k_2^- - k_{T,2}^2)\,(2\pi)^{d-2}\delta^{d-2}(\vec{q}_T-\vec{k}_{T,1}-\vec{k}_{T,2})\\ \times\,\delta^-(q^- - p_a^- + k_1^- + k_2^-)\,\delta^+(q^- - p_b^+ + k_1^+ + k_2^+)\end{aligned} \tag{4.63}$$

leaving the Heaviside theta functions implicit for the moment and where the factor 1/2 is the Jacobian for the change of coordinates. In this equation, can first eliminate the (d-2)-dimensional delta function by integrating it in q_T, so as to get rid of any vector quantity in the regularized integration measure. Then we can use eq.(4.40) for integrating the delta functions $\delta(k_1^2)$, $\delta(k_2^2)$ in $k_{T,1}^2$, $k_{T,2}^2$. After these steps, the cross-section eq.(4.62) in the $\overline{\text{MS}}$-scheme is equal to

$$\begin{aligned}\hat{\sigma}^i_{RR} = \left(\frac{\alpha_s}{4\pi}\right)^2\frac{(e^{\gamma_E}\mu^2)^{2\varepsilon}}{\Gamma(1-\varepsilon)^2}\,4\,\hat{\sigma}_B^{\gamma\gamma}\int dk_1^+\,dk_1^-\,dk_2^+\,dk_2^-\,(k_1^+k_1^-k_2^+k_2^-)^{-\varepsilon}\\ \times\,\delta^-(q^- - p_a^- + k_1^- + k_2^-)\,\delta^-(q^+ - p_b^+ + k_1^+ + k_2^+)\,T^i_{RR\,\text{soft}}(k_1^\pm,k_2^\pm)\,.\end{aligned} \tag{4.64}$$

At this point, we are left with four integrals, over the plus and minus components of the gluons momenta, and two constraints, given by the two remaining delta functions δ^-

and δ^+. Because we want to treat k_1 and k_2 on an equal footing, it is useful to change coordinates to the sum and difference of lightcone momenta, so that the integration measure modifies as

$$dk_1^+\, dk_1^-\, dk_2^+\, dk_2^- = \frac{1}{4}\, d(k_1^+ + k_2^+)\; d(k_1^+ - k_2^+) d(k_1^- + k_2^-)\, d(k_1^- - k_2^-)\,. \tag{4.65}$$

In this way, the delta functions δ^+ and δ^- now depend only on one of the new variables and can thus be trivially integrated out. In particular, their argument fixes the value of the variables z_a and z_b, given by

$$\begin{aligned} z_a &= \frac{q^-}{p_a^-} = 1 - \frac{k_1^- + k_2^-}{p_a^-} \\ z_b &= \frac{q^+}{p_b^+} = 1 - \frac{k_1^+ + k_2^+}{p_b^+}\,. \end{aligned} \tag{4.66}$$

As last, we still have two non-trivial integrals over $(k_1^+ - k_2^-)$ and $(k_1^- - k_2^-)$ to perform. Their domain is fixed by the Heaviside functions $\theta(k_1^0)$, $\theta(k_1^+ k_1^-)$ and $\theta(k_2^0)$, $\theta(k_2^+ k_2^-)$, which set

$$k_1^+ - k_2^+ < |k_1^+ + k_2^+| \qquad \wedge \qquad k_1^- - k_2^- < |k_1^- + k_2^-|\,. \tag{4.67}$$

Eventually substituting the values of the soft hadronic structure functions $T^i_{RR,\text{soft}}$ given by eq.(4.59) into eq.(4.64) and integrating over $(k_1^+ - k_2^+)$ and $(k_1^- - k_2^-)$, we obtain the following partonic cross-sections

$$\begin{aligned} \hat{\sigma}^{\text{incl}}_{RR} &= \left(\frac{\alpha_s}{4\pi}\right)^2 4\,\hat{\sigma}_B^{\gamma\gamma} C_F^2 \left[-4^{1+2\varepsilon} \frac{(e^{\gamma_E}\mu^2)^{2\varepsilon}}{\Gamma(1-\varepsilon)^2} \frac{\Gamma(-\varepsilon)\Gamma(1/2+\varepsilon)}{\Gamma(1/2-\varepsilon)\Gamma(1+\varepsilon)} \frac{p_a^- p_b^+}{(\pi\,\text{Cot}(\varepsilon\pi))^{-1}} \right] (k_{mp} k_{pp})^{1-2\varepsilon} \\ \hat{\sigma}^0_{RR} &= \left(\frac{\alpha_s}{4\pi}\right)^2 4\,\hat{\sigma}_B^{\gamma\gamma} C_F^2 \left[2^{1+4\varepsilon} \frac{(e^{\gamma_E}\mu^2)^{2\varepsilon}}{\Gamma(1-\varepsilon)^2} \frac{\pi\Gamma(-\varepsilon^2)}{\Gamma(1/2-\varepsilon)^2} \right] (k_{mp} k_{pp})^{-2\varepsilon} \Bigg\} \end{aligned} \tag{4.68}$$

where we have introduced the short-hand notation $k_{pp} = k_1^+ + k_2^+ = p_a^- \bar{z}_a$ and $k_{mp} = k_1^- + k_2^- = \bar{z}_b p_b^+$ and divided by the jacobian of the change of coordinates eq.(4.65). Expressing k_{pp} and k_{pm} in terms of $\bar{z}_a$ and $\bar{z}_b$, the cross-sections eq.(4.68) are only functions of these ratios and the hard scale Q. At this point, the zeroth cross-section can be simply evaluated by expanding around $\varepsilon = 0$ and is given by

$$\hat{\sigma}^0_{RR} = \left(\frac{\alpha_s}{4\pi}\right)^2 4\,\hat{\sigma}_B^{\gamma\gamma} C_F \left[\frac{2}{\varepsilon^2} + \frac{4}{\varepsilon} \ln\!\left(\frac{\mu^2}{Q^2 \bar{z}_a \bar{z}_b}\right) + 4\ln^2\!\left(\frac{\mu^2}{Q^2 \bar{z}_a \bar{z}_b}\right) - \pi^2 \right]. \tag{4.69}$$

Instead, we work the inclusive helicity cross-section by using the distribution identity eq.(4.47) and then expanding around four spacetime dimensions. Minimally subtracting

the singular part,

$$
\begin{aligned}
[\hat{\sigma}^{\rm incl}_{RR}]_{\rm sing} = \left(\frac{\alpha_s}{4\pi}\right)^2 4\,\hat{\sigma}^{\gamma\gamma}_B\, C_F^2 \Bigg\{ & \frac{\delta(\bar{z}_a)\delta(\bar{z}_b)}{\varepsilon^4} \\
& - \frac{2}{\varepsilon^3}\big(\delta(\bar{z}_a)\mathcal{L}_0(\bar{z}_b) + \delta(\bar{z}_b)\mathcal{L}_0(\bar{z}_a) - \delta(\bar{z}_a)\delta(\bar{z}_b)\log M^2\big) \\
& + \frac{1}{\varepsilon^2}\Big\{2\delta(\bar{z}_a)\delta(\bar{z}_b)\Big[-\frac{\pi^2}{4} + \log^2 M^2\Big] + 4\Big[\delta(\bar{z}_a)\mathcal{L}_1(\bar{z}_b) + \delta(\bar{z}_b)\mathcal{L}_1(\bar{z}_a) \\
& \qquad + \mathcal{L}_0(\bar{z}_a)\mathcal{L}_0(\bar{z}_b) - \log M^2\big(\delta(\bar{z}_a)\mathcal{L}_0(\bar{z}_b) + \delta(\bar{z}_b)\mathcal{L}_0(\bar{z}_a)\big)\Big]\Big\} \\
& + \frac{1}{\varepsilon}\Big\{\delta(\bar{z}_a)\delta(\bar{z}_b)\Big[\frac{4}{3}\log^3 M^2 - \pi\log M^2 - \frac{14\zeta(3)}{3}\Big] - 8(\mathcal{L}_0(\bar{z}_a)\mathcal{L}_1(\bar{z}_b) + \mathcal{L}_0(\bar{z}_b)\mathcal{L}_1(\bar{z}_a)) \\
& \qquad + \big(\delta(\bar{z}_a)\mathcal{L}_1(\bar{z}_b) + \delta(\bar{z}_b)\mathcal{L}_1(\bar{z}_a)\big)[\pi^2 - 4\log^2 M^2] + \\
& \qquad + 8\log M^2\big(\delta(\bar{z}_a)\mathcal{L}_1(\bar{z}_b) + \delta(\bar{z}_b)\mathcal{L}_1(\bar{z}_a) + \mathcal{L}_0(\bar{z}_a)\mathcal{L}_0(\bar{z}_b)\big)\Big\}\Bigg\}, \qquad (4.70)
\end{aligned}
$$

where $M^2 = \mu^2/Q^2$ as before, we then obtain that the finite part of the double real inclusive cross-section read

$$
\begin{aligned}
\hat{\sigma}^{\rm incl}_{RR} = \left(\frac{\alpha_s}{4\pi}\right)^2 4\,\hat{\sigma}^{\gamma\gamma}_B\, C_F^2 \Bigg\{ & \delta(\bar{z}_a)\delta(\bar{z}_b)\Big[\frac{2}{3}\log^4 M^2 - \pi^2\log^2 M^2 - \frac{28\zeta(3)}{3}\log M^2 + \frac{\pi^4}{24}\Big] \\
& + \big(\delta(\bar{z}_a)\mathcal{L}_0(\bar{z}_b) + \delta(\bar{z}_b)\mathcal{L}_0(\bar{z}_a)\big)\Big[-\frac{8}{3}\log^3 M^2 + 2\pi^2\log M^2 + \frac{28}{3}\zeta(3)\Big] \\
& + \big(\delta(\bar{z}_a)\mathcal{L}_1(\bar{z}_b) + \delta(\bar{z}_b)\mathcal{L}_1(\bar{z}_a) + \mathcal{L}_0(\bar{z}_a)\mathcal{L}_0(\bar{z}_b)\big)\big[8\log^2 M^2 - 2\pi^2\big] \\
& + 16\mathcal{L}_1(\bar{z}_a)\mathcal{L}_1(\bar{z}_b)\Bigg\}. \qquad (4.71)
\end{aligned}
$$

These results eventually conclude our full theory calculations.

Chapter 5

Soft threshold factorization

In this chapter, we derived the LP and NNLP soft functions and compute them at NLO and NNLO. We expect the inclusive partonic helicity cross-section for real and double real emission to be exactly reproduced by the LP soft factorization theorem, as these results are already present in the literature. Instead, the NNLP factorization theorem will be here derived for the first time. The outcome of its application to the calculation of the real and double real zeroth cross-section is then tested using the results derived in the previous chapter in the full QCD theory.

5.1 LP soft function

5.1.1 Derivation of the LP factorization formula

The derivation of the LP factorization formula presented in this section closely follows the one carried out in ref.[60], of which it is just a readaptation in terms of our normalization and conventions. For proving this fomula, we start from the hadronic tensor defined in eq.(3.5) and write the delta function in terms of its Fourier transform (see app. A). Since the operator P acting on $|pp\rangle$ and $|X\rangle$ has eigenvalue $(P_a + P_b)$ and p_X respectively, the hadronic tensor becomes

$$W^{\mu\nu} = \int d^4x e^{-iq\cdot x} \sum\!\!\!\!\!\!\int_X \langle pp|e^{ix\cdot P} J^{\mu\dagger}(0) e^{-ix\cdot P}|X\rangle \langle X|J^{\nu}(0)|pp\rangle \,. \tag{5.1}$$

In the first matrix element, we can moreover use that the translation operator acting on the current determines the relation $J^{\dagger}_{\mu}(x) = e^{ix\cdot P} J^{\dagger}_{\mu}(0) e^{-ix\cdot P}$. This, together with the fact that $|X\rangle$ forms a complete set of states, implies that we can write

$$W^{\mu\nu} = \int d^4x e^{-iq\cdot x} \langle pp|J^{\mu\dagger}(x) J^{\nu}(0)|pp\rangle \,. \tag{5.2}$$

In order to derive the LP factorization formula, we now have to write down an explicit form for this current. Because this factorization formula gives the inclusive cross section, and for the double real amission case we have only considered $V = \gamma^*$, this current just

corresponds to the QED current of eq.(3.3). Writing it in terms of SCET operators and performing decoupling transformations of eq.(2.66), we hence arrive to the following expression

$$J^\mu(x) = eQ_f \int dr \int dt\, C_V(r,t)\, \bar\chi_{\bar c}(x+rn) S^\dagger_{\bar n}(x) S_n(x) \gamma^\mu_\perp \chi_c(x+t\bar n), \tag{5.3}$$

where C_V is the hard matching coefficient. This current is the same as the one $J^\mu(x)$ used by Becher in ref.[60] with a different normalization, and describes the electromagnetic interaction between an energetic quark moving in the direction of P_a with an anti-quark moving in the direction of P_b. After the decoupling transformations, the collinear and soft fields do not interact with each other, so that inserting the current eq.(5.3) into the hadronic tensor eq.(5.2) results in

$$\begin{aligned}\frac{W^{\mu\nu}}{e^2Q_f^2} = \int d^4x e^{-iq\cdot x} \int dr\, dr'\, dt\, dt' C_V(r,t) C_V^*(r',t')\ \langle 0|\bar T\{S_n^\dagger(x) S_{\bar n}(x)\}\, T\{S_{\bar n}^\dagger(0) S_n(0)\}|0\rangle \\ \times \langle pp|\bar\chi_c(x+t'\bar n)\gamma^\mu_\perp \chi_{\bar c}(x+r'n)\bar\chi_{\bar c}(rn)\gamma^\nu_\perp \chi_c(t\bar n)|pp\rangle\,.\end{aligned} \tag{5.4}$$

Namely, the hadronic tensor factorizes into a collinear matrix element, where the collinear and anti-collinear field $\chi_{c,\bar c}$ act on the two protons state, and a soft matrix element where the soft Wilson lines $S_{n,\bar n}$ act on the vacuum. Indeed, the two protons only contain collinear degrees of freedom, being the relevant energy scale of a soft parton much higer than the energy scale of the hadrons momenta $P_a \sim P_b \sim \Lambda_{QCD}$. Consequently, soft partons can only be created from the vacuum. In addition, the soft matrix element include the anti-time ordering $\bar T$ and time ordering T operator, which order Wilson lines with $+i0$ and $-i0$ propagator prescription respectively.

The bispinor products of collinear operators in the collinear matrix elements can be now rearranged using Fierz identities. These read,

$$\bar u_1 \Gamma_1 u_2\, \bar u_3 \Gamma_2 u_4 = \sum C_{AB}\, \bar u_1 \Gamma_A u_4\, \bar u_3 \Gamma_B u_2 \tag{5.5}$$

where $u_{1,2,3,4}$ are spinors, $\Gamma_{1,2}$, $\Gamma_{A,B}$ are elements of the Clifford algebra and C_{AB} are numerical coefficients. The lhs of eq.(5.5) in terms of the bilinears of collinear fields appearing in eq.(5.4), involve $\Gamma_1 = \gamma^\mu_\perp$ and $\Gamma_2 = \gamma^\nu_\perp$. Therefore, the rhs must be transverse as well. Among the elements of the Clifford algebra, there is the identity, gamma matrices and products of these last, the metric and the Levi Civita symbol, respectively used for constructing symmetric and antisymmetric bilinears. However, since the collinear fields satisfy

$$\bar\chi_c \gamma^\mu \chi_c = n^\mu \bar\chi_c \frac{\bar{\not n}}{2} \chi_c, \qquad\qquad \bar\chi_c \chi_c = 0, \tag{5.6}$$

the only tensor structures we can form are the one constructed out of $g^{\mu\nu}_\perp$, $\epsilon^{\mu\nu}$ and $\bar n^\mu$, $\bar n^\mu$. Moreover, considering that the collinear fields also satisfy $\bar{\not n}\chi_{\bar c} = \bar{\not n}\chi_c = 0$ and that the final tensor structure must be a symetric one with two perpendicular indices, we eventually find that there is only one possibility, that is

$$\bar\chi_c \gamma^\mu_\perp \chi_{\bar c} \bar\chi_{\bar c} \gamma^\nu_\perp \chi_c = \frac{g^{\mu\nu}_\perp}{(D-2)} \bar\chi_c \frac{\bar{\not n}}{2} \chi_c \bar\chi_{\bar c} \frac{\bar{\not n}}{2} \chi_{\bar c}\,, \tag{5.7}$$

with $(D-2)^{-1}$ normalization factor. (The proof that this factor indeed yields to the correct normalization can be obtained by contracting both sides of the identity with $g_{\mu\nu,\perp}$). Because the product of bilinears involving collinear fields separate into a collinear and an anticollinear acting separately on $|pp\rangle = |p(P_a)\rangle \otimes |p(P_b)\rangle$, the hadronic tensor becomes

$$\begin{aligned}\frac{W^{\mu\nu}}{e^2Q_f^2} = \int d^4x e^{-iq\cdot x} \int dr\, dr'\, dt\, dt' C_V(r,t)C_V^*(r',t') \\ \times \langle 0|\bar{T}\{\,[S_n^\dagger(x)S_{\bar{n}}(x)]_{ih}\,\}\, T\{\,[S_{\bar{n}}^\dagger(0)S_n(0)]_{kj}\,\}|0\rangle \\ \times g_\perp^{\mu\nu}\,\langle p(P_a)|\bar{\chi}_c(x+t'\bar{n})_i\,\frac{\bar{n}\!\!\!/}{2}\,\chi_c(t\bar{n})_j\,|p(P_a)\rangle \\ \times \langle p(P_b)|\bar{\chi}_{\bar{c}}(rn)_k\,\frac{n\!\!\!/}{2}\,\chi_{\bar{c}}(x+r'n)_h\,|p(P_b)\rangle \end{aligned} \tag{5.8}$$

expliciting the color indices. Averaging over these indices, the collinear fields satisfy

$$(\bar{\chi}_{c,i}\,\frac{\bar{n}\!\!\!/}{2}\,\chi_{c,j})(\bar{\chi}_{\bar{c},k}\,\frac{n\!\!\!/}{2}\,\chi_{\bar{c},h}) \to \frac{1}{N_c^2}(\delta_{ij}\bar{\chi}_{c,m}\,\frac{\bar{n}\!\!\!/}{2}\,\chi_{c,m})(\delta_{kh}\bar{\chi}_{\bar{c},n}\,\frac{n\!\!\!/}{2}\,\chi_{\bar{c},n}) \tag{5.9}$$

and, summing over the indices, the delta functions ensures that the color indices of the soft Wilson lines gets contracted among themselves. This makes sense because the soft and collinear matrix elements do not interact with each other, and therefore all their color indices must be individually contracted, leading to color-singlet expressions.

Because our goal is to compare the prediction for the cross section obtained via the soft factorization formula with the inclusive cross section derived in the full theory, we contract the hadronic tensor with the metric $(-g_{\mu\nu})$, that gives a factor $(D-2)$ when this acts to the transverse metric $g_\perp^{\mu\nu}$. At the end, putting everything together, we arrive to the following expression

$$\begin{aligned}W^{incl} = -\frac{e^2Q_f^2}{N_c} \int d^4x e^{-iq\cdot x} \int dr\, dr'\, dt\, dt' C_V(r,t)C_V^*(r',t')\, \tilde{S}_{LP}(x) \\ \times \langle p(P_a)|\bar{\chi}_c(x+t'\bar{n})\,\frac{\bar{n}\!\!\!/}{2}\,\chi_c(t\bar{n})\,|p(P_a)\rangle\,\langle p(P_b)|\bar{\chi}_{\bar{c}}(rn)\,\frac{n\!\!\!/}{2}\,\chi_{\bar{c}}(x+r'n)\,|p(P_b)\rangle \end{aligned} \tag{5.10}$$

where $\tilde{S}_{LP}(x)$ denotes the leading power soft function in position space

$$\tilde{S}_{LP}(x) = \frac{1}{N_c}\,\mathrm{Tr}\,\langle 0|\bar{T}\{S_n^\dagger(x)S_{\bar{n}}(x)\}\,T\{S_{\bar{n}}^\dagger(0)S_n(0)\}|0\rangle\,. \tag{5.11}$$

As last, one can relate the collinear matrix elements to the quark and antiquark parton distribution functions by performing an expansion in small momentum components. Here, we state the result from Becher *et. al* [60], which use that the conjugate position variable to the vector boson momentum q scales as $x^\mu \sim (1,1,\lambda^{-1})$ and that the transverse momentum of the colliding partons is of order Λ_{QCD}. In this way, the collinear matrix element is relate to the normalized parton distribution functions via

$$\langle p(P_a)|\bar{\chi}_c(x+t'\bar{n})\,\frac{\bar{n}\!\!\!/}{2}\,\chi_c(t\bar{n})\,|p(P_a)\rangle = \bar{n}\cdot P_a \int_{-1}^{1} d\xi_a\, f_q(\xi_a,\mu)\, e^{i\xi_a(x_+ + t'\bar{n} - t\bar{n})\cdot P_a}\,, \tag{5.12}$$

and a similar expression can be also written down for the anticollinear matrix, except for a minus sign since antiquark distribution satisfy $f_{\bar{q}}(\xi) = f^*_{\bar{q}}(\xi) = -f_q(-\xi)$. Putting everything together, and restricting the integration domain over the PDF to only positive values, we thus obtain that

$$W^{incl} = \frac{e^2 Q_f^2}{N_c} E_{cm}^2 \int_0^1 d\xi_a \int_0^1 d\xi_b |\tilde{C}_V(-\hat{s},\mu)|^2 \int d^4x\, \tilde{S}_{LP}(x)\, e^{ix\cdot(\xi_a P_a + \xi_b P_b - q)} \\ [f_q(\xi_a,\mu) f_{\bar{q}}(\xi_b,\mu) + f_{\bar{q}}(\xi_a,\mu) f_q(\xi_b,\mu)]\,. \tag{5.13}$$

Here, we have used that $E_{cm}^2 = (n\cdot P_a)(\bar{n}\cdot P_b) = P_a^- P_b^+$, defined the Fourier transform of the hard matching coefficient

$$\tilde{C}_V(-\hat{q}^2) = \int dr \int dt\, C_V(r,t)\, e^{ix_1\, t\, \bar{n}\cdot P_a}\, e^{-ix_2\, r\, n\cdot P_b} \tag{5.14}$$

where at soft threshold we can replace $\hat{s}$ with $\hat{q}^2$, and added to the expression the second term of the current eq.(5.3) where the quark and the antiquark are exchanged, which is crucial to identify the PDF as probability densities. Now that we have the brought the inclusive hadronic tensor in the form eq.(5.13), we can calculate the differential cross section, that according to the definition given in section 3.2 can be written as

$$d\sigma^{\text{incl}} = \frac{d^4q}{(2\pi)^4}\, \frac{1}{2E_{cm}^2}\, L_{\gamma\gamma,+}\, W^{incl}\,. \tag{5.15}$$

Substituting the eq.(5.13), one can also express the LP soft function in momentum space by taking its Fourier transform. In particular, expressing both the measures d^4q and d^4x in lightcone coordinates and using the integral representation of the delta function, it holds that

$$\int \frac{d^2q_\perp}{(2\pi)^2} \int d^2x_\perp\, \tilde{S}_{LP}(x^+,x^-,\vec{x}_\perp)\, e^{i\vec{q}_\perp\cdot\vec{x}_\perp} = \tilde{S}_{LP}(x^+,x^-,\vec{0}_\perp)\,. \tag{5.16}$$

In this way, the inclusive cross section is equal to

$$\frac{d\sigma^{\text{incl}}}{dq^+\,dq^-} = \sum_{i,j=q,\bar{q}} \int_0^1 d\xi_a \int_0^1 d\xi_b\, f_i(\xi_a) f_j(\xi_b) \Bigg[\hat{\sigma}_B^{\gamma\gamma} |\tilde{C}_V(-\hat{s},\mu)|^2 \\ \times \frac{1}{4} \int \frac{dx^+}{2\pi} \int \frac{dx^-}{2\pi}\, \tilde{S}_{LP}(x^+,x^-,\vec{0}_\perp)\, e^{i(\xi_a - x_a)P_a^-/2}\, e^{i(\xi_b - x_b)P_b^+/2} \Bigg] \tag{5.17}$$

where the factor 1/4 is the jacobian of the change of coordinates. Recalling that $(\xi_a - x_a)P_a^- = k^-$ and $(\xi_b - x_b)P_b^+ = k^+$, the second line of the expression above thus corresponds to the Fourier transform of the soft function $\tilde{S}_{LP}(x)$, which gives the following expression for the LP soft function in momentum space

$$S_{LP}(k^+,k^-) = \frac{1}{N_c}\, \text{Tr}\, \langle 0|\bar{T}\{S_n^\dagger S_{\bar{n}}\}\, \delta^-(k^- - \hat{p}^-)\delta^+(k^+ - \hat{p}^+)\, T\{S_{\bar{n}}^\dagger S_n\}|0 \tag{5.18}$$

where the delta functions enforce that the eigenvalues of the operators $\hat{p}^+$, $\hat{p}^-$ acting on an hadronic state correspond to the lightcone coordinates of the soft radiative emission. Eventually expressing dq^+dq^- in terms of the bare momentum fractions x_a and x_b, which introduces the jacobian $P_a^- P_b^+ = Q^2/\xi_a\xi_b$, the hadronic cross section can be written as

$$\frac{d\sigma^{incl}}{dx_a dx_b} = \sum_{i,j=q,\bar{q}} \int \frac{d\xi_a}{\xi_a} \int \frac{d\xi_b}{\xi_b} f_i(\xi_a,\mu)\, f_j(\xi_b,\mu)\; \hat{\sigma}_{ij}^{\rm incl}\left(\frac{x_a}{\xi_a}, \frac{x_b}{\xi_b}, Q^2\right), \tag{5.19}$$

where we have kept the same normalization as in the full theory, with the partonic cross section given by

$$\hat{\sigma}_{ij}^{\rm incl}(z_a, z_b, Q^2) = \hat{\sigma}_B^{\gamma\gamma}\, Q^2\, |C_V(-\hat{q}^2,\mu)|^2\, S_{LP}(k^+,k^-)\,. \tag{5.20}$$

5.1.2 LP soft function at NLO

For evaluating the LP soft function at NLO order, we start by inserting a complete set of hadronic states, that is

$$\sum\!\!\!\!\!\!\int_X |X\rangle\langle X| = 1 \tag{5.21}$$

into eq.(5.18) before the time ordering operator T. In this way, the soft function separates into two different matrix elements, related to each other by conjugation, and can therefore be treated as an amplitude squared. Therefore, using that the integral sum above reads in full

$$\sum\!\!\!\!\!\!\int_X = \sum_X \int d^4p_X \prod_{i\in X} \int \frac{d^4p_i}{(2\pi)^3} \delta^2(p_i^2)\theta(p^0)\delta^4\left(\sum_{i\in X} p_i - p_X\right) \tag{5.22}$$

and that at NLO the only relevant states $|X\rangle$ are the vacuum state $|0\rangle$ and rhe single gluon state $|\ell\rangle$, the soft function $S_{LP}(k^+,k^-)$ consists of a sum of a real and a virtual contribution

$$S_{LP}(k^+,k^-) = S_{LP}^V(k^+,k^-) + S_{LP}^R(k^+,k^-)\,. \tag{5.23}$$

Here, the virtual contribution is given by the term $|X\rangle = |0\rangle$; since there are no particles in this state, the total phase space only consist and integral over the delta function $\delta^4(p_X)$, which indeed impose that there is not hadronic radiation p_X. The virtual soft function is therefore equal to

$$S_{LP}^V(k^+,k^-) = \frac{1}{N_c}\,\mathrm{Tr}\,\langle 0|\bar{T}\{S_n^\dagger S_{\bar{n}}\}|0\rangle\langle 0|T\{S_{\bar{n}}^\dagger S_n\}|0\rangle \tag{5.24}$$

and consists of the diagrams displayed in fig 5.1. Evaluating these diagrams in dimensional regularization and using the Wilson lines Feynman rules reported in ref.[61], we obtain that

$$S_{LP}^V(k^+,k^-) = -4g_s^2\mu^{2\varepsilon} C_F \int \frac{d^dk}{(2\pi)^d} \frac{1}{(k^2+i0)(\bar{n}\cdot k + i0)(\bar{n}\cdot k - i0)} \tag{5.25}$$

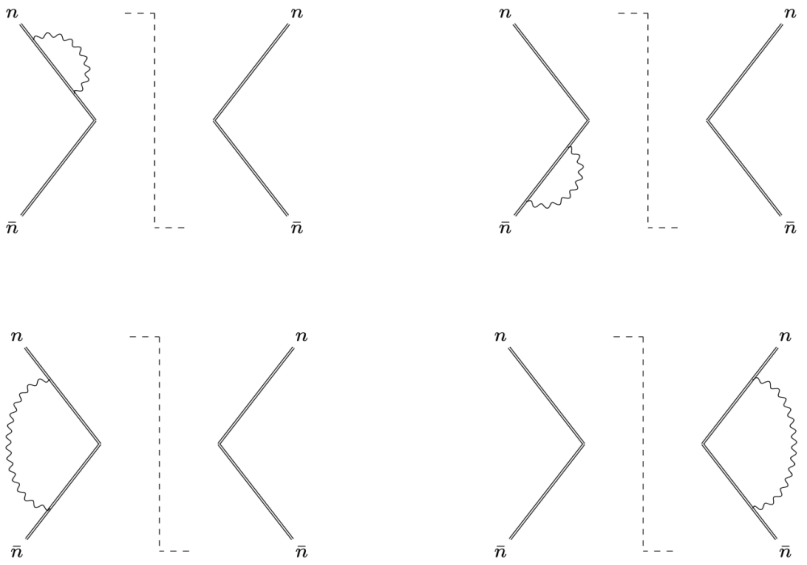

Figure 5.1: Virtual diagrams contributing to the LP soft function at NNLO. The self energy diagrams (top row) vanish due to $n^2 = \bar{n}^2 = 0$, so that the function $S^V_{LP}(k^+, k^-)$ is only given by the vertex diagrams on the bottom row.

which is a scaless integral, and therefore vanishes in dimensional regularization. The real contribution instead is determined by the action of the soft Wilson lines on the one gluon state $|X\rangle = |l\rangle$. Expressing the gluon phase space in lightcone coordinates, this reads

$$S^R_{LP}(k^+, k^-) = \frac{1}{2N_c} \int \frac{d^{d-2}\ell_\perp}{(2\pi)^{d-2}} \int \frac{dk^+ dk^-}{2\pi}\, \delta^-(k^- - \ell^-)\, \delta(k^+ - \ell^+)\, \theta(\ell^0) \\ \times \delta(\ell^+\ell^- - \ell_\perp^2)\, \mathrm{Tr}\, \langle 0|\bar{T}\{S_n^\dagger S_{\bar{n}}\}|\ell\rangle \langle \ell| T\{S_{\bar{n}}^\dagger S_n\}|0\rangle \tag{5.26}$$

where the matrix element is given by the sum of the diagrams of fig 5.2. Integrating now the delta functions $\delta(k^- - \ell^-)$ and $\delta(k^+ - \ell^+)$ against the integration measure, and using eq.(4.40) for expressing the integral over the transverse momentum in spherical coordinates, the real contribution to the LP soft function becomes

$$S^R_{LP}(k^+, k^-) = \frac{1}{16\pi^2 N_c} \frac{(4\pi\mu^2)^\varepsilon}{\Gamma(1-\varepsilon)} \int d\ell_\perp^2\, \delta(k^+k^- - \ell_\perp^2)\, \theta(k^0)\, (\ell_\perp^2)^{-\varepsilon} \left(\frac{4g_s^2}{k^+k^-} \mathrm{Tr}[t_a t_a] \right) \tag{5.27}$$

Eventually integrating out also $\ell_\perp^2$, expressing k^+ and k^- in terms of $\bar{z}_a$ and $\bar{z}_b$ and exploiting that the virtual contribution yields zero, the LP soft function at NLO in the $\overline{\mathrm{MS}}$ corresponds to

$$S^R_{LP}(k^+, k^-) = \left(\frac{\alpha_s}{4\pi} \right) \frac{e^{\varepsilon\gamma_E}}{\Gamma(1-\varepsilon)}\, \mu^{2\varepsilon}\, 4C_F\, \theta(\bar{z}_a)\, \theta(\bar{z}_b)\, (Q^2 \bar{z}_a \bar{z}_b)^{-1-\varepsilon}\,. \tag{5.28}$$

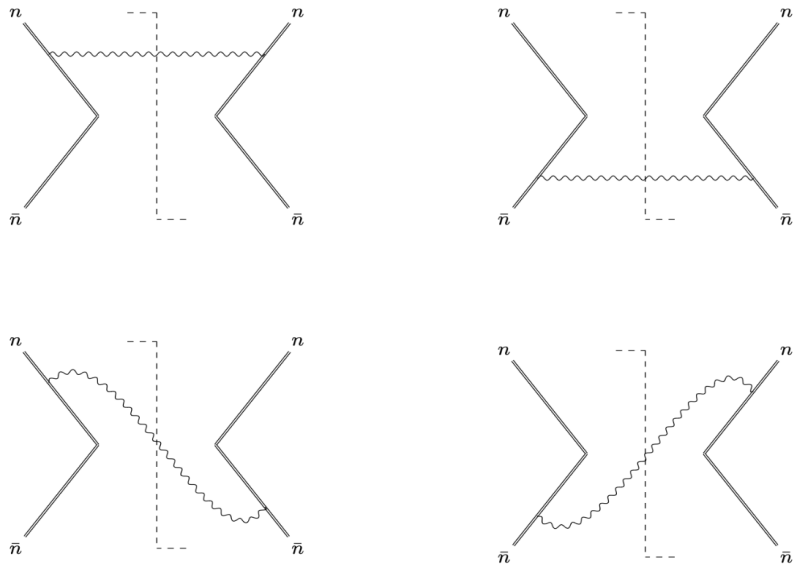

Figure 5.2: Real cut diagrams contributing the LP soft function at NLO. Similarly to the virtual ones, the diagrams on the first row vanish as a consequence of the identity $n^2 = \bar{n}^2 = 0$, so that the soft function $S^R_{LP}(k^+, k^-)$ is only determined by the diagrams on the second row.

With respect to the inclusive partonic cross section of the full theory, eq.(4.41), eq.(4.46), the soft function involve an extra power of Q^{-2} which is however compensated by the same factor in the inclusive partonic cross section we have obtained via factorization formula. Therefore, putting everything together, we finally obtain that

$$\frac{\hat{\sigma}^{\text{incl}}_R}{|C_V(-\hat{q}^2,\mu)|^2} = \left(\frac{\alpha_s}{4\pi}\right)\frac{e^{\varepsilon\gamma_E}}{\Gamma(1-\varepsilon)}\,\mu^{2\varepsilon}\,4\,\hat{\sigma}^{\gamma\gamma}_B\,C_F\,\frac{(Q^2\bar{z}_a\bar{z}_b)^{-\varepsilon}}{\bar{z}_a\bar{z}_b} \tag{5.29}$$

which, expanded around $\varepsilon = 0$, exactly gives the LP contriution to the inclusive partonic cross section eq.(4.50).

5.1.3 LP soft function at NNLO

The calculation for the LP soft funciton at NNLO follows the same steps as the NLO one. Thus, we first insert a complete set of states as in eq.(5.21), (5.22) and use that virtual diagrams do not contributesince they are scaless. Therefore, the soft function in d dimensions is equal to

$$S^{RR}_{LP}(k^+,k^-) = \frac{1}{N_c}\prod_{i=1,2}\int\frac{d^d\ell_i}{(2\pi)^{d-1}}\,\delta^2(\ell_i^2)\,\theta(\ell_i^0)\,\delta(k^- - (\ell_1^- + \ell_2^-))\,\delta(k^+ - (\ell_1^+ + \ell_2^+))$$
$$\text{Tr}\,\langle 0|\bar{T}\{S_n^\dagger S_{\bar{n}}\}|\ell\,\ell\rangle\,\langle\ell\,\ell|T\{S_{\bar{n}}^\dagger S_n\}|0\rangle \tag{5.30}$$

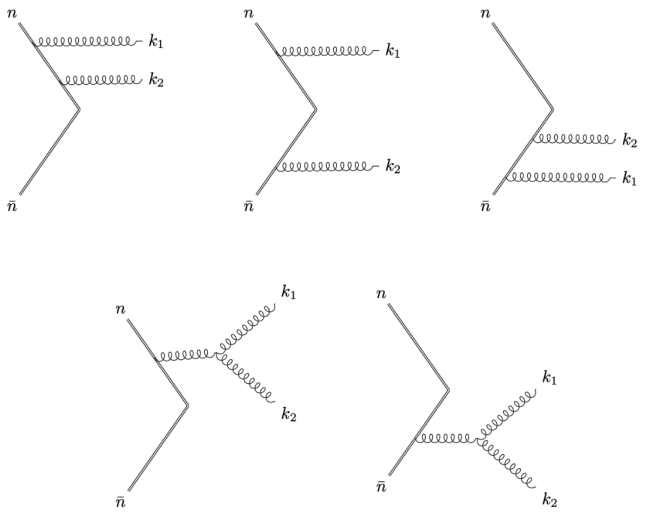

Figure 5.3: Soft Wilson line attachments that, together with their permutation (not showed) determine the LP soft function at NNLO. As for the full theory calculation, the diagrams on the first row are responsible for the abelian contribution C_F^2 and the non abelian $C_A C_F$, while diagrams on the second row for the $C_A C_F$ only.

where we have used that the only non vanishing contribution is given by the two-gluon state $|X\rangle = |\ell\,\ell\rangle = |\ell\rangle \otimes |\ell\rangle$. The matrix element in the integrand of the soft function above can be evaluated from the vertices fig.5.3. Selecting the abelian contribution only, we obtain that the LP soft function is given by

$$S_{LP}^{RR}(k^+,k^-) = \mu^{4\varepsilon} \int \frac{d^d\ell_1}{(2\pi)^{d-1}} \frac{d^d\ell_2}{(2\pi)^{d-1}} \delta^2(\ell_1^2)\,\delta^2(\ell_2^2)\,\theta(\ell_1^0)\,\theta(\ell_2^0) \times \delta(k^- - (\ell_1^- + \ell_2^-))\,\delta(k^+ - (\ell_1^+ + \ell_2^+)) \left[\frac{8g^4 C_F^2}{\ell_1^+\ell_1^-\ell_2^+\ell_2^-}\right]. \tag{5.31}$$

Eventually expressing the differential $d^d\ell_1$ and $d^d\ell_2$ in lightcone coordinates and using eq.(4.40) to carry out the integration of the delta functions $\delta(\ell_1^2)$, $\delta(\ell_2)$ over the gluons transverse momenta $\ell_{1,T}$, $\ell_{2,T}$, the soft function in the $\overline{\text{MS}}$-scheme can be written as

$$S_{LP}^{RR}(k^+,k^-) = \left(\frac{\alpha_s}{4\pi}\right)^2 \frac{(e^{\varepsilon\gamma_E}\mu^2)^{2\varepsilon}}{\Gamma(1-\varepsilon)^2}\, 4C_F^2 \int d\ell_1^+\, d\ell_1^-\, d\ell_2^+\, d\ell_2^-\, (\ell_1^+\ell_2^+\ell_1^-\ell_2^-)^{-\varepsilon} \times \delta^-(k^- - (\ell_1^- + \ell_2^-))\,\delta^+(k^+ - (\ell_1^+ + \ell_2^+)) \left[\frac{1}{\ell_1^+\ell_2^+\ell_1^-\ell_2^-}\right]. \tag{5.32}$$

where we have divided by 1/2 because the integration measure is symmetric under the exchange $\ell_1 \longleftrightarrow \ell_2$. Notice that this soft function is the same as the double real cross section eq.(4.68) apart from a factor $Q^2 = p_a^- p_b^+$ and the multiplication for born cross

section $\hat{\sigma}_B^{\gamma\gamma}$, that comes from the definition of inclusive cross section eq.(5.20). Therefore, putting everything together, we have indeed that

$$\frac{\hat{\sigma}_{RR}^{\text{incl}}}{|C_V(-\hat{q}^2,\mu)|^2} = \left(\frac{\alpha_s}{4\pi}\right)^2 \frac{(e^{\varepsilon\gamma_E}\mu^2)^{2\varepsilon}}{\Gamma(1-\varepsilon)^2}\, 4\,\hat{\sigma}_B^{\gamma\gamma}\, C_F^2 \int d\ell_1^+\, d\ell_1^-\, d\ell_2^+\, d\ell_2^-\, (\ell_1^+\ell_2^+\ell_1^-\ell_2^-)^{-\varepsilon} \times \delta^-(k^- - (\ell_1^- + \ell_2^-))\,\delta^+(k^+ - (\ell_1^+ + \ell_2^+))\left[\frac{p_a^- p_b^+}{\ell_1^+\ell_2^+\ell_1^-\ell_2^-}\right] \tag{5.33}$$

which is equal to the cross section $\hat{\sigma}_{RR}^{\text{incl}}$ calculated in the full-theory at the integrand level.

5.2 Derivation of the NNLP factorization formula

In the previous section, we have found an expression for the inclusive cross section in terms of the LP soft function to compare with the inclusive cross section we have calculated in the full theory. The purpose of this section, is to derive an equivalent expression for the NNLP soft function, which we expect to reproduce the cross section $\hat{\sigma}^0$. The reason why we can focus on the NNLP term only, is because the structure function W^0 is, at both NLO and NNLO in α_s, suppressed by two powers of λ with respect to W^{incl}, and scales as λ^0 (after phase space integration).

The derivation of the NNLP factorization formula follows the same steps as in the derivation of the LP factorization formula of section 5.1.1. Hence, the first thing to do, is to write down the correct current such that, inserted in the hadronic tensor eq.(5.2) and contracted with the longitudinal projector $P^0_{\mu\nu} = 2 z_\mu z_\nu$ exactly reproduces the cross section σ^0. The complete NNLP current written in terms of power-suppressed operators that couple with longitudinal polarization states has been calculated in ref.[70]. This current consists of two contributions, a hard and a hard-collinear contribution. Because the matching coefficient of this last one is suppressed by one-loop, for describing real emission only we just retain the hard current. In position space, this current is given by

$$J^\mu(x) = e\,Q_f\,\frac{n^\mu - \bar{n}^\mu}{2Q}\int dr \int dt\, C_V(r,t)\,\bar{\chi}_{\bar{c}}(x+rn)\,\mathcal{O}^{(1),\rho}_{n,\bar{n}}(x)\,\gamma_{\rho,\perp}\,\chi_c(x+t\bar{n}) \tag{5.34}$$

where the operator $\mathcal{O}^{(1),\mu}_{n,\bar{n}}$ describes the interaction between the collinear and soft sectors at NNLP and is equal to

$$\mathcal{O}^{(1),\rho}_{n,\bar{n}} = g\mathcal{B}^{\bar{n},\rho}_{s,\perp}\, S^\dagger_{\bar{n}}\, S_n + S^\dagger_{\bar{n}}\, S_n\, g\mathcal{B}^{n,\rho}_{s,\perp} \tag{5.35}$$

Here, the $\mathcal{B}^{n_i\mu}_{s,\perp}$ fields are the transverse components of the gluon field strengths in the soft sector, and are defined by the action of the covariant derivative along the transverse direction on soft Wilson lines, that is

$$\mathcal{B}^{n_i,\rho}_{s,\perp} = \frac{1}{g}[S^\perp_{n_i}\, iD^\rho_\perp\, S_{n_i}] \qquad n_i = n, \bar{n}\,. \tag{5.36}$$

The one gluon and double gluon Feynman rules for these fields are respectively given by

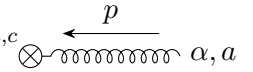

$$= \delta^{ca}\left(g_\perp^{\mu\alpha} - \frac{p_\perp^i n_i^\alpha}{n_i\cdot p}\right) \tag{5.37}$$

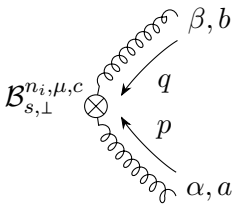

$$= igf^{cab}\left[\frac{g_\perp^{\mu\beta}n_i^\alpha}{n_i\cdot p} - \frac{g_\perp^{\mu\alpha}n_i^\beta}{n_i\cdot q} + \left(\frac{p_\perp^\mu}{n_i\cdot q} - \frac{q_\perp^\mu}{n_i\cdot p}\right)\frac{n_i^\alpha n_i^\beta}{n_i\cdot(p+q)}\right] \tag{5.38}$$

We can now insert the current eq.(5.34) into the hadronic tensor eq.(5.2). As noted before, soft partons cannot be part of the colliding protons because the energy scale of soft radiation is much higher compared to the relevant energy scale of the protons momenta. Analogously, also the transverse momentum gained by the vector boson cannot be given by the transverse momenta of the protons, since this is also of order $\sim \Lambda_{\rm QCD}$. Therefore, the hadronic tensor again factorizes into a collinear and soft-transverse part, where the collinear part is the same as eq.(5.4) and where the soft matrix element features the operator $\mathcal{O}^{(1),\mu}_{n,\bar n}$ acting on the vacuum state, that is

$$W^{\mu\nu} = \frac{(n^\mu-\bar n^\mu)(n^\nu-\bar n^\nu)}{4Q^2(Q_f e)^{-2}}\int d^4x e^{-iq\cdot x}\int dr\,dr'\,dt\,dt'\,C_V(r,t)\,C_V^*(r',t') \tag{5.39}$$
$$\times\langle 0|\mathcal{O}^{(1),\rho\,\dagger}_{n,\bar n}(x)\,\mathcal{O}^{(1),\sigma}_{n,\bar n}(0)|0\rangle\,\langle pp|\bar\chi_c(x+t'\bar n)\gamma_{\rho,\perp}\chi_{\bar c}(x+r'n)\bar\chi_{\bar c}(rn)\gamma_{\sigma,\perp}\chi_c(t\bar n)|pp\rangle\,.$$

Since the collinear matrix element is the same as in the LP case, we can use the Fierz identity eq.(5.7) to factorize this tensor into a collinear and an anticollinear part and then average over color indices using eq.(5.9). The delta functions arising from these identities constraint the product $\mathcal{O}^{(1),\rho\,\dagger}_{n,\bar n}(x)\,\mathcal{O}^{(1),\sigma}_{n,\bar n}(0)$ to be a color singlet, and therefore , after color average, the NNLP soft matrix element appears inside a trace. In addition, we project the hadronic tensor into its zeroth component by contracting it with the projector

$$P^0_{\mu\nu} = 2z_\mu z_\nu = 2\,\frac{n_\mu-\bar n_\mu}{2}\,\frac{n_\nu-\bar n_\nu}{2}, \tag{5.40}$$

where in the second equality we have expressed the z axis in lightcone coordinates, as given in [64]. As a result, eventually using eq.(5.12) to related the collinear and anticollinear matrix elements to the protons PDFs, we get that

$$W^0 = \frac{2Q_f^2e^2E_{\rm cm}^2}{Q^2N_c(D-2)}\int_0^1 d\xi_a\int_0^1 d\xi_b|\tilde C_V(-\hat s,\mu)|^2\int d^4x\,\widetilde S_{NNLP}(x)\,e^{ix\cdot(x_1P_a^-/2+x_2P_b^+/2-q)}$$
$$[f_{q/N_1}(\xi_a,\mu)f_{\bar q/N_2}(\xi_b,\mu)+f_{\bar q/N_1}(\xi_b,\mu)f_{q/N_2}(\xi_a,\mu)] \tag{5.41}$$

where eq.(5.14) has been used and where we have added the second part of the current with $q\longleftrightarrow\bar q$. The term $\tilde S_{\rm NNLP}(x)$ in this expression gives the NNLP soft function, defined

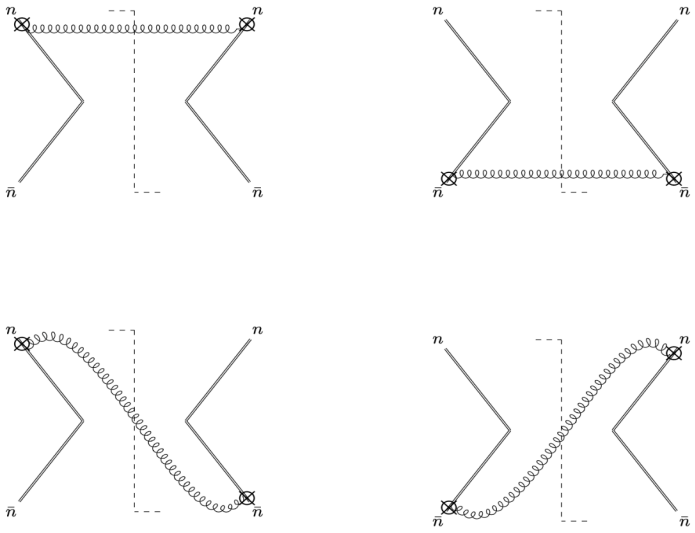

Figure 5.4: Set of diagrams contributing to the NNLP soft function at NLO. The crossed circle on the n and $\bar{n}$ side of the cusp denotes the attachment of the $\mathcal{B}_{s,\perp}^{n,\mu}$ and $\mathcal{B}_{s,\perp}^{\bar{n},\mu}$ respectively.

explicitly as

$$S_{\rm NNLP}(k^+,k^-) = -\frac{g_{\rho\sigma,\perp}}{N_c}\,{\rm Tr}\langle 0|\mathcal{O}_{n,\bar{n}}^{(1),\rho\,\dagger}(x)\,\delta^-(k-\hat{p}^-)\,\delta^+(k^+-\hat{p}^+)\,\mathcal{O}_{n,\bar{n}}^{(1),\sigma}(0)|0\rangle\,. \tag{5.42}$$

With the hadronic tensor eq.(5.41) at hand, the cross-section σ^0 can be computed in the same way as given by eq.(5.15) and the momentum space NNLP soft function $S_{\rm NNLP}(k^+,k^-)$ can be obtained via performing a Fourier transform done in eq.(5.16), (5.17). At the end, putting everything together and using that $dq^+dq^- = Q^2/\xi_a\xi_b dx_a dx_b$, the cross section in dimension $D=4$ reads

$$\frac{d\sigma^0}{dx_a\,dx_b} = \sum_{i,j=q,\bar{q}}\int\frac{d\xi_a}{\xi_a}\int\frac{d\xi_b}{\xi_b}\,f_i(\xi_a,\mu)\,f_j(\xi_b,\mu)\;\hat{\sigma}_{ij}^0\left(\frac{x_a}{\xi_a},\frac{x_b}{\xi_b},Q^2\right), \tag{5.43}$$

where the partonic cross-section is given by

$$\hat{\sigma}_{ij}^0 = |\tilde{C}_V(-\hat{q}^2,\mu)|^2\,\hat{\sigma}_B^{\gamma\gamma}\,S_{\rm NNLP}(k^+,k^-) \tag{5.44}$$

and indeed, by dimensional analysis, is suppressed by a factor of Q^2 with respect to inclusive one.

5.2.1 NNLP soft function at NLO

After inserting of a complete set of states into the NNLP soft function eq.(5.42), only the single gluon state $|X\rangle = |\ell\rangle$ gives a non-vanishing contribution, and therefore we obtain

that

$$S^R_{\rm NNLP}(k^+,k^-) = -\frac{g_{\rho\sigma,\perp}}{N_c}\, g^2\mu^{2\varepsilon}\int \frac{d^d\ell}{(2\pi)^{d-1}}\,\delta(\ell^2)\theta(\ell^0)\,\delta^-(k^- - \ell^-)\,\delta^+(k^+ - \ell^+)$$
$$\times \mathrm{Tr}\Big\{\langle 0|S_n^\dagger S_{\bar n}(\mathcal{B}^{\bar n,\rho}_{s,\perp})^\dagger|\ell\rangle\langle\ell|\mathcal{B}^{\bar n,\sigma}_{s,\perp}S^\dagger_{\bar n}S_n|0\rangle + \langle 0|S_n^\dagger S_{\bar n}(\mathcal{B}^{\bar n,\rho}_{s,\perp})^\dagger|\ell\rangle\langle\ell|S^\dagger_{\bar n}S_n\mathcal{B}^{n,\sigma}_{s,\perp}|0\rangle$$
$$+ \langle 0|(\mathcal{B}^{n,\rho}_{s,\perp})^\dagger S_n^\dagger S_{\bar n}|\ell\rangle\langle\ell|\mathcal{B}^{\bar n,\sigma}_{s,\perp}S^\dagger_{\bar n}S_n|0\rangle + \langle 0|(\mathcal{B}^{n,\rho}_{s,\perp})^\dagger S_n^\dagger S_{\bar n}|\ell\rangle\langle\ell|S^\dagger_{\bar n}S_n\mathcal{B}^{n,\sigma}_{s,\perp}|0\rangle\Big\}\,, \quad (5.45)$$

where we have used the explicit expression of the operator $\mathcal{O}^{(1),\mu}_{n,\bar n}$ in terms of the $\mathcal{B}^\mu_{s,\perp}$ fields (5.35). The amplitude in the integrand can be then evaulated from the diagram of Fig.(5.4), which gives

$$S^R_{\rm NNLP}(k^+,k^-) = \frac{g^2\mu^{2\varepsilon}}{2(2\pi)}\,4C_F\int\frac{d^{d-2}\ell_T}{(2\pi)^{d-2}}\int d\ell^+\,d\ell^-\,\delta^-(k^- - \ell^-)\,\delta^+(k^+ - \ell^+)$$
$$\delta(\ell^+\ell^- - \ell_T^2)\left[(D-2) - \frac{\ell_T^2}{\ell^+\ell^-}\right]. \quad (5.46)$$

Hence, integrating the δ^+ and δ^- against the integration measure and using the identity eq.(4.40) for working out the integral over the gluons transverse component ℓ_T, we obtain that in $d = 4-2\varepsilon$, the NNLP soft function at NLO is equal to

$$S^R_{\rm NNLP}(k^+,k^-) = \left(\frac{\alpha_s}{4\pi}\right)\frac{(1-2\varepsilon)e^{\varepsilon\gamma_E}\mu^{2\varepsilon}}{\Gamma(1-\varepsilon)}\,4C_F\,(k^+k^-)^{-\varepsilon}\,\theta(k^0)\theta(k^+k^-)\,. \quad (5.47)$$

Eventually plugging this expression into eq.(5.44) and expanding around $\varepsilon = 0$, we obtain that the $\hat\sigma^0$ cross section is given by this soft function multiplied by the Born cross section $\hat\sigma_B$, which make it equal to the full theory cross section $\sigma^0_R(z_a,z_b)$ of eq.(4.41).

5.2.2 NNLP soft function at NNLO

As last, we compute the NNLP soft function at NLO, which has the same expression as the soft function $S^R_{\rm NNLP}$ of eq.(5.45) but with the single gluon state replaced by the two gluon state $|\ell\,\ell\rangle = |\ell\rangle\otimes|\ell\rangle$ and where the phase space in d dimension is

$$\sum\!\!\!\!\!\!\int_X = \int\frac{d^d\ell_1}{(2\pi)^{d-1}}\int\frac{d^d\ell_2}{(2\pi)^{d-1}}\,\delta(\ell_1^2)\,\delta(\ell_2^2)\,\theta(\ell_1^0)\,\theta(\ell_2^0)\,, \quad (5.48)$$

with $\ell_1+\ell_2 = p_X$. The abelian contribution of the amplitude in the integrand can be evaluated from the diagrams of Fig.5.5 and their permutations. Hence, expressing the phase space eq.(5.48) in lightcone coordinates and dividing by 1/2, the NNLP soft function at NNLO is given by

$$S^{RR}_{\rm NNLP}(k^+,k^-) = \frac{g^4\mu^{4\varepsilon}C_F^2}{4(2\pi)^2}\,8\int d\ell_1^+\,d\ell_1^-\,d\ell_2^+\,d\ell_2^-$$
$$\times\,\delta^-(k^- - \ell^-)\,\delta^+(k^+ - \ell^+)\,\delta(\ell_1^+\ell_1^- - \ell_{1,T}^2)\,\delta(\ell_2^+\ell_2^- - \ell_{2,T}^2)$$
$$\int\frac{d^{d-2}\ell_{1,T}}{(2\pi)^{d-1}}\int\frac{d^{d-2}\ell_{2,T}}{(2\pi)^{d-1}}\left[\frac{-2\vec\ell_{1,T}\cdot\vec\ell_{2,T} + \ell_1^+\ell_1^- + \ell_2^+\ell_2^-}{\ell_1^+\ell_2^+\ell_1^-\ell_2^-}\right]. \quad (5.49)$$

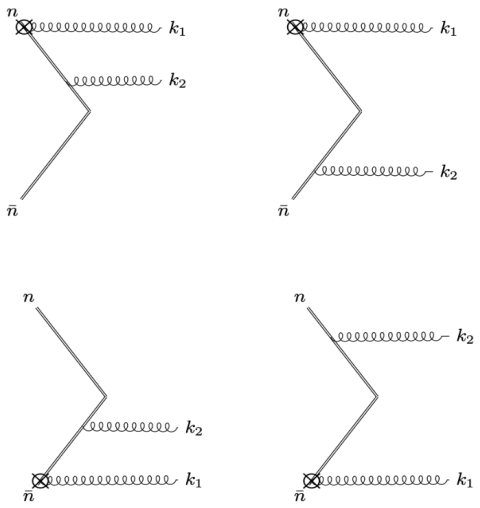

Figure 5.5: Set of diagrams giving the abelian contribution to the NNLP soft function at NNLO. The attachment of the $\mathcal{B}^{n,\mu}_{s,\perp}$ and $\mathcal{B}^{\bar{n},\mu}_{s,\perp}$ is signaled by a crossed circle. The other attachment correspond to soft Wilson lines S_n and $S_{\bar{n}}$.

Comparing the structure function at the integrand with the $T^i_{RR,\text{soft}}$ of eq.(4.59), in the NNLP soft function we have an extra term proportional to $\vec{\ell}_{1,T}\cdot\vec{\ell}_{2,T}$. However, when decomposing the $d-2$ dimensional integral over the emitted gluons transverse momenta using eq. 4.38, we have

$$\int d\Omega_{d-2}\,\vec{\ell}_{1,T}\cdot\vec{\ell}_{2,T} = 0 \tag{5.50}$$

by symmetry. Because the other terms of the soft function do not depend on the transverse momenta, using the identity eq.(4.40) to perform the integral over $\vec{k}_{1,T}$ and $\vec{k}_{2,T}$. Inserting the expression thus obtained into the definition of the cross section eq.(5.44), we finally obtain that

$$\begin{aligned}\frac{\hat{\sigma}^0_{RR}}{|\tilde{C}_V(-\hat{q}^2,\mu)|^2} = \left(\frac{\alpha_s}{4\pi}\right)^2 \frac{e^{2\varepsilon\gamma_E}}{\Gamma(1-\varepsilon)^2}\, 8\,\hat{\sigma}^{\gamma\gamma}_B\, C_F^2 \int d\ell_1^+\, d\ell_1^-\, d\ell_2^+\, d\ell_2^-\, (\ell_1^+\ell_2^+\ell_1^-\ell_2^-)^{-\varepsilon} \\ \times\, \delta(k^- - \ell^-)\,\delta(k^+ - \ell^+)\left[\frac{1}{\ell_1^+\ell_1^-} + \frac{1}{\ell_2^+\ell_2^-}\right].\end{aligned} \tag{5.51}$$

Comparing this expression with the one calculated in the full theory and given in eq.(4.64), we find that they also agree apart from a factor of 2. However, because the NNLP soft function exactly reproduced the cross-section $\hat{\sigma}^0_R$ at NLO and it is also in full agreement with the functional form of the NNLO cross-section $\hat{\sigma}^0_{RR}$, there are strong indications that that factor might just come from an inaccuracy in our last calculations.

Chapter 6

Conclusions

In this thesis, we have calculated the soft threshold limit of the Drell-Yan process angular coefficients in both full QCD and in the Soft Collinear Effective Theory. Because of their sensitivity to initial state radiation, their calculation provides an important test for probing the accuracy of perturbative QCD predictions. With the wealth of data collected from experiments like those at the LHC, precise theoretical predictions of the angular coefficients allow for stringent tests against experimental results. Discrepancies between theory and experiment can point to either the need for improved calculations or hints of new phenomena. In addition, although we have only focused on the case of γ^* and Z boson production, and lately only on the electromagnetic case, these results can be straightforwardly extended to $W^\pm$ bosons production, and could ultimately provide important tests for the mass and couplings of the electroweak sector of the SM.

In the following, we summarize and discuss the main results of this thesis and point out possible future research directions.

- Using the CS tensor decomposition, we have calculated the structure functions for single gluon emission, which agree with the ones already present in the literature, and the structure functions for double gluons emission. Because the LP contribution of the parity even and parity odd structure functions was the same, at NNLO we have restricted our analysis to the case that the intermediate vector boson was a virtual photon. However, even in this simpler scenario, we have found that the double real structure functions at soft threshold feature the product of gluons transverse momenta in the denominator. Therefore, we have furthermore restricted our attention to the abelian contribution only. Despite these simplifications, the inclusive and zeroth structure functions still displayed a pattern for verifying the exponentiation properties of the eikonal amplitude. Nonetheless, the double real emission case could be more thoroughly studied including Z boson production and the non-abelian contribution as well, thus obtaining a complete expression for the helicity cross sections for the neutral current Drell-Yan process at soft threshold.

- That the abelian contribution of the inclusive eikonal helicity amplitude displayed

an exponential pattern was manifest from the explicit form of the real and double real form of the inclusive structure functions. However, at NLO order, we have found that at soft threshold, $T^0_{R,\text{soft}}$ was simply equal to one. Because the eikonal exponentiation was difficult to point out in this case, we have rederived the helicity cross sections using effective field theory methods. Specifically, soft factorization theorems constitute a very powerful tool, as they correspond to an all-order Ansatz. Using these theorems, we have rederived the LP soft function, already present in the literature, and applied it to the calculation of the inclusive real and double real helicity cross sections. Comparing the results obtained within SCET and in full QCD, we have verified that they agree. What constitute the original contribution of this thesis, was instead the derivation of the NNLP soft function. In particular, against using the QCD results to cross-check the ones obtained in the effective theory, we have verified that the NNLP soft function indeed reproduces the zeroth real and double real (in this case, except for a factor of 2) structure functions calculated in the full theory. This factorization formula could be then used for future studies and for deriving all-order statements on the nature of the projection of the amplitude into longitudinal polarization states.

Appendix A

Notation and Conventions

A.1 Distributions

In this thesis, we use the following conventions for the Fourier transform

$$\begin{aligned} \tilde{f}(x) &= \int \frac{d^4k}{(2\pi)^4} f(k)\, e^{-ik\cdot x} \\ f(k) &= \int d^4x\, \tilde{f}(x)\, e^{ik\cdot x}\,. \end{aligned} \tag{A.1}$$

Because by the argument of the function is clear if we are working in position or momentum space, the tilde will always be omitted. Moreover, the dot product in the argument of the exponential is in Minkowski metric. That is, we have that

$$k\cdot x = k^\mu g_{\mu\nu} x^\nu, \qquad g_{\mu\nu} = \mathrm{diag}(+1,-1,-1,-1) \tag{A.2}$$

with the above convention for the choice of the signature. The Fourier trasform of the identity gives the delta function, that is

$$\begin{aligned} \mathcal{F}[1] &= \int d^4x\, e^{ik\cdot x} = (2\pi)^4 \delta^4(k) \\ \mathcal{F}^{-1}[1] &= \int \frac{d^4k}{(2\pi)^4} e^{-ik\cdot x} = \delta^4(x)\,. \end{aligned} \tag{A.3}$$

Alternatively, the delta function can be defined as the derivative of the Heaviside theta function $\theta(x)$, defined by

$$\theta(x) = \begin{cases} 1 & x > 0 \\ 0 & x < 0 \end{cases} \tag{A.4}$$

In addition, for the application of subtraction schemes, we make use of the plus distribution $[f(\xi)]_+$, defined as

$$\int_x^1 d\xi\, g(\xi)[f(\xi)]_+ \equiv \int_x^1 d\xi [g(\xi) - g(1)] f(\xi) - g(1) \int_0^x d\xi\, f(\xi) \tag{A.5}$$

with $g(\xi)$ smooth test function.

A.2 Spinors

A.2.1 Dirac Matrices

The Dirac gamma matrices $\{\gamma^0, \gamma^1, \gamma^2, \gamma^3\}$ are the basis of the spinor algebra. These are hermitian traceless matrices satisfying the anti-commutation relations

$$\{\gamma^\mu, \gamma^\nu\} = 2g^{\mu\nu}$$

and satisfying the following properties:

$$\begin{aligned}
&\mathrm{Tr}(\gamma^\mu) = 0 \\
&\mathrm{Tr}(\gamma^\mu\gamma^\nu) = 4g^{\mu\nu} \\
&\mathrm{Tr}(\gamma^5) = \mathrm{Tr}(\gamma^\mu\gamma^\nu\gamma^5) = 0 \\
&\mathrm{Tr}(\gamma^\mu\gamma^\nu\gamma^\rho\gamma^\sigma\gamma^5) = -4i\epsilon^{\mu\nu\rho\sigma} \\
&\mathrm{Tr}(\gamma^{\mu_1}\cdots\gamma^{\mu_n}) = 0 \qquad n \quad \text{odd}\,.
\end{aligned} \tag{A.6}$$

A.2.2 Completness relations for spinor fields

The completeness relations for spinors u and v of momentum k are given by

$$\begin{aligned}
\sum_s u_i^s(k)\bar{u}_j^s(k) &= \sum_s \bar{u}_j^s(k)u_i^s(k) = (\not{k} + m\mathbb{I})_{ij} \\
\sum_s v_i^s(k)\bar{v}_j^s(k) &= \sum_s \bar{v}_j^s(k)v_i^s(k) = (\not{k} - m\mathbb{I})_{ij}
\end{aligned} \tag{A.7}$$

where the sum runs over spin states s.

Appendix B

Hadronic decomposition

B.1 Spherical harmonics

$$
\begin{aligned}
g_{-1}(\vartheta,\varphi) &= 1+\cos^2\vartheta & g_2(\vartheta,\varphi) &= \frac{1}{2}\sin^2\vartheta\cos(2\varphi) & g_5(\vartheta,\varphi) &= \sin^2\vartheta\sin(2\varphi)\\
g_0(\vartheta,\varphi) &= 1-\cos^2\vartheta & g_3(\vartheta,\varphi) &= \sin\vartheta\cos\varphi & g_6(\vartheta,\varphi) &= \sin(2\vartheta)\sin\varphi\\
g_1(\vartheta,\varphi) &= \sin(2\vartheta)\cos\varphi & g_4(\vartheta,\varphi) &= \cos\vartheta & g_7(\vartheta,\varphi) &= \sin\vartheta\sin\varphi
\end{aligned}
$$

B.2 Interference γ^*/Z at $\mathcal{O}(\alpha_s)$

The interferenxe between the virtual photon γ^* and the Z boson can be calculated in the same way as at tree level. The amplitude, averaged over spin, color and polarization indices, is equal to

$$\mathcal{M}_\gamma \mathcal{M}_Z^* = L_{\mu\nu,\gamma Z} W_{\gamma Z}^{\mu\nu} \tag{B.1}$$

where the leptonic tensor and the hadronic tensor are defined as

$$L_{\gamma Z,R}^{\mu\nu} = \frac{e^2}{q^4} P_Z(q^2)\,\mathrm{Tr}[\not{p}_1\gamma^\mu\not{p}_2\gamma^\nu] \tag{B.2}$$

$$W_{\gamma Z,R}^{\mu\nu} = -g_s\,\frac{Q_f\,e^2\,C_F}{4N_c}\,\mathrm{Tr}[\not{p}_b S^{\mu\alpha}\not{p}_a S_{\alpha 5}{}^{\nu}]\,. \tag{B.3}$$

As seen in section 4.1, the tensor $S_5^{\mu\nu}$ defined in eq.(4.5) consists of a symmetric part proprtional to $S^{\mu\nu}$ and of an antisymmetric part involving the trace of γ^5, so that the hadronic tensor is explicitly given by

$$W_{\gamma Z,R}^{\mu\nu} = -g_s\,\frac{Q_f\,e^2\,C_F}{4N_c}\left[v_f\,\mathrm{Tr}[\not{p}_b S^{\mu\alpha}\not{p}_a S_\alpha{}^{\nu}] - a_f\,\mathrm{Tr}[\not{p}_b S^{\mu\alpha}\not{p}_a S_{\alpha 5}{}^{\nu}]\right]. \tag{B.4}$$

For the decomposition of this tensor into structure functions we just make use of the previous results. The first trace in the above expression is non vanishing for $i \in \{-1,0,1,2\}$

and zero for all the other indices, while the second is non vanishing only for $i = 3, 4$. Including the correct overall factor, the parity-even structure functions are equal to

$$
\begin{aligned}
W^{-1}_{\gamma Z,R} &= \frac{Q_f C_F}{N_c} 16\pi^2 \alpha_{em}\alpha_s \cdot v_f \left\{ \left(\frac{2(q^2-u)(q^2-t)-ut}{ut} \right) \cdot \left(\frac{q^2-u}{q^2-t} + \frac{q^2-t}{q^2-u} \right) \right\} \\
W^{0}_{\gamma Z,R} &= \frac{Q_f C_F}{N_c} 16\pi^2 \alpha_{em}\alpha_s \cdot v_f \left\{ 2 \left(\frac{q^2-u}{q^2-t} + \frac{q^2-t}{q^2-u} \right) \right\} \\
W^{1}_{\gamma Z,R} &= \frac{Q_f C_F}{N_c} 16\pi^2 \alpha_{em}\alpha_s \cdot v_f \left\{ 2\sqrt{\frac{q^2 s}{tu}} \left(\frac{q^2-u}{q^2-t} - \frac{q^2-t}{q^2-u} \right) \right\} \\
W^{2}_{\gamma Z,R} &= \frac{Q_f C_F}{N_c} 16\pi^2 \alpha_{em}\alpha_s \cdot v_f \left\{ 2 \left(\frac{q^2-u}{q^2-t} + \frac{q^2-t}{q^2-u} \right) \right\} .
\end{aligned}
\tag{B.5}
$$

while the parity-odd structure functions and the inclusive structure function are equal to

$$
\begin{aligned}
W^{3}_{\gamma Z,R} &= \frac{Q_f C_F}{N_c} 16\pi^2 \alpha_{em}\alpha_s (-a_f) \left\{ 4\sqrt{\frac{(q^2-u)(q^2-t)}{ut}} \left(\frac{q^2-u}{q^2-t} - \frac{q^2-t}{q^2-u} \right) \right\} \\
W^{4}_{\gamma,Z} &= \frac{Q_f C_F}{N_c} 16\pi^2 \alpha_{em}\alpha_s (-a_f) \left\{ 4\sqrt{\frac{q^2 s}{(q^2-t)(q^2-u)}} \left(\frac{(q^2-u)^2+(q^2-t)^2}{ut} \right) \right\} \\
W^{incl}_{\gamma Z,R} &= \frac{Q_f C_F}{N_c} 16\pi^2 \alpha_{em}\alpha_s \cdot v_f \left\{ 2\sqrt{\frac{q^2 s}{(q^2-t)(q^2-u)}} \left(\frac{(q^2-u)^2+(q^2-t)^2}{ut} \right) \right\} .
\end{aligned}
\tag{B.6}
$$

As expected, these structure functions are proportional to the functions T^i_R given in eq.(4.11), (4.15) with a different normalization factor involving electroweak couplings and numerical factors.

Bibliography

[1] Georges Aad et al. Observation of a new particle in the search for the Standard Model Higgs boson with the ATLAS detector at the LHC. *Phys. Lett. B*, 716:1–29, 2012.

[2] Serguei Chatrchyan et al. Observation of a New Boson at a Mass of 125 GeV with the CMS Experiment at the LHC. *Phys. Lett. B*, 716:30–61, 2012.

[3] Georges Aad et al. Measurements of the Higgs boson production and decay rates and constraints on its couplings from a combined ATLAS and CMS analysis of the LHC pp collision data at $\sqrt{s} = 7$ and 8 TeV. *JHEP*, 08:045, 2016.

[4] S. D. Drell and Tung-Mow Yan. Massive Lepton Pair Production in Hadron-Hadron Collisions at High-Energies. *Phys. Rev. Lett.*, 25:316–320, 1970. [Erratum: Phys.Rev.Lett. 25, 902 (1970)].

[5] John C. Collins and Davison E. Soper. Angular Distribution of Dileptons in High-Energy Hadron Collisions. *Phys. Rev. D*, 16:2219, 1977.

[6] E. Mirkes. Angular decay distribution of leptons from W bosons at NLO in hadronic collisions. *Nucl. Phys. B*, 387:3–85, 1992.

[7] Markus A. Ebert, Johannes K. L. Michel, Iain W. Stewart, and Frank J. Tackmann. Drell-Yan q_T resummation of fiducial power corrections at N^3LL. *JHEP*, 04:102, 2021.

[8] Murray Gell-Mann. Symmetries of baryons and mesons. *Phys. Rev.*, 125:1067–1084, 1962.

[9] A. P. Balachandran, G. Marmo, B. S. Skagerstam, and A. Stern. *Gauge Theories and Fibre Bundles - Applications to Particle Dynamics*, volume 188. 1983.

[10] Chen-Ning Yang and Robert L. Mills. Conservation of Isotopic Spin and Isotopic Gauge Invariance. *Phys. Rev.*, 96:191–195, 1954.

[11] L. D. Faddeev and V. N. Popov. Feynman Diagrams for the Yang-Mills Field. *Phys. Lett. B*, 25:29–30, 1967.

[12] A. A. Slavnov. Ward Identities in Gauge Theories. *Theor. Math. Phys.*, 10:99–107, 1972.

[13] J. C. Taylor. Ward Identities and Charge Renormalization of the Yang-Mills Field. *Nucl. Phys. B*, 33:436–444, 1971.

[14] C. Becchi, A. Rouet, and R. Stora. Renormalization of Gauge Theories. *Annals Phys.*, 98:287–321, 1976.

[15] M. Z. Iofa and I. V. Tyutin. Gauge Invariance of Spontaneously Broken Nonabelian Theories in the Bogolyubov-Parasiuk-HEPP-Zimmerman Method. *Teor. Mat. Fiz.*, 27:38–47, 1976.

[16] William A. Bardeen, A. J. Buras, D. W. Duke, and T. Muta. Deep Inelastic Scattering Beyond the Leading Order in Asymptotically Free Gauge Theories. *Phys. Rev. D*, 18:3998, 1978.

[17] Gerard 't Hooft and M. J. G. Veltman. Regularization and Renormalization of Gauge Fields. *Nucl. Phys. B*, 44:189–213, 1972.

[18] Johannes Michel. *Factorization and Resummation for Precision Physics at the LHC*. PhD thesis, U. Hamburg (main), Hamburg U., 2020.

[19] K. A. Olive et al. Review of Particle Physics. *Chin. Phys. C*, 38:090001, 2014.

[20] Curtis G. Callan, Jr. Broken scale invariance in scalar field theory. *Phys. Rev. D*, 2:1541–1547, 1970.

[21] K. Symanzik. Small distance behavior in field theory and power counting. *Commun. Math. Phys.*, 18:227–246, 1970.

[22] S. A. Larin and J. A. M. Vermaseren. The Three loop QCD Beta function and anomalous dimensions. *Phys. Lett. B*, 303:334–336, 1993.

[23] F. Herzog, B. Ruijl, T. Ueda, J. A. M. Vermaseren, and A. Vogt. The five-loop beta function of Yang-Mills theory with fermions. *JHEP*, 02:090, 2017.

[24] T. van Ritbergen, J. A. M. Vermaseren, and S. A. Larin. The Four loop beta function in quantum chromodynamics. *Phys. Lett. B*, 400:379–384, 1997.

[25] Georges Aad et al. A precise determination of the strong-coupling constant from the recoil of Z bosons with the ATLAS experiment at $\sqrt{s} = 8$ TeV. 9 2023.

[26] David J. Gross and Frank Wilczek. Ultraviolet Behavior of Nonabelian Gauge Theories. *Phys. Rev. Lett.*, 30:1343–1346, 1973.

[27] H. David Politzer. Reliable Perturbative Results for Strong Interactions? *Phys. Rev. Lett.*, 30:1346–1349, 1973.

[28] Kenneth G. Wilson. Confinement of Quarks. *Phys. Rev. D*, 10:2445–2459, 1974.

[29] L. D. Landau. On analytic properties of vertex parts in quantum field theory. *Nucl. Phys.*, 13(1):181–192, 1959.

[30] George F. Sterman. Partons, factorization and resummation, TASI 95. In *Theoretical Advanced Study Institute in Elementary Particle Physics (TASI 95): QCD and Beyond*, pages 327–408, 6 1995.

[31] Davison E. Soper. Basics of QCD perturbation theory. In *Theoretical Advanced Study Institute in Elementary Particle Physics (TASI 2000): Flavor Physics for the Millennium*, pages 267–316, 11 2000.

[32] T. Kinoshita. Mass singularities of Feynman amplitudes. *J. Math. Phys.*, 3:650–677, 1962.

[33] T. D. Lee and M. Nauenberg. Degenerate Systems and Mass Singularities. *Phys. Rev.*, 133:B1549–B1562, 1964.

[34] John C. Collins, Davison E. Soper, and George F. Sterman. Factorization of Hard Processes in QCD. *Adv. Ser. Direct. High Energy Phys.*, 5:1–91, 1989.

[35] John Collins. *Foundations of Perturbative QCD*, volume 32 of *Cambridge Monographs on Particle Physics, Nuclear Physics and Cosmology*. Cambridge University Press, 7 2023.

[36] R. P. Feynman. Photon-hadron interactions. 1973.

[37] Gillian Hendrik Hubertus Lustermans. *Scaling up the Detail in Particle Collisions: Factorization and resummation for predictions of multi-differential cross sections*. PhD thesis, Amsterdam U., 2019.

[38] Richard D. Ball et al. Parton distributions for the LHC Run II. *JHEP*, 04:040, 2015.

[39] A. D. Martin, W. J. Stirling, R. S. Thorne, and G. Watt. Parton distributions for the LHC. *Eur. Phys. J. C*, 63:189–285, 2009.

[40] Xiangdong Ji. Parton Physics on a Euclidean Lattice. *Phys. Rev. Lett.*, 110:262002, 2013.

[41] Michiel Botje. Lecture notes particle physics ii, quantum chromodynamics: The qcd improved parton model, 2013.

[42] John C. Collins and Davison E. Soper. Parton Distribution and Decay Functions. *Nucl. Phys. B*, 194:445–492, 1982.

[43] V. N. Gribov and L. N. Lipatov. Deep inelastic e p scattering in perturbation theory. *Sov. J. Nucl. Phys.*, 15:438–450, 1972.

[44] Yuri L. Dokshitzer. Calculation of the Structure Functions for Deep Inelastic Scattering and e+ e- Annihilation by Perturbation Theory in Quantum Chromodynamics. *Sov. Phys. JETP*, 46:641–653, 1977.

[45] Guido Altarelli and G. Parisi. Asymptotic Freedom in Parton Language. *Nucl. Phys. B*, 126:298–318, 1977.

[46] Aneesh V. Manohar. Introduction to Effective Field Theories. 4 2018.

[47] Enrico Fermi. Tentativo di una teoria dell'emissione dei raggi beta. *Ric. Sci.*, 4:491–495, 1933.

[48] Matthias Neubert. B decays and the heavy quark expansion. *Adv. Ser. Direct. High Energy Phys.*, 15:239–293, 1998.

[49] Matthias Neubert. Heavy quark effective theory and weak matrix elements. In *1997 Europhysics Conference on High Energy Physics*, pages 243–268, 1 1998.

[50] A. G. Grozin. Heavy quark effective theory. *Springer Tracts Mod. Phys.*, 201:1–213, 2004.

[51] S. Scherer. Chiral Perturbation Theory: Introduction and Recent Results in the One-Nucleon Sector. *Prog. Part. Nucl. Phys.*, 64:1–60, 2010.

[52] Johan Bijnens and Gerhard Ecker. Mesonic low-energy constants. *Ann. Rev. Nucl. Part. Sci.*, 64:149–174, 2014.

[53] Ilaria Brivio and Michael Trott. The Standard Model as an Effective Field Theory. *Phys. Rept.*, 793:1–98, 2019.

[54] Christian W. Bauer, Sean Fleming, and Michael E. Luke. Summing Sudakov logarithms in $B \to X_s\gamma$in effective field theory. *Phys. Rev. D*, 63:014006, 2000.

[55] Christian W. Bauer, Sean Fleming, Dan Pirjol, and Iain W. Stewart. An Effective field theory for collinear and soft gluons: Heavy to light decays. *Phys. Rev. D*, 63:114020, 2001.

[56] Christian W. Bauer and Iain W. Stewart. Invariant operators in collinear effective theory. *Phys. Lett. B*, 516:134–142, 2001.

[57] Christian W. Bauer, Dan Pirjol, and Iain W. Stewart. Soft collinear factorization in effective field theory. *Phys. Rev. D*, 65:054022, 2002.

[58] Christian W. Bauer, Sean Fleming, Dan Pirjol, Ira Z. Rothstein, and Iain W. Stewart. Hard scattering factorization from effective field theory. *Phys. Rev. D*, 66:014017, 2002.

[59] Christian W. Bauer, Dan Pirjol, and Iain W. Stewart. On Power suppressed operators and gauge invariance in SCET. *Phys. Rev. D*, 68:034021, 2003.

[60] Thomas Becher, Alessandro Broggio, and Andrea Ferroglia. *Introduction to Soft-Collinear Effective Theory*, volume 896. Springer, 2015.

[61] Ian W. Stewart. Lectures on the soft-collinear effective theory. MIT OpenCourseWare, 2013.

[62] R. Gauld, A. Gehrmann-De Ridder, T. Gehrmann, E. W. N. Glover, and A. Huss. Precise predictions for the angular coefficients in Z-boson production at the LHC. *JHEP*, 11:003, 2017.

[63] Daniel Boer and Werner Vogelsang. Drell-Yan lepton angular distribution at small transverse momentum. *Phys. Rev. D*, 74:014004, 2006.

[64] Markus A. Ebert, Johannes K. L. Michel, Iain W. Stewart, and Frank J. Tackmann. Drell-Yan q_T resummation of fiducial power corrections at N^3LL. *JHEP*, 04:102, 2021.

[65] E. Mirkes and J. Ohnemus. Angular distributions of Drell-Yan lepton pairs at the Tevatron: Order $\alpha - s^2$ corrections and Monte Carlo studies. *Phys. Rev. D*, 51:4891–4904, 1995.

[66] Georges Aad et al. Measurement of the angular coefficients in Z-boson events using electron and muon pairs from data taken at $\sqrt{s} = 8$ TeV with the ATLAS detector. *JHEP*, 08:159, 2016.

[67] C. S. Lam and Wu-Ki Tung. A Systematic Approach to Inclusive Lepton Pair Production in Hadronic Collisions. *Phys. Rev. D*, 18:2447, 1978.

[68] Leszek Motyka, Mariusz Sadzikowski, and Tomasz Stebel. Lam-Tung relation breaking in Z^0 hadroproduction as a probe of parton transverse momentum. *Phys. Rev. D*, 95(11):114025, 2017.

[69] Iain W. Stewart, Frank J. Tackmann, and Wouter J. Waalewijn. Factorization at the LHC: From PDFs to Initial State Jets. *Phys. Rev. D*, 81:094035, 2010.

[70] Markus A. Ebert, Anjie Gao, and Iain W. Stewart. Factorization for azimuthal asymmetries in SIDIS at next-to-leading power. *JHEP*, 06:007, 2022. [Erratum: JHEP 07, 096 (2023)].